Synthesis of flat-sheet thin film composite forward osmosis membranes

Wei, Jing

2013

Wei, J. (2013). Synthesis of flat-sheet thin film composite forward osmosis membranes. Doctoral thesis, Nanyang Technological University, Singapore.

https://hdl.handle.net/10356/54655

https://doi.org/10.32657/10356/54655

NANYANG TECHNOLOGICAL UNIVERSITY

SYNTHESIS OF FLAT-SHEET THIN FILM COMPOSITE FORWARD OSMOSIS MEMBRANES

WEI JING

SCHOOL OF CIVIL AND ENVIRONMENTAL ENGINEERING

2013

SYNTHESIS OF FLAT-SHEET THIN FILM COMPOSITE FORWARD OSMOSIS MEMBRANES

WEI JING

SCHOOL OF CIVIL AND ENVIRONMENTAL ENGINEERING

A thesis submitted to the Nanyang Technological University
in partial fulfillment of the requirement for the degree of
Doctor of Philosophy

2013

Acknowledgements

First and foremost, I would like to extend my deepest gratitude to my supervisor, Associate Professor Tang Chuyang, and my co-supervisor, Associate Professor Wang Rong. Prof. Tang and Prof. Wang gave me consistent guidance on each step of my PhD study, to solve my questions on the graduate courses, to discuss the experimental progress, and to review my manuscripts and presentations. Their profound knowledge and wisdom not only guided me on my PhD study but also taught me how to become an open-minded and independent researcher in the future. It is my great honor to be their student and I owe all my achievements to them.

I would like to acknowledge the Singapore Membrane Technology Centre (SMTC) and School of Civil & Environmental Engineering (CEE), Nanyang Technological University for providing me the scholarship and facilities to fulfill my PhD research. An acknowledgement also goes to the Environment and Water Industry Development Council (EWI) of Singapore and Singapore Economic Development Board for funding my research project.

My special thanks go to Dr. Qiu Changquan, a former Research Fellow in CEE/SMTC. He patiently taught me and generously shared his knowledge on membrane fabrication from the very beginning of my PhD study. This research could not go so smoothly without his inspiration and contribution.

I take this opportunity to sincerely thank Dr. Ma Ning, Dr. Wang Yining, Liu Xin, Liau Wei Min and Eugene Chen Jian Hong for their earnest cooperation in my experiments. I am also very grateful to all of our group members, Qi Saren, Zhao Yang, She Qianhong, Gu Yangshuo, Xiao Dezhong, Zou Shan, Gao Yiben, Do Thanh Van, Dr. Jin Xue, Dr. Li Weiyi, Dr. Zhang Yan, Zhang Minmin, Pan Fanfan, Wang Can, Lee Jian Yuan, Li Ye and Hou Dianxun. I feel so lucky to be part of this warm and cheerful group.

I would like to sincerely thank all the colleagues in the SMTC. They always extend

their kindly help when I encounter problems. My thanks also go to all the staff in the Environmental Lab of CEE for providing me the necessary research facilities, professional training, and patient assistance during my study.

Last but not least, I would like to convey my heartfelt gratitude to my dear family and friends for supporting me in the past years, and for sharing with me each laughter and tear. I would not go this far on my research without their support.

Table of contents

Abstract

Forward osmosis (FO) is an emerging membrane separation technology. It is different from the well-studied pressure-driven membrane separation processes. The FO process is based on water transport under an osmotic pressure difference across a semi-permeable membrane. The distinct operating conditions lead to unique technical challenges during the exploitation of FO technology. According to a comprehensive literature investigation, one of the stringent barriers is lacking of effective FO membranes. The objectives of this research were to develop high performance FO membranes, and furthermore, to systematically study the mass transport and the governing mechanisms in FO process.

Thin film composite (TFC) FO membranes with a tailored support structure were developed in this study. The membranes consisted of a highly porous substrate with finger-like pore structure, which was prepared via phase inversion, and a polyamide rejection layer synthesized by interfacial polymerization. The TFC FO membranes had small structural parameters due to the thin cross-section, low tortuosity, and high porosity of the substrates. The membrane rejection layers exhibited superior separation properties (higher water permeability and excellent selectivity) relative to commercial FO membranes. Under FO testing conditions, these membranes achieved high water flux while maintaining relatively low solute reverse diffusion. Comparison of the synthesized TFC FO membranes with commercial FO and reverse osmosis (RO) membranes revealed the critical importance of the substrate structure, with a straight finger-like pore structure preferred over a spongy pore structure to minimize internal concentration polarization (ICP), a unique and critical problem resulting in low water flux in the osmotically driven membrane processes. In addition, membranes with high water permeability and excellent selectivity are preferred to achieve both high FO water flux and low solute flux. The results proved that TFC membranes with a tailored porous substrate and rejection layer are promising for FO applications.

In the study of polyamide rejection layer synthesis, the influence of monomer

concentrations (i.e., m-phenylenediamine (MPD) and trimesoyl chloride (TMC) concentrations) on the membrane separation properties as well as the FO performance was systematically investigated. A strong trade-off between the water permeability and salt rejection of the membranes was observed, where reducing the MPD concentration or increasing the TMC concentration may result in a higher membrane permeability but a lower salt rejection. In FO tests, membranes with poor salt rejection had severe solute reverse diffusion, which enhanced the severity of ICP. It was found that the FO water flux was governed by both the membrane water permeability and solute rejection. For a membrane with higher water permeability but lower solute rejection, the reduced membrane frictional resistance was compensated simultaneously by the more severe solute-reverse-diffusion-induced ICP. The net effect on the FO water flux depends on the competition of these two opposing mechanisms. Under conditions where solute reverse diffusion may cause severe ICP (e.g., high draw solution concentration and high water flux level), membranes need to be optimized to achieve a high salt rejection even if this is at the expense of lower water permeability.

In view of the importance of the water permeability and salt permeability on FO performance, a systematic comparison study of prevailing semi-permeable FO membranes with nanofiltration (NF)-like and RO-like separation properties in terms of flux performance and fouling behavior was conducted. Due to the crucial influence of solute reverse diffusion on FO water flux, the high-rejection RO-like FO membranes generally performed better than the NF-like counterparts in sodium chloride based FO tests. On the other hand, the high permeability of NF-like FO membranes could achieve higher water flux, when proper draw solutes were used to minimize draw solute leakage. Fouling tests suggested that the NF-like TFC FO membranes tended to be more fouling resistant due to their relatively smooth membrane surface. This work further elucidated the major mechanisms that govern the FO performance. These mechanisms were summarized as a frictional resistance loss mechanism (M_R), solute-reverse-diffusion-induced ICP ($M_{ICP\text{-}Js}$), concentration of feed solutes (concentrative ICP or $M_{ICP\text{-}feed}$ in the active-layer-facing-draw-solution orientation) and dilution of draw solutes (dilutive ICP or $M_{ICP\text{-}draw}$ in the

active-layer-facing-feed-solution orientation). These mechanisms are related to the properties of membrane, draw and feed solutions. This work led to a set of systematic criteria for the selection of FO membranes, draw solution and optimization of other operating conditions, of which the practicability was demonstrated in potential FO applications.

List of tables

List of figures

List of symbols

Symbol	Description
A	Water permeability coefficient of membrane
A_m	Effective membrane area
B	Salt permeability coefficient of membrane
B_{draw}	Draw solute permeability coefficient of membrane
B_{feed}	Feed solute permeability coefficient of membrane
C	Molar concentration
C_{draw}	Concentration of draw solution
C_{feed}	Concentration of feed solution
C_p	Concentration of permeate
C_0	Initial concentration of solution
C_t	Concentration of solution at time t
D	Diffusion coefficient of solute
D_{draw}	Diffusion coefficient of draw solute
D_{eff}	Effective diffusion coefficient of solute
D_{feed}	Diffusion coefficient of feed solute
J_s	Solute flux
J_v	Water flux
K_m	Mass transfer coefficient
l	Thickness of membrane support
l_{eff}	Effective thickness of membrane support
Δm_{feed}	Weight change of feed solution
m_{wet}	Wet mass of membrane sample

Symbol	Description
m_{dry}	Dry mass of membrane sample
n	Crosslinking density of polyamide film
ΔP	Trans-membrane pressure
R	Salt rejection of membrane
R_g	Universal gas constant
R_{rms}	Root mean square roughness
S	Structural parameter
T	Absolute temperature
Δt	Sampling time interval
V_0	Initial volume of solution
V_t	Volume of solution at time t
ΔV_{feed}	Volume change of feed solution
β	Dimensionless van't Hoff factor
ε	Porosity of membrane support
ε_{eff}	Effective porosity of membrane support
π	Osmotic pressure
π_{draw}	Osmotic pressure of draw solution
π_{feed}	Osmotic pressure of feed solution
$\Delta\pi$	Osmotic pressure difference
$\Delta\pi_{eff}$	Effective osmotic pressure difference
ρ_w	Density of wetting solvent
ρ_m	Density of polymer
ρ_{feed}	Density of feed solution
σ	Reflection coefficient
τ	Tortuosity of membrane support

List of abbreviations

Abbreviation	Description
AFM	Atomic force microscopy
AL-DS	Active-layer-facing-draw-solution orientation
AL-FS	Active-layer-facing-feed-solution orientation
ATR-FTIR	Attenuated total reflection-Fourier transform infrared spectroscopy
BSA	Bovine serum albumin
CA	Cellulose acetate
CTA	Cellulose triacetate
DS	Draw solution
ECP	External concentration polarization
FO	Forward osmosis
FS	Feed solution
HTI	Hydration Technology Innovations
ICP	Internal concentration polarization
LBL	Layer-by-layer assembly
MBR	Membrane bioreactor
MD	Membrane distillation
MF	Microfiltration
$M_{ICP\text{-}draw}$	Dilutive internal concentration polarization of draw solution
$M_{ICP\text{-}feed}$	Concentrative internal concentration polarization of feed solution
$M_{ICP\text{-}Js}$	Solute reverse diffusion induced internal concentration polarization
MNPs	Superparamagnetic nanoparticles
MPD	M-phenylenediamine

Abbreviation	Description
M_R	Membrane frictional resistance loss mechanism
NF	Nanofiltration
NMP	N-Methyl-2-pyrrolidone
OMBR	Osmotic membrane bioreactor
PAH	Poly(allylamine hydrochloride)
PAI	Poly(amide-imide)
PAN	Polyacrylonitrile
PBI	Polybenzimidazole
PEG	Polyethylene glycol
PEI	Polyethyleneimine
PES	Polyethersulfone
PIP	Piperazine
PRO	Pressure-retarded osmosis
PSS	Poly(sodium 4-styrene-sulfonate)
PVP	Polyvinyl pyrrolidone
RO	Reverse osmosis
SDS	Sodium dodecyl sulfate
SEM	Scanning electron microscope
TEA	Triethylamine
TFC	Thin film composite
TFN	Thin film nanocomposite
TMC	Trimesoyl chloride
UF	Ultrafiltration

List of publications

Journal articles

1. **Wei, J.**, Qiu, C., Tang, C.Y., Wang, R., Fane, A.G. (2011), "Synthesis and characterization of flat-sheet thin film composite forward osmosis membranes", Journal of Membrane Science, Vol. 372, No. 1-2, pp. 292-302.

2. **Wei**, **J.,** Liu, X., Qiu, C., Wang, R., Tang, C.Y. (2011), "Influence of monomer concentrations on the performance of polyamide-based thin film composite forward osmosis membranes", Journal of Membrane Science, Vol. 381, No. 1-2, pp. 110-117.

3. Ma, N., **Wei, J.,** Liao, R., Tang, C.Y. (2012), "Zeolite-polyamide thin film nanocomposite membranes: Towards enhanced performance for forward osmosis", Journal of Membrane Science, Vol. 405-406, pp. 149-157.

4. Jin, X., Shan, J., Wang, C., **Wei, J.**, Tang, C.Y. (2012), "Rejection of pharmaceuticals by forward osmosis membranes", Journal of Hazardous Materials, Vol. 227-228, pp. 55-61.

5. **Wei, J.**, Qiu, C., Wang, Y.N., Wang, R., Tang, C.Y. (2013), "Comparison of NF-like and RO-like thin film composite osmotically-driven membranes - Implications for membrane selection and process optimization", Journal of Membrane Science, Vol. 427, pp. 460-471.

6. Wang, Y.N., **Wei, J.**, She, Q., Pacheco, F., Tang, C.Y. (2012) "Microscopic characterization of FO/PRO membranes - A comparative study of CLSM, TEM and SEM", Environmental Science and Technology, Vol. 46, No. 18, pp. 9995-10003.

7. Qi, S., Li, W., Zhao, Y., Ma, N., **Wei, J.**, Chin, T.W., Tang, C.Y. (2012), "Influence of the properties of layer-by-layer active layers on forward osmosis performance", Journal of Membrane Science, Vol. 423-424, pp. 536-542.

Patents

1. Tang, C.Y., Qiu, C., **Wei, J.**, Wang, R., Fane, A.G. "Synthesis of thin film composite flat-sheet forward osmosis membranes", Provisional US Patent #61/435,959, filed on 25 Jan 2011.

2. Tang, C.Y., Qiu, C., **Wei, J.** "Synthesis of nanofiltration-type thin film composite forward osmosis membranes", Provisional US Patent #61/552,157, filed on 27 Oct 2011.

3. Tang, C.Y., Qiu, C., **Wei, J.**, Wang, R., Fane, A.G. "A forward osmosis membrane and method of forming a forward osmosis membrane", Patent Cooperation Treaty PCT/SG2012/000023 (provisional), filed on 25 Jan 2012.

4. Tang, C.Y., She, Q., Ma, N., **Wei, J.**, Sim, V.S.T., Fane, A.G. "Reinforced membranes for producing osmotic power in pressure retarded osmosis", Provisional US Patent #61/683,475, filed on 15 Aug 2012.

Conference presentations

1. **Wei, J.**, Tang, C.Y., Wang, R. (2010), "Modeling the effect of membrane separation properties and structure on forward osmosis performance", Young Water Talents Symposium 2010, Singapore.

2. **Wei, J.**, Qiu, C., Tang, C.Y., Wang, R., Fane, A.G. (2011), "Fabrication and characterization of thin film composite membranes for forward osmosis",

Young Water Talents Symposium 2011, Singapore.

3. **Wei, J.**, Liu, X., Qiu, C., Wang, R., Tang, C.Y. (2011), "Influence of monomer concentration on the performance of polyamide-based thin film composite forward osmosis membranes", International Congress on Membranes and Membrane Processes (ICOM) 2011, Amsterdam, the Netherlands.

4. **Wei, J.**, Qiu, C., Tang, C.Y., Wang, R., Fane, A.G. (2011), "Synthesis and characterization of flat-sheet thin film composite forward osmosis membranes", International Congress on Membranes and Membrane Processes (ICOM) 2011, Amsterdam, the Netherlands.

5. **Wei, J.**, Tang, C.Y., Qiu, C., Wang, Y., Wang, R. (2012), "Comparison of NF-like and RO-like thin film composite forward osmosis membranes in osmotically driven membrane processes", Euromembrane 2012, London, UK.

Chapter 1
Introduction

1.1 Background

Forward osmosis (FO) is an osmotically driven membrane process where water diffuses through a semi-permeable membrane under an osmotic pressure difference ($\Delta\pi$) across the membrane (Cath et al., 2006). The osmotic pressure difference is generated when two solutions, i.e., a low osmotic pressure solution (feed solution or FS) and a high osmotic pressure solution (draw solution or DS), are separated by the semi-permeable membrane. The osmosis phenomenon has been studied centuries ago. The first reported study can be traced back to 1748 when Abbé Nollet observed diffusion of pure water through an animal bladder into wine (Lonsdale, 1982). From the middle of last century, researchers started to explore the engineering applications of osmotically driven membrane process. One of the preliminary attempts was the hydroelectric pile to produce electric power by mixing freshwater and salt water (Pattle, 1954). A few more studies were reported from the 1970s on. Interesting topics included drinking water extraction (Kessler and Moody, 1976; Moody and Kessler, 1976), osmotic power plant (Loeb, 1975; 1976; Loeb et al., 1976), and osmotic pump for drug delivery (Theeuwes and Yum, 1976; Eckenhoff and Yum, 1981). More recently, especially in the past decade, FO technology has been proposed for many more applications, such as wastewater treatment (Holloway et al., 2007; Cornelissen et al., 2008; Achilli et al., 2009b; Lay et al., 2011; Xiao et al., 2011), biomass concentration (Zou et al., 2011), seawater desalination (McCutcheon et al., 2005b; Elimelech, 2007; Cath et al., 2010), osmotic power generation (Achilli et al., 2009a; She et al., 2012b), microbial fuel cell (Zhang et al., 2011a; Ge and He, 2012), food processing (Petrotos and Lazarides, 2001; Jiao et al., 2004; Sant'Anna et al., 2012), pharmaceutical devices (Waterman et al., 2009; Ajay Babu et al., 2010), etc.

Compared to pressure-driven membrane processes such as reverse osmosis (RO) and nanofiltration (NF), FO can operate at a very low hydraulic pressure (Cath et al.,

2006; Xu et al., 2010). Where a high osmotic pressure draw solution is naturally available or can be easily regenerated, the energy consumption of the FO process can be potentially lower than that of pressure-driven processes (Cath et al., 2006; McGinnis and Elimelech, 2007). FO is also expected to have reduced risk of membrane fouling (Holloway et al., 2007; Cornelissen et al., 2008; Achilli et al., 2009b), though further research is still required to understand the mechanisms involved (Lay et al., 2010; Mi and Elimelech, 2010b; Tang et al., 2010; Wang et al., 2010c; Zou et al., 2011). In addition, FO is ideal for some sensitive applications where high pressure and high temperature need to be avoided, e.g., food processing (Dova et al., 2007; Garcia-Castello et al., 2009), pharmaceutical applications (Eckenhoff and Yum, 1981; Guan et al., 2009), etc.

1.2 Problem statement

Despite the many potential applications of FO technology, there are a few technological barriers that have yet to be overcome. One stringent problem is lack of suitable membranes. In principle, any semi-permeable membrane that rejects the draw agents can be used as FO membrane (Cath et al., 2006). However, it is found that conventional semi-permeable membranes for pressure-driven membrane processes (e.g., RO membranes) achieved poor FO water flux (Mehta and Loeb, 1978; Loeb et al., 1997; Wei et al., 2011b). Lack of a suitable membrane has greatly impeded the development of FO technology.

The main reason why conventional semi-permeable membranes fail in the FO process is a severe concentration polarization occurring within the membrane support layer. Like pressure-driven membrane processes, FO has concentration polarization at the solution-membrane interface (external concentration polarization or ECP), which can be controlled by improving the hydraulic conditions (Wang et al., 2010c). Moreover, concentration polarization can occur within the membrane support layer in the FO process, which is known as internal concentration polarization (ICP) (Loeb et al., 1997; McCutcheon and Elimelech, 2006; Tang et al., 2010). ICP is a unique problem in osmotically driven membrane processes. As the water flux in FO is on the opposite direction to the solute flux, there will be either

(1) a concentrative ICP for the active-layer-facing-draw-solution (AL-DS) orientation, where the solutes from the feed solution accumulate in the porous support layer as a result of retention by the active rejection layer, or (2) a dilutive ICP for the active-layer-facing-feed-solution (AL-FS) orientation, caused by dilution of the draw solution inside the support layer (McCutcheon and Elimelech, 2006; Tang et al., 2010). In addition, ICP can be enhanced by the solute diffusion from DS to FS for low-rejection membranes (Tang et al., 2010; Xiao et al., 2011; Zou et al., 2011). In all cases, the effective driving force (i.e., $\Delta\pi$ across the rejection layer) would be dramatically reduced, resulting in severe reduction of the water flux (McCutcheon and Elimelech, 2006; Tang et al., 2010). One essential solution to improve the performance of current FO technology is developing membranes suitable for the FO process.

Up to the present, commercial FO membranes are still limited in terms of both manufacturers and choice of membrane chemistries. The only commercial FO membranes widely available are the cellulose triacetate asymmetric membranes from Hydration Technologies Innovations (HTI, Albany, OR) (McCutcheon and Elimelech, 2006; Tang et al., 2010; Wang et al., 2010c). In parallel, the synthesis of FO membranes is still in the preliminary stage. There have been only a handful of FO membranes reported (Herron, 2005; Wang et al., 2009; Chou et al., 2010; Su et al., 2010a; Wang et al., 2010b; Yip et al., 2010; Qiu et al., 2011a; Qiu et al., 2011b; Saren et al., 2011; Setiawan et al., 2011; Tiraferri et al., 2011; Yu et al., 2011; Fang et al., 2012; Ma et al., 2012; Qi et al., 2012b; Wang et al., 2012b). The demand for FO membrane development is stringent. One obstacle faced by FO membrane fabrication is the absence of systematic knowledge of mass transport in the FO process. Unlike pressure-driven membrane process, the flux in the FO process is highly non-linear with respect to membrane properties (such as water permeability and solute rejection) and osmotic driving force (Tang et al., 2010). The influence of these factors on FO performance has yet to be studied. Meanwhile, trade-off relationships among membrane properties due to the limitation of fabrication techniques impose constraints for membrane optimization. Thus, systematic studies are necessary to provide guidelines for FO membrane fabrication as well as future

engineering applications of FO technology.

1.3 Objectives

The overall objectives of this study were to synthesize high-performance FO membranes and to systematically investigate the mechanisms that govern the FO performance. The specific tasks were as follows:

(1) to study the effects of support layer properties on the FO performance;

(2) to determine the influence of the rejection layer, particularly the combination of permeability and selectivity, on the FO performance;

(3) to investigate the impact of membrane fabrication conditions on the FO performance;

(4) to fabricate flat-sheet thin film composite (TFC) FO membranes with both support and rejection layers optimized for the FO process;

(5) to study the competing effects of membrane properties and operating conditions, and to set out criteria for membrane selection and process optimization. The conclusions of this study would be applicable to not only the flat-sheet membranes but also other configurations such as hollow fibre membranes.

1.4 Scope and organization of the thesis

This thesis focused on the synthesis and characterization of optimal TFC FO membranes. The thesis includes eight chapters. The contents of each chapter are as follows.

The working principle of the FO process, and the advantages and critical problems encountered by FO technology are briefly introduced in Chapter 1. The objectives of this research are also introduced.

A comprehensive literature review is presented in Chapter 2, which introduces the basic concepts, potential applications and challenges of FO technology. The influential factors governing FO performance are investigated. Solutions are developed from the membrane point of view and promising technologies to fabricate high-performance FO membranes are reviewed.

Chapter 3 introduces the methodology and experimental design of this study. Preparation methods of flat-sheet TFC FO membranes are presented. Characterization of membrane chemistry, morphology and separation properties is provided. Systematic FO experiments are designed to study membrane performance in different testing conditions.

In Chapter 4, TFC FO membranes with optimized support structures and rejection layer are developed. Characteristics of the resulting FO membranes are examined and compared with commercial FO membranes as well as RO membranes, to illustrate the effects of the support layer structure and the active rejection layer separation properties. This part of work has been published in the Journal of Membrane Science (Wei et al., 2011b). Copyright permission for using this work is attached at the end of this thesis.

Chapter 5 is to study the effect of polyamide layer fabrication conditions on the performance of TFC FO membranes. In particular, the influence of monomer concentrations used in interfacial polymerization and the resulting polyamide rejection layer separation properties on FO performance are systematically studied. The constraint on FO performance imposed by the rejection layer synthesis is investigated to provide insights into membrane optimization and selection of suitable membranes for given FO applications. This part of work has been published in the Journal of Membrane Science (Wei et al., 2011a). Copyright permission for using this work is attached at the end of this thesis.

Chapter 6 systematically compares NF-like and RO-like FO membranes in terms of their FO performance and fouling behavior. NF-like and RO-like TFC FO

membranes were prepared on identical porous substrates. The influence of membrane surface characteristics and separation properties on the FO performance (water flux, solute rejection, and fouling behavior) is studied. Implications on the membrane selection and process operation in FO applications are discussed. This work has been published in the Journal of Membrane Science (Wei et al., 2013). Copyright permission for using this work is attached at the end of this thesis.

Modeling work is presented in the Appendix to theoretically demonstrate the influence of membrane properties (structural parameters, water permeability and solute permeability) on FO performance. An ICP model is used to predict the water flux when membranes with different properties are used.

Chapter 2

Literature review

2.1 Forward osmosis

Osmosis is the transport of solvent through a semi-permeable membrane from a lower osmotic pressure phase to a higher osmotic pressure phase (Moody and Kessler, 1976; Cath et al., 2006). The semi-permeable membrane is permeable to the solvent but impermeable to the solutes. As a spontaneous phenomenon, osmosis has been discovered centuries ago and was explored for applications such as preservation of foods and sterilization (Cath et al., 2006). Engineering applications of osmosis as a membrane separation technology have been proposed since the middle of the last century (Pattle, 1954; Loeb, 1975; Kessler and Moody, 1976; Loeb, 1976; Loeb et al., 1976; Moody and Kessler, 1976), although large scale applications were not developed at that time. In recent years, there is a recurring surge of study on osmotically driven membrane technologies due to the stringent water and fossil energy shortage. The proposed applications have covered many fields like wastewater treatment (Holloway et al., 2007; Cornelissen et al., 2008; Achilli et al., 2009b; Xiao et al., 2011), seawater desalination (McCutcheon et al., 2005b; Elimelech, 2007; Cath et al., 2010), power generation (Achilli et al., 2009a), osmotic microbial fuel cells (Zhang et al., 2011a), etc. In this section, basic concepts of osmotically driven membrane technologies (the forward osmosis technology in particular) as well as their potential applications are introduced.

2.1.1 Working principles of forward osmosis

The working principles of osmotically driven membrane processes are shown in Figure 2-1. When a high osmotic pressure draw solution and a lower osmotic pressure feed solution are separated by a semi-permeable membrane, concentration of the FS and dilution of the DS will take place at the same time under the osmotic pressure difference ($\Delta\pi = \pi_{draw} - \pi_{feed} > 0$) (Cath et al., 2006).

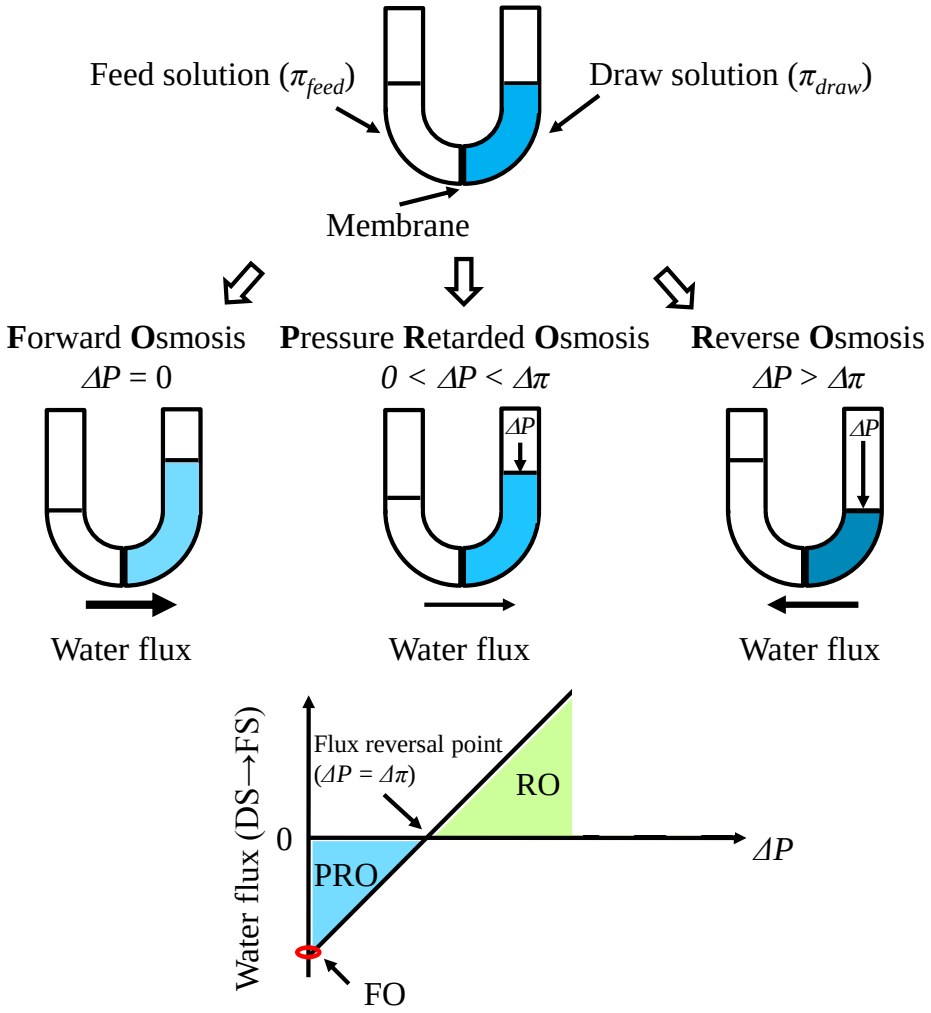

Figure 2-1 Schematic drawing of forward osmosis, pressure-retarded osmosis and reverse osmosis processes (modified from Ref. (Cath et al., 2006) with copyright permission).

An osmotic pressure difference is generated due to the chemical potential difference of solvent in the DS and FS (Cath et al., 2006). With identical solutes in both solutions, the chemical potential of solvent in the low concentration solution is higher and thus drives the solvent transport into the high concentration solution until equal chemical potentials are reached, e.g., identical solute concentrations in both solutions, or $\Delta\pi$ is counterbalanced by a hydrostatic pressure difference ΔP (Figure 2-1), etc. (Mulder, 1996). In the FO process, $\Delta\pi$ is usually created by using a DS that has a higher osmotic pressure than that of the FS. The osmotic pressure of a solution can be calculated using the van't Hoff equation (Mulder, 1996):

$$\pi = \beta C R_g T \tag{2-1}$$

where β is the dimensionless van't Hoff factor, C is the molar concentration of solution, R_g is the gas constant, and T is the absolute temperature. The van't Hoff factor is a function of the dissociation degree of the solute in the solution. It can be seen from this equation that osmotic pressure is a colligative property determined by the solution concentration and dissociation of solutes. The physical meaning of π can be interpreted as the pressure needed to prevent the transport of pure water through an ideal semi-permeable membrane into this solution (Mulder, 1996; Cath et al., 2006).

There are two other membrane processes that are closely related to forward osmosis, i.e., reverse osmosis and pressure-retarded osmosis (PRO). The separation mechanism of RO membranes is similar to that of FO membranes, via the solution-diffusion mechanism. Therefore, these two types of membranes could have similar semi-permeable properties. Instead of using an osmotic pressure difference as the driving force, however, the RO process applies a hydraulic pressure on a feed stream (e.g., seawater) to overcome its osmotic pressure and to extract pure water from the feed (Figure 2-1) (Cath et al., 2006). Compared to FO, RO is a more well-established and leading membrane technology today, widely used in industry especially in desalination (Lee et al., 2011). Another emerging osmotically driven membrane technology is PRO. In the PRO process, a hydraulic pressure lower than $\Delta\pi$ is applied on the DS side to retard the water permeation. The solvent flux is in the direction from FS to DS (Figure 2-1) (Cath et al., 2006). The work of osmotic flux can be used to generate power by a hydroturbine (Yip and Elimelech, 2011; She et al., 2012b). The PRO process has been studied to harvest osmotic energy since the 1970s and becomes increasingly attractive recently in view of the abundant osmotic energy sources worldwide (Aaberg, 2003).

The FO, RO and PRO processes are compared in terms of applied hydraulic pressure and the direction of water flux in Figure 2-1. A general equation for the water flux (J_v) in these three processes is as follows (Cath et al., 2006):

$$J_v = A(\sigma\Delta\pi - \Delta P) \quad (2\text{-}2)$$

where A is the water permeability of membrane and σ is the reflection coefficient. In the FO process, the hydraulic pressure applied on the system is zero ($\Delta P = 0$) and thus the water flux is from the FS to the DS under the osmotic pressure gradient ($\Delta\pi$). A $\Delta P < \Delta\pi$ is applied on the high osmotic pressure side in the PRO process and the water flux is still from the FS to the DS. In the RO process, a $\Delta P > \Delta\pi$ is applied on the brine side to exceed the osmotic pressure difference; thus, the water flux is generated from the brine. The operating pressure in an RO process could be very high (e.g., 10-100 bar, (Mulder, 1996)) due to the high osmotic pressure of the brine, which makes it a very energy-intensive process.

2.1.2 Potential applications of FO technology

In order to utilize the renewable osmotic energy and to reduce the pumping energy in membrane processes, osmotically driven membrane technologies have been studied for many applications such as wastewater treatment, water purification, FO desalination, osmotic power generation, food processing, pharmaceutical devices, and osmotic microbial fuel cells, etc. (Cath et al., 2006; Zhao et al., 2012b). A few of the applications with great interest are introduced in the following to shed light on future studies of FO membrane synthesis.

2.1.2.1 Osmotic membrane bioreactor

The membrane bioreactor (MBR) is a prevalent water reclamation technology that combines biological degradation and membrane separation (Judd, 2008). Conventionally, microfiltration (MF) or ultrafiltration (UF) is used in an MBR system to filter the mixed liquor (Judd, 2008); effluent post-treatments such as RO are required if the product is high quality water. Recently, an innovative osmotic membrane bioreactor (OMBR) technology has been extensively studied (Cornelissen et al., 2008; Achilli et al., 2009b; Qin et al., 2010; Cornelissen et al., 2011; Lay et al., 2011; Xiao et al., 2011; Alturki et al., 2012; Lay et al., 2012a; Lay et al., 2012b; Yap et al., 2012; Zhang et al., 2012a; Zhang et al., 2012b). A schematic of a submerged OMBR is shown in Figure 2-2. In this system, an FO

membrane module is contacted with the mixed liquor. Water in the mixed liquor permeates through the membrane into draw solution that is circulated within the module. A downstream desalination process (e.g., RO or membrane distillation (MD)) is combined to reconcentrate the diluted draw solution and to release the high quality water (Cath et al., 2005a; Cath et al., 2005b; Holloway et al., 2007; Cornelissen et al., 2008; Achilli et al., 2009b).

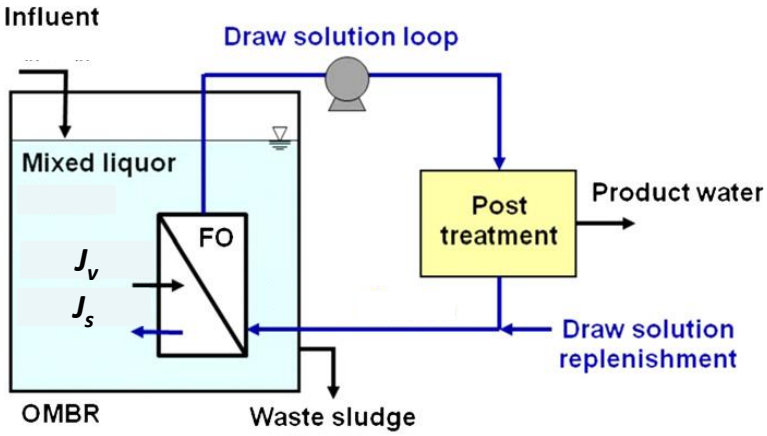

Figure 2-2 Schematic of an osmotic membrane bioreactor (reproduced from Ref. (Lay et al., 2012a) with copyright permission).

Compared to an MBR using porous MF or UF membranes, the OMBR has a higher removal efficiency to a wide spectrum of pollutants due to the high-rejection FO membranes (Achilli et al., 2009b; Alturki et al., 2012; Xie et al., 2012a). It was also reported that less fouling was observed in the FO process, probably due to the low flux condition and the special characteristics (e.g., roughness and hydrophilicity) of the used FO membrane (Cornelissen et al., 2008; Achilli et al., 2009b; Lay et al., 2010; Lay et al., 2012a). The cleaning efficiency is also expected to be higher in OMBR as a result of the mild FO fouling. Achilli (Achilli et al., 2009b) compared the fouling behavior between the OMBR and conventional MBR, showing that the OMBR required less backwashing frequency while maintaining a high water flux recovery rate.

A problem faced by OMBR technology is severe salt accumulation in the bioreactor, which is attributed to the continuous concentration of influent salts as well as the

reverse diffusion of draw solutes. Salinity build-up in the bioreactor not only reduces the water flux but also has a potential inhibition and toxicity effect on the microbial communities (Alturki et al., 2012). According to Xiao's modeling work (Xiao et al., 2011), salt accumulation in an OMBR can be controlled by the OMBR operating conditions (the hydraulic retention time/sludge retention time ratio) and membrane selectivity (salt permeability/water permeability ratio). From a membrane optimization point of view, the membrane selectivity was suggested to be $B/A \sim 0.1\pi_{feed}$ (Xiao et al., 2011). It is noticed that the types of FO membranes available currently are still very limited, which cannot offer enough choices for optimal OMBR operation yet. Meanwhile, most of the current OMBR studies are using the commercial cellulose triacetate FO membranes. This material is susceptible to biological degradation. Thus, future research should be focused on fabrication of robust membranes to meet the development of OMBR technology.

2.1.2.2 FO desalination

Due to the freshwater scarcity and booming water demand, seawater and brackish water desalination has become an important water source in many countries and areas such as Singapore, the Middle East, etc. Among the desalination technologies, membrane-based technologies have grown fast since the 1960s and become dominant over thermal technology in new desalination plants due to the lower energy consumption (2-6 kWh/m^3) (Subramani et al., 2011). Nevertheless, even with the most energy-efficient RO desalination technology, the energy consumption due to high pumping pressure still needs to be cut down considering the rising energy cost (Subramani et al., 2011). Moreover, water recovery in RO desalination is typically 35%-50% (McCutcheon et al., 2005b). Disposal of the concentrated RO brine is of concern because regulations on brine discharge have become more stringent. Recently, FO desalination has been considered to solve these problems.

In FO based desalination, an osmotic pressure difference instead of hydraulic pressure is used as the driving force to concentrate the seawater, whereby it is possible to greatly minimize the pumping pressure. Where a high osmotic pressure DS is economically available, FO could be a low-energy desalination technology.

Fouling and scaling are also supposed to be more reversible in FO desalination due to the less compact fouling layer formed (Mi and Elimelech, 2010b; a). Early FO desalination studies can be traced back to the 1970s when the FO extractor was proposed to produce drinking water from seawater (Kessler and Moody, 1976; Moody and Kessler, 1976). It has undergone rapid development recently owing to the progress in draw agents and process design. For example, an FO desalination system using ammonium bicarbonate as the draw solute is shown in Figure 2-3. The diluted draw solution after the FO unit will be heated to decompose the draw solute and to produce fresh water. Then the released ammonia and carbon dioxide can be reused to regenerate the draw solution (McCutcheon et al., 2005a; McCutcheon et al., 2005b; McCutcheon et al., 2006; Patel-Predd, 2006; McGinnis and Elimelech, 2007; Low, 2009). A pilot plant based on this approach has been built by Oasys Water recently (Elimelech, 2007). Other hybrid FO desalination processes, e.g., FO/RO (Bamaga et al., 2009; Choi et al., 2009; Bamaga et al., 2011), FO/MD (Martinetti et al., 2009), FO/NF (Tan and Ng, 2010; Zhao et al., 2012a) and FO/UF (Ling and Chung, 2011a) were reported as well. To promote the economic feasibility, regeneration-free FO based desalination techniques were also proposed, such as controlled dilution of a seawater feed by impaired water to reduce the energy consumption in RO desalination, controlled dilution of high-salinity RO brine before discharge, and osmotic backwashing, etc. (Hoover et al., 2011; Phuntsho et al., 2011; Yangali-Quintanilla et al., 2011; Phuntsho et al., 2012a; Phuntsho et al., 2012b).

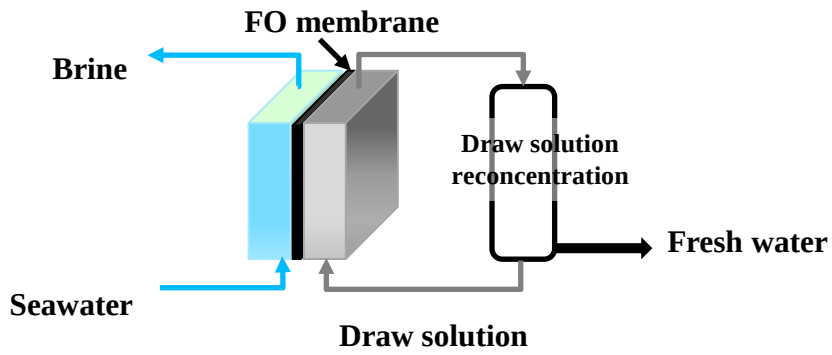

Figure 2-3 Schematic of an FO desalination system (reproduced from Ref. (McCutcheon et al., 2005b) with copyright permission).

Further development of FO desalination technology calls for more breakthroughs in membrane materials. First of all, a salt rejection as high as that of seawater RO membranes will be a crucial criterion, considering the high concentration feed and draw solutions. In addition, the high salinity on the feed side will greatly reduce the osmotic driving force. Optimization of the membranes for higher water flux is necessary for economic practicability.

2.1.2.3 Water purification

FO based water purification is one of the relatively established fields among the FO applications for which commercialized products have been available in the market. Similar to RO membranes, FO membranes have high rejection to particles and solutes. Thus with suitable draw agents, high quality water can be produced. The operating condition with low or even zero hydraulic pressure also makes the system design relatively simple and flexible. In small scale, direct purification from contaminated water sources can be performed by FO devices when potable water is lacking. For example, HTI has commercialized several portable FO filtration units (e.g., SeaPack, HydroPack, Expedition, LifePack, Hydrowell and X-Pack, see www.htiwater.com). These products are basically FO membrane pouches that contain a sport drink syrup or powder. By dipping the FO unit in water sources, water diffuses into the pouch and generates a clean energy drink (Cohen, 2004; Gourley, 2006; Bolto et al., 2007). Impurities like particles, colloids, bacteria, viruses will be effectively removed without hydraulic pressure or chemical addition. Purification of other contaminated water sources via FO has been studied as well, e.g., wastewater reuse in space missions (Cath et al., 2005a; Cath et al., 2005b; Cartinella et al., 2006; Gormly et al., 2009), water recovery from sewage concentration (Lutchmiah et al., 2011), potable water extraction from brackish water (Wallace et al., 2008), etc. In industry, an oilfield wastewater reclamation system (named Green Machine) for reclaiming drilling wastewater from gas exploration operations for hydraulic fracturing has been designed by HTI (Schultz, 2010). More applications including dewatering of toxic landfill leachate, concentrating digester waste streams, and other industrial and municipal wastewaters are studied by this company as well. Generally speaking, FO

technology is able to recover purified water from a variety of water sources. To maintain the consistent water flux and quality in the long run, membranes with high chemical and biological stability, as well as high fouling resistance will be preferable.

2.1.2.4 Osmotic power generation

A schematic of osmotic power generation via PRO is shown in Figure 2-4. In this process, freshwater and pressurized seawater are synchronously pumped into a membrane module where the two streams are separated by a semi-permeable membrane. As water permeates into the draw solution, a portion of the diluted seawater will be depressurized by a hydroturbine to generate power, while the rest of seawater goes to a pressure exchanger to pressurize influent seawater (Achilli and Childress, 2010; She et al., 2012b). It is well-known that the osmotic power (namely blue energy) exists in a huge amount worldwide. For example, the osmotic pressure of seawater is about 25 bar and that of RO brine is about 50 bar. A great amount of energy can be harvested by controlled mixing of salt water with freshwater, e.g., about 1600 TWh/year of osmotic power could be produced in the estuaries globally (Achilli and Childress, 2010).

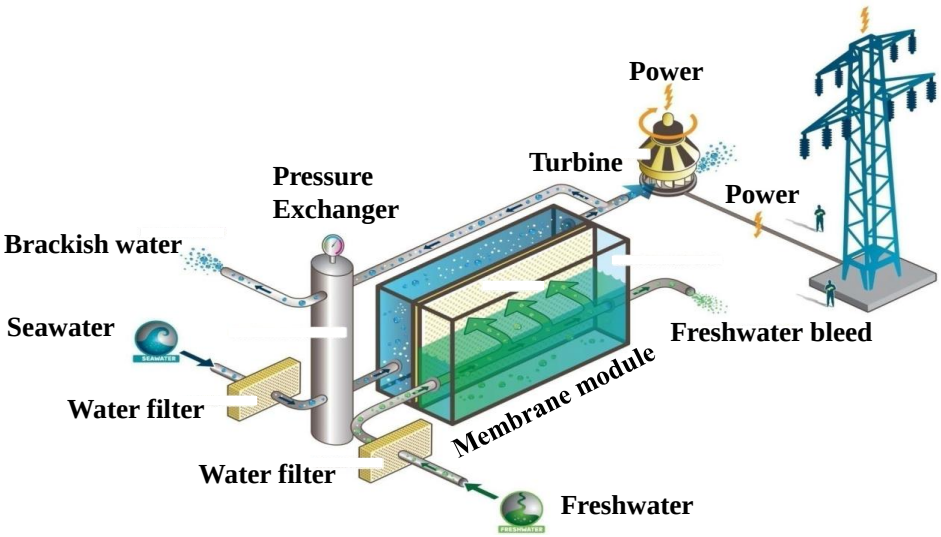

Figure 2-4 Schematic of an osmotic power plant (reproduced from www.statkraft.com).

Studies of osmotic energy exploitation were started in the early 1950s when Pattle

(Pattle, 1954) proposed a hydroelectric pile, in which electric power was produced by mixing freshwater and salt water. More research was conducted from the 1970s on (Gregor, 1974; Levenspiel and De Nevers, 1974; Loeb, 1975; Norman, 1975; Loeb, 1976; Loeb et al., 1976; Mehta and Loeb, 1978; Mehta and Loeb, 1979; Reali, 1980; 1981); however, low power density was observed in these early studies and hampered the development of osmotic power plants for a few decades. This is mainly because efficient PRO membranes were not available at that time (Lee et al., 1981; Vigo and Uliana, 1986). In 2001, the Norwegian state power company Statkraft and research partners developed two types of PRO membranes, i.e., thin film composite membranes and asymmetric cellulose acetate membranes (Gerstandt et al., 2008), and started a pioneering PRO power plant in 2003 on the Norwegian west coast (Aaberg, 2003). Potential power densities of the TFC and asymmetric membranes were reported to be 5 W/m^2 and 1.3 W/m^2, respectively (Gerstandt et al., 2008; Skilhagen et al., 2008). Later in 2009, an osmotic power plant was launched at Tofte on the Oslo fjord, Norway (Patel, 2010). Other research using optimized FO membranes was also reported recently, showing even better results (power density >10 W/m^2) (Chou et al., 2012). Increasing attention has been paid to PRO studies from membrane fabrication to system design (Post et al., 2007; Achilli et al., 2009a; Thorsen and Holt, 2009; Yip and Elimelech, 2011; Chou et al., 2012; Kim and Elimelech, 2012; She et al., 2012b), which are supposed to greatly promote the practical application of PRO technology.

Nevertheless, most of the PRO membranes currently available were designed to have thin and highly porous supports for high osmotic flux. Ideally, the peak power density can be reached at $\Delta P = \Delta\pi/2$. However, membrane deformation under such a high pressure may occur, which would destroy the membrane integrity and reduce the flow channels of the feed solution (She et al., 2012b). Therefore, membranes with high mechanical strength will be important in PRO applications.

2.2 Internal concentration polarization

Under ideal FO conditions, the FO membrane is assumed to be completely impermeable to solutes; thus, water transports through the membrane under the

osmotic pressure difference while all solutes are retained (Moody and Kessler, 1976). Meanwhile, perfect mixing is provided to maintain identical concentrations between the bulk phase and the solution-rejection-layer interface (Moody and Kessler, 1976). The corresponding osmotic pressure profile is shown in Figure 2-5. Here the membrane works as a mere barrier to reject solutes and there is no resistance to mass diffusion on either the FS side or DS side. Therefore, the effective osmotic driving force will be $\Delta\pi$ between the bulk FS and DS. The osmotic water flux J_v through membrane is proportional to $\Delta\pi$ in the bulk phases, as shown in the following equation (McCutcheon and Elimelech, 2006):

$$J_v = A(\pi_{draw} - \pi_{feed}) \tag{2-3}$$

where A is the water permeability of membrane, π_{draw} and π_{feed} are the osmotic pressures of the DS and FS, respectively.

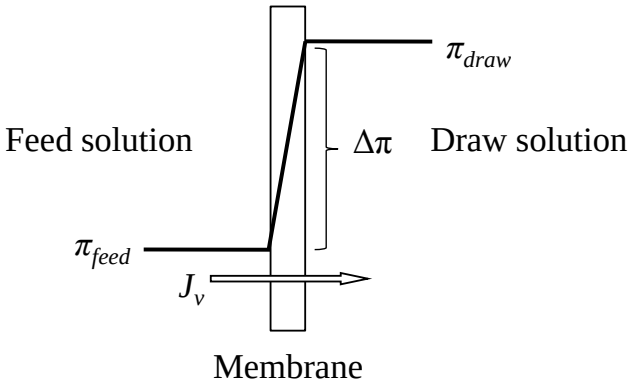

Figure 2-5 Osmotic pressure profile across the membrane in an ideal FO process (reproduced from Ref. (Cath et al., 2006) with copyright permission).

In prior FO studies, however, the experimental water flux appeared to be much lower than the product of membrane water permeability and osmotic pressure difference of the bulk solutions (Equation 2-3) (Lee et al., 1981; McCutcheon et al., 2005a; Cath et al., 2006; McCutcheon et al., 2006). Moody derived three mathematical models for an example of an FO extractor to explain this lower-than-expected water flux (Moody and Kessler, 1976). It was revealed to be the result of concentration polarization and reverse diffusion of the solute.

Concentration polarization is a universal problem existing in all membrane processes for liquid separation (Sablani et al., 2001). With an applied driving force, e.g., a hydraulic pressure for pressure-driven processes or an osmotic pressure difference for FO, water permeates through the membrane while the transport of solutes is hindered. The retained solutes will accumulate at the membrane surface and form a boundary layer (Mulder, 1996). This phenomenon of retained components accumulating and permeating components being depleted at the membrane surface is referred to as concentration polarization (Strathmann, 1981; Mulder, 1996). In the FO process, concentration polarization would exist externally on both sides of the membrane if solutes are present in both the FS and DS. The accumulation of solutes on the FS side is referred to as concentrative external concentration polarization (concentrative ECP) as in pressure-driven processes, while the depletion of solutes on the DS side due to water permeation is referred to as dilutive external concentration polarization (dilutive ECP) (McCutcheon and Elimelech, 2006).

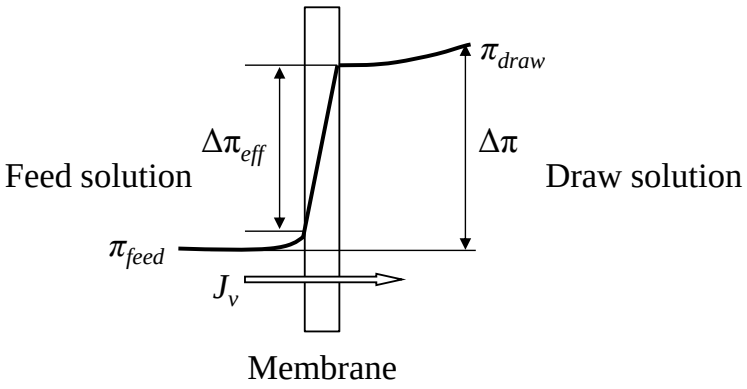

Figure 2-6 Osmotic pressure profile across the membrane in the presence of ECP (modified from Ref. (McCutcheon and Elimelech, 2006) with copyright permission).

Figure 2-6 illustrates the osmotic pressure profile when ECP occurs. ECP can reduce the effective driving force $\Delta\pi_{eff}$ and leads to lower water flux than that estimated with $\Delta\pi$ in bulk phase. In pressure-driven processes, the influence of ECP on membrane performance has been well studied and modeled by prior studies (Strathmann, 1981; Mulder, 1996; Elimelech and Bhattacharjee, 1998; Sablani et al.,

2001), which may have a similar effect in the FO process. Nevertheless, it is found that the influence of ECP on the FO flux is relatively small, which could be mitigated by controlling the flux and mass transfer coefficient. Effective measures to reduce ECP may include increasing cross-flow velocity, using spacers, vibrations, ultrasound, etc. (Lee et al., 1981; Sablani et al., 2001; Cath et al., 2006).

A more severe problem contributing to the low water flux in the FO process is internal concentration polarization. In the ideal case, perfect mixing should be provided on the membrane surface to homogenize the solutions and to mitigate the effect of concentration polarization. Under FO conditions, however, concentration polarization also takes place within the membrane as the membrane usually has a porous support layer beneath the selective layer for handling strength (McCutcheon et al., 2005b). This porous support tends to resist mass diffusion and thus forms a concentration polarization layer within it. This phenomenon is observed uniquely in osmotically driven membrane processes and is referred to as internal concentration polarization (Mehta and Loeb, 1978; Loeb et al., 1997; McCutcheon and Elimelech, 2006).

In the FO process, the asymmetric semi-permeable membrane can be loaded with the active rejection layer either facing the DS (the AL-DS orientation, Figure 2-7(a)) or facing the FS (the AL-FS orientation, Figure 2-7(b)). In the AL-DS orientation, water permeates from the FS through the membrane rejection layer while the feed solutes transport into the porous support due to convection. As the feed solutes are retained by the semi-permeable rejection layer, a boundary layer is formed within the support. On the other hand, the diffusion of solutes back into the bulk phase will be hindered by the support. This phenomenon is referred to as concentrative ICP (McCutcheon et al., 2005b; McCutcheon and Elimelech, 2006). ICP also takes place in another orientation. In the AL-FS orientation, water permeates through the rejection layer and dilutes the draw solution in the support layer. Draw solutes have to diffuse towards the rejection-layer-support interface to restore the osmotic driving force; however, this movement will be hindered by the support layer and leads to depletion of draw solutes near the rejection-layer-support interface, which

is referred to as dilutive ICP (McCutcheon et al., 2005b; McCutcheon and Elimelech, 2006). Both concentrative and dilutive ICP may lead to a severe reduction in the osmotic pressure difference across the rejection layer (represented by $a\ \Delta\pi_{eff} < \Delta\pi$ as in Figure 2-7). According to Equation 2-3, the water flux should increase linearly with the osmotic pressure difference when the ECP is minimized; however, many studies showed a non-linear dependence of flux on $\Delta\pi$, i.e., the discrepancy between the experimental and predicted flux tended to increase under a higher osmotic driving force (McCutcheon et al., 2005b; Gray et al., 2006; Tang et al., 2010; Xu et al., 2010; Chanukya et al., 2012). This is because the influence of ICP is enhanced at higher water flux levels. The ICP phenomenon can be considered as hindered solute diffusion in the membrane support layer, for which the resistance can be represented by a K (or $1/K_m$) value in modeling studies (Lee et al., 1981; Loeb et al., 1997; Loeb, 2002; Gray et al., 2006; Tang et al., 2010).

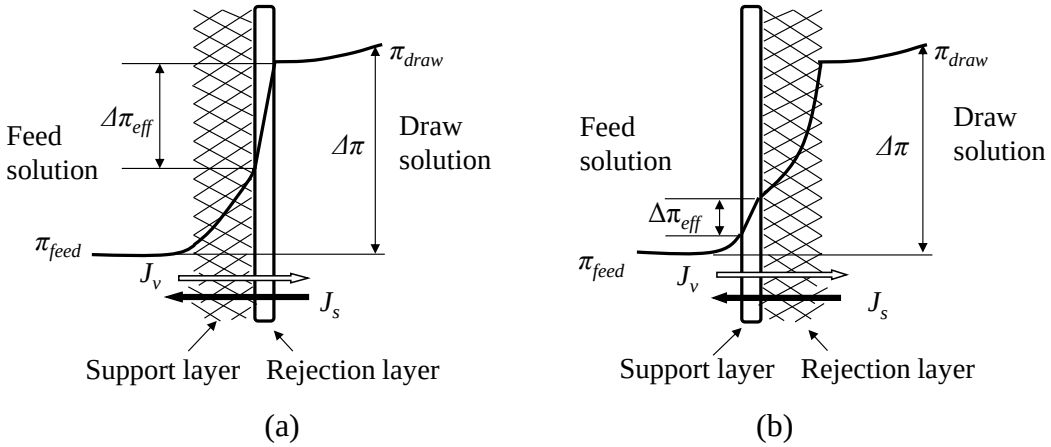

Figure 2-7 Osmotic pressure profiles across an FO membrane in the (a) AL-DS and (b) AL-FS orientations (reproduced from Ref. (Cath et al., 2006) with copyright permission).

As the FO membranes are usually not ideally impermeable to solutes, the water flux J_v would be accompanied by a solute flux J_s (Tang et al., 2010). If identical solutes are used in FS and DS, J_s will be in the opposite direction to J_v. Leakage of draw solutes can enhance the ICP by increasing the FS concentration (in the AL-DS orientation) or reducing the DS concentration (in the AL-FS orientation) near the rejection layer and thus further reducing $\Delta\pi_{eff}$. Even when pure water is used as the

feed and the AL-DS orientation is adapted, which was expected to have insignificant ICP (Gray et al., 2006; Alturki et al., 2012), concentrative ICP still can take place due to the reverse diffusion of draw solutes. Therefore, the reverse diffusion of draw solutes is considered as one of the most important problems in osmotically driven membrane processes. Several studies have been carried out to understand the effect of the solute diffusion on the FO performance. Lee (Lee et al., 1981) first pointed out the enhancement of ICP by solute reverse diffusion. An ICP model combining the effect of the solute reverse diffusion on the predicted FO water flux was developed by Loeb (Loeb et al., 1997), which is widely adapted in many FO studies today. Recently, Tang (Tang et al., 2010) developed a model to evaluate the solute flux in FO.

Several fundamental studies on the influence of ICP and ECP have been carried out (Loeb et al., 1997; McCutcheon and Elimelech, 2006; McCutcheon and Elimelech, 2007; Tan and Ng, 2008; Tang et al., 2010). It is proved that ICP is a major factor contributing to the FO flux reduction, especially under conditions of high flux and/or high DS concentration (Tang et al., 2010). Moreover, unlike ECP that can be mitigated by optimizing external hydraulic conditions, ICP was found to be less affected by external shear or turbulence due to the protection of the membrane support layer (Lee et al., 1981; Qin et al., 2009). Approaches to characterize ICP (e.g., electrochemical impedance spectroscopy (Gao et al., 2012), network modeling (Li et al., 2011c), computational fluid dynamics simulations (Gruber et al., 2011), etc.) have been proposed. According to prior studies, membrane optimization would be an efficient and critical task to reduce ICP.

2.3 Influential factors for FO performance

There are several factors that play important roles in the FO performance. From the process optimization point of view, these factors can be attributed to the FO membrane, the draw solution and the operating conditions. In this section, the influence of key factors is summarized to find out their relationships with membrane properties. Furthermore, this review is to indicate how to enhance FO performance by membrane improvement.

2.3.1 Membrane properties

Membranes used in the FO processes typically comprise a semi-permeable rejection layer and a porous support layer that has no rejection to solutes. The influence of the support layer and rejection layer on FO performance is individually discussed in the following.

2.3.1.1 Membrane support layer

A critical and unique problem in the FO process is the ICP that causes a dramatic reduction in the osmotic driving force across the rejection layer as well as the obtainable water flux. The influence of the membrane support on ICP has been identified in several FO studies. Researchers (McCutcheon et al., 2005b; Garcia-Castello et al., 2009) conducted a comparison between one commercial FO membrane and RO membranes under FO conditions. It was found that notably higher water flux was achieved by the FO membrane despite its slightly lower water permeability than that of the RO membranes. In microscopic examination of the membrane structure, the asymmetric FO membrane showed a small thickness of ~50 μm. An open reinforcing polyester mesh was embedded within the semi-permeable cellulose triacetate layer to minimize its contribution to the overall thickness. In contrast, the evaluated RO membranes, with either a polyamide-base thin film composite structure or cellulose acetate asymmetric structure, had an asymmetric polymer layer (~50 μm thick) and were further supported with a thick reinforcing fabric (~90 μm thick). This structure was to provide sufficient mechanical strength under the high pressure RO conditions. During the FO process, however, the thick and dense supports of the RO membranes resisted the solute diffusion between the bulk solution and rejection-layer-support interface. As a result, severe ICP occurred for the RO membranes and the membranes showed poor FO water flux compared to that of the FO membrane.

Modeling of concentration polarization within the membrane support in the FO process was first proposed by Lee (Lee et al., 1981). An ICP model was then developed by Loeb to predict the FO water flux in the presence of a porous support layer (Loeb et al., 1997). It was revealed that the support layer primarily affected

ICP by several structural characteristics, i.e., thickness, porosity and tortuosity of the support. A parameter K_m can be used to measure the mass transfer coefficient in the support layer (Tang et al., 2010).

$$K_m = \frac{D_{eff}}{l_{eff}} = \frac{D\varepsilon}{l\tau} = \frac{D}{l\tau/\varepsilon} = \frac{D}{S} \tag{2-4}$$

where D_{eff} and D are the effective and theoretical solute diffusion coefficients, respectively; l_{eff} and l are the effective and actual thickness of the support layer, respectively; τ is the tortuosity of the support layer; ε is the porosity of the support layer and S is the structural parameter of the membrane support. In some FO studies (Lee et al., 1981; Loeb et al., 1997; Gray et al., 2006), a K value was also used to represent the resistance of the porous support to solute diffusion, which is equal to the reciprocal of K_m.

The structural parameter, S, is a critical parameter to assess the ICP propensity of FO membranes. The physical meaning of this parameter can be interpreted as the thickness of the ICP boundary layer (Tang et al., 2010). It can be seen from Equation 2-4 that the mass transfer coefficient of the FO support increases with a higher diffusion coefficient of the solute, while it decreases with a larger structural parameter. Therefore, FO membranes with a small S value are preferable, which means that the concentration at the rejection-layer-support interface can be restored more easily by mass diffusion from/toward bulk solution (Yip et al., 2011). It has been noticed that the ideal FO support layer shall be thin, highly porous, and have minimal tortuosity to reduce the S value (McCutcheon and Elimelech, 2007; Tan and Ng, 2008; Bui et al., 2011; Tiraferri et al., 2011). In addition, a finger-like pore structure of the substrate is likely to have smaller S value than that of the sponge-like structure but further investigation is still needed (Yip et al., 2010; Widjojo et al., 2011). The above findings explain the poor FO performance of conventional RO membranes. In the RO process, the water flux is mainly governed by the rejection layer while the support layer has minor influence on the flux behavior. Thus, the support layer is designed to be thick and compact to withstand the high hydraulic

pressure. This kind of supports has a large thickness, high tortuosity and low porosity. Correspondingly, the RO membranes encounter severe ICP under FO conditions due to the inherently large *S* value (McCutcheon and Elimelech, 2007).

Another important property of the FO support layer is its hydrophilicity, in addition to the structural parameter. According to McCutcheon (McCutcheon and Elimelech, 2008), an FO support with poor wetting tended to have vapor or air trapped in the pores, which blocked the water pathway and reduced the water continuity (wetted porosity (Bui et al., 2011)), thereby enhancing the ICP. Arena (Arena et al., 2011) modified two commercial TFC RO membranes by coating hydrophilic polydopamine onto the membrane support. A significantly higher FO water flux was achieved by the modified membranes. Widjojo (Widjojo et al., 2011) compared TFC FO membranes of which the substrates were prepared with different casting solutions. It was reported that blending of sulphonated material in the substrate could reduce the contact angle of the substrate from 77 ° to 15-20 °, which led to an improved FO water flux.

According to the above, it can be summarized that the support layer of an FO membrane should have a structural parameter as small as possible. As the fabrication technology of FO membranes is still under development at this point, more research on the effects of related parameters, i.e., porosity, tortuosity and thickness of support layer need to be conducted in the future. Other properties of suitable substrates may also include hydrophilicity, sufficient mechanical strength and high stability in harsh operating conditions, etc., which should be improved during membrane fabrication as well.

2.3.1.2 Membrane rejection layer

In membrane processes, separation of mixed components in the feed stream is achieved as the membranes can transport some components from the feed stream more readily than the other components (Mulder, 1996). The primary parameters to evaluate the separation efficiency of membranes are their permeability and selectivity. Similarly, water flux is one of the key parameters to determine the

performance of an FO process. According to Equation 2-3, the FO water flux is equal to the product of the membrane water permeability and the osmotic driving force. Therefore, increasing the intrinsic water permeability of an FO membrane is expected to achieve a better FO water flux. For example, in a comparison study by Yip (Yip et al., 2011), membranes prepared with identical support layers but different permeabilities showed different FO water fluxes. Increasing the membrane water permeability from 1.63 L/(m^2 h bar) to 4.35 L/(m^2 h bar) resulted in a higher FO water flux. Nevertheless, the FO water flux does not linearly increase with membrane water permeability due to ICP. At a high water flux level, dilution of the draw solution (AL-FS) or concentration of the feed solution (AL-DS) will be enhanced inside the support layer that inhibits the increase of the water flux.

Membrane selectivity is another critical parameter in osmotically driven membrane processes. In principle, efficient FO membranes should have high rejection to draw solutes in order to maintain a high osmotic driving force across the membrane. In the case of low-rejection membranes, the reverse diffusion of draw solutes through membrane could significantly reduce the osmotic driving force and further exacerbate the concentrative/dilutive ICP, resulting in water flux decline. According to prior research, the FO solute flux/water flux ratio is proportional to the membrane selectivity (i.e., the salt permeability/water permeability ratio) (Tang et al., 2010). Other adverse effects of low membrane selectivity were also reported. Diffusion of the draw solute, especially fouling precursors (Mg^{2+}, Ca^{2+}, etc.), into the feed solution may increase the fouling potential on the FS side (Zou et al., 2011; She et al., 2012a). In the OMBR, draw solute leakage also contributed to salinity build-up in the bioreactor, which would have inhibition or toxicity effects on the microbial community and cause deterioration of biological activity (Xiao et al., 2011; Alturki et al., 2012). Other concerns include contamination of the feed product, high cost of draw solution dosing, etc. On the other hand, salt flux from the FS to DS will occur as well if different solutes exist in the FS and DS (Hancock and Cath, 2009; Hancock et al., 2011; She et al., 2012a). In general, diffusion of feed solutes into the draw solution may have a negative effect when downstream processes (RO, NF, MD, etc.) are combined to regenerate the draw solution, or the

diluted draw solution is a product for further use, but it may have a benefit due to mitigation of the salinity build-up in feed, which deserves more investigation. In addition, membrane rejection to contaminants, e.g., pharmaceuticals (Jin et al., 2012a), boron and arsenic (Jin et al., 2011; Jin et al., 2012b) is also of concern as it determines the contaminant removal efficiency of the FO process (Jin et al., 2011; Jin et al., 2012a; Jin et al., 2012b).

According to above investigation, the rejection layer of FO membranes should have a high water permeability and high selectivity (low solute permeability) (McCutcheon and Elimelech, 2007). Nevertheless, the membrane water permeability and solute permeability are usually interrelated (Geise et al., 2011). Membranes with a high affinity to water are likely to have a high affinity to the solute as well. The trade-off between water permeability and selectivity has been demonstrated in FO membrane fabrication (Saren et al., 2011; Yip et al., 2011; Zhang et al., 2011b). In the FO process, although high water permeability tends to increase the water flux, a coupled high salt permeability could induce severe salt leakage and cut down the water flux. It has been found that the ratio of the reverse salt flux/water flux in the FO process is determined by the intrinsic properties of the membrane rather than operating condition, although salt flux is proportional to the effective draw solution concentration. This ratio, referred to as the specific reverse salt flux or reverse flux selectivity in some studies, is proportional to the ratio of the solute permeability/water permeability of the membrane (Tang et al., 2010). It can be used to evaluate the efficiency of the FO separation process, i.e., the mass of draw solute leakage with a unit of water permeate. Since both the water flux and salt flux/water flux ratio are important for an FO process, the optimal combination between membrane permeability and selectivity should be determined. Thus, it is worthwhile to conduct more studies on these competing mechanisms and their relationships with operating conditions.

2.3.2 Draw solutes

In the FO process, draw solutes work as the “engine” to provide the osmotic driving force for water flux. Thus, FO performance greatly depends on the properties of the

draw solutes. According to the literature, inorganic salts (e.g., NaCl, $MgCl_2$, NH_4HCO_3) are commonly used as draw solutes. Permeation of this kind of inorganic draw solute through an FO membrane and their FO performance have attracted wide attention (Hancock and Cath, 2009; Achilli et al., 2010; Hancock et al., 2011). Recently, new draw solutes with advanced properties were employed in FO studies (Chekli et al., 2012). These draw solutes are summarized and compared in Table 2-1.

Table 2-1 Summary and comparison of recently reported draw solutes for FO process

Category	Draw solutes	Advantages	Disadvantages	References
Inorganic electrolytes	NaCl, $MgCl_2$, $CaCl_2$, KCl, Na_2SO_4, $MgSO_4$, etc.	• Commercially available at low cost. • Natural sources may be available, such as seawater, brackish water, RO brine, etc.	• Relatively high solute permeability.	(Hancock and Cath, 2009; Achilli et al., 2010; Hancock et al., 2011; She et al., 2012a)
Thermolytic solutes	NH_4HCO_3, $(NH_4)_2CO_3$, etc.	• Draw solute can be effectively separated from water by decomposing upon moderate heating.	• Draw solute recovery relies on proximity of economic heat source.	(McCutcheon et al., 2005b; McCutcheon et al., 2006; McGinnis and Elimelech, 2007; McGinnis et al., 2007; Low, 2009)
Superparamagnetic nanoparticles (MNPs)	Magnetic iron oxide nanoparticles, dextran coated MNPs, poly(ethylene glycol) diacid-coated MNPs, 2-Pyrrolidone MNPs, triethylene glycol MNPs, polyacrylic acid MNPs, etc.	• Feasibility to be functionalized for good solubility and high osmotic pressure. • Low permeability in membrane. • Easy recovery of draw solute by magnetic field or UF with low energy consumption.	• Aggregation of MNPs. • High ICP propensity. • Possible deterioration of magnetic properties of MNPs during recycle. • Trend to adhere on supporting fabric.	(Ling et al., 2010; Bai et al., 2011; Ge et al., 2011; Kim et al., 2011; Li et al., 2011d; Ling and Chung, 2011b; a; Liu et al., 2011)

Category	Draw solutes	Advantages	Disadvantages	References
Organic solutes and macromolecules	Fructose, glucose, sucrose, polyethylene glycol, 2-Methylimidazole-based organic compounds, poly(acrylic acid) sodium, etc.	• Possibility to be functionalized for good solubility and high osmotic pressure. • Low solute permeability. • Easy recycle by low pressure membrane process.	• High ICP potential due to high viscosity and low diffusion coefficient. • Possibly high cost.	(Petrotos et al., 1998; Yen et al., 2010; Ge et al., 2012a; Ge et al., 2012b; Sarp et al., 2012)
Hydrogel		• Highly concentrated hydrophilic groups. • Ability to draw large volume of water. • Properties, e.g., hydrophilicity, can transit via environmental stimuli that release water at low energy cost.	• High ICP potential.	(Li et al., 2011a; Li et al., 2011b)
Fertilizers		• Applicability in FO desalination. Diluted fertilizer solution can be directly used for fertigation and thus the process is reconcentration-free.	• Concerns on irrigation water quality, e.g., ionic species, nutrient concentrations. • Fouling potential.	(Phuntsho et al., 2011; Phuntsho et al., 2012a; Phuntsho et al., 2012b)

The criteria for draw solute selection have been studied by a few researchers (McCutcheon et al., 2005b; Achilli et al., 2010; Kim et al., 2012). Achilli (Achilli et al., 2010) proposed a protocol to screen efficient draw solutes among a variety of inorganic compounds. This protocol included high osmotic pressure, high water solubility, and minimal reverse diffusion of the draw solute (small solute permeability). Other concerns included technologies for draw solute separation and recycle, toxicity, compatibility with membrane material, dosing cost, etc.

The osmotic pressure of the draw solution is a function of the solute molar concentration and the number of species dissociated in the solution (Equation 2-1) (Mulder, 1996). Therefore, solutes with small molecular weight, high dissociation degree and high water solubility would be preferred as they can provide a high osmotic driving force. NaCl is such a solute and is widely used in FO studies. According to Equation 2-4, the mass transfer coefficient K_m increases with the diffusion coefficient of the draw solute. As small molecules usually have higher diffusion coefficients, they are supposed to diffuse more easily through the membrane support (Gray et al., 2006). In contrast, draw solutes containing large hydrated ions (e.g., multivalent electrolytes, large molecules) tend to have a lower diffusivity and higher viscosity. More severe ICP may occur with this kind of draw solutes when the porous support layer is placed against the draw solution (AL-FS) (Zhao and Zou, 2011b). Besides, solutes such as magnesium salts and calcium salts could act as fouling or scaling precursors (Achilli et al., 2010; Zou et al., 2011; She et al., 2012a). A high concentration of these solutes should be avoided when the system has a high fouling/scaling propensity. On the other hand, large molecules usually have lower permeability through the membrane and thus can minimize the reverse diffusion (Achilli et al., 2010). Several advanced draw solutes (e.g., macromolecules, superparamagnetic nanoparticles, hydrogels) were studied in view of their high retention by membrane. These large-molecule draw solutes seem to be advantageous in certain cases; however, a high ICP potential will be a problem to be considered.

Due to the aforementioned trade-off relationships, selection of the draw solute is

considered to be one of the main challenges in FO technology. A promising solution to this problem is membrane optimization. As to the membrane support layer, reducing the structural parameter of the membrane support layer can effectively increase the mass transfer coefficient (Equation 2-4), thus alleviating the severity of the ICP when a large-molecule DS is used. Moreover, an optimal combination of membrane separation properties and draw solutes should be designed, e.g., RO-like membrane/NaCl DS, NF-like membrane/$MgCl_2$. However, few comprehensive studies integrating both FO membrane optimization and draw solute selection are found in this literature investigation.

2.3.3 Membrane orientation

In the FO tests, the asymmetric-structure membranes are orientated with the rejection layer facing either the draw solution or the feed solution, where concentrative ICP and dilutive ICP will take place, respectively (Section 2.2). Gray and McCutcheon (Gray et al., 2006; McCutcheon and Elimelech, 2006) studied the influence of concentrative and dilutive ICP on FO performance. It was revealed that membrane orientation played an important role on the FO flux behavior. Significantly lower water flux was achieved in the AL-FS orientation than in the AL-DS orientation, especially when a low concentration FS (e.g., pure water) was used. The influence of dilutive ICP is more severe than concentrative ICP. A similar trend has been reported in other FO studies.

Despite the potentially lower degree of ICP, the AL-DS orientation may not be a preferred configuration in some FO processes as it is susceptible to fouling. The membrane fouling behavior in the AL-DS and AL-FS orientations was compared by Tang (Tang et al., 2010). In the AL-DS orientation, foulants in the feed solution can easily enter the support and cause pore clogging. A cake layer formed within the support reduces the porosity and increases the tortuosity of the membrane support. As a result, the mass diffusion resistance of the support layer is drastically increased and the concentrative ICP is enhanced. Due to the pore clogging enhanced ICP, a more decline of the water flux was observed in the AL-DS orientation (Tang et al., 2010). In comparison, a more stable water flux was observed in the alternative AL-

FS orientation due to less fouling. A visual examination of these phenomena by direct microscopic observation has been reported by Wang (Wang et al., 2010c). Additionally, it was found that a lower rejection to contaminants in the feed solution was exhibited in the AL-DS orientation due to contaminant build-up near the rejection-layer-support interface (Jin et al., 2011; Xie et al., 2012b). Interestingly, a fouling layer (e.g., alginate) forming on the rejection layer in the AL-FS orientation would possibly enhance the rejection to contaminants (Jin et al., 2012b).

To solve the dilemma of either the high fouling potential in the AL-DS orientation or the severe dilutive ICP in the AL-FS orientation, an innovative FO membrane with a rejection layer on both surfaces would be an ideal design. Tang (Tang et al., 2011) published a modeling paper to predict the performance of such double-skinned FO membranes. In contrast to conventional single-skinned membranes, double-skinned FO membranes will have (1) a highly permeable and nonporous feed skin to reject foulants without a substantial contribution to the hydraulic resistance, and (2) a draw skin with a suitable combination of water permeability and solute rejection. According to the modeling results, it was suggested that an optimal double-skinned FO membrane should have an RO-like draw skin such as that needs for brackish water desalination while a low rejection NF-like feed skin. Besides, the support layer should have a mass transfer coefficient as high as possible to reduce ICP.

2.4 Synthesis of FO membranes

2.4.1 Commercial membranes for FO study

In early FO research, conventional semi-permeable membranes such as commercial RO membranes were studied due to their high permeability and selectivity in pressure-driven process; however, very low water flux was achieved as a result of severe ICP (Lee et al., 1981). These RO membranes typically comprised a thick and robust porous layer that has dense sponge-like pore structure. This support layer of RO membranes hinders solute diffusion between the bulk solution and the rejection-layer-support interface, reducing $\Delta\pi_{eff}$ across the rejection layer and leading to low FO water flux (McCutcheon et al., 2005b). In some studies (McCutcheon and

Elimelech, 2008; Tang and Ng, 2008), the low FO water flux was also attributed to hydrophobicity of the support layer since insufficient wetting could disrupt the water continuity and enhance ICP. Arena (Arena et al., 2011) modified the hydrophilicity of two TFC RO membranes (Dow Water & Process Solutions BW30 and SW30-XLE) by coating the support layer with hydrophilic polydopamine. An improved FO water flux was achieved by the modified membranes but was still not high enough (e.g., $J_v < 25$ L/(m^2 h) with 1.5 M NaCl DS in the AL-DS orientation) in view of their high water permeability. It was demonstrated that conventional RO membranes are not suitable for osmotically driven membrane processes.

Lack of effective FO membranes has been a bottleneck in FO technology for a few decades until commercial FO membranes were developed. Up to date, the only widely available commercial FO membranes are produced by HTI (Herron, 2005). Another two companies, Catalyx Inc. (Anaheim, CA) (2009c; 2009a; 2009b) and Oasys Water (Cambridge, MA) (2010; Pearce, 2010-2011), also announced the startup of FO membrane manufacture but commercial products are not widely available yet. According to newsletters (2010), the Oasys membranes were developed based on a thin film composite FO membrane, of which the lab-scale research has been published by Yip (Yip et al., 2010).

The FO membranes produced by HTI are cellulose triacetate (CTA) based integral asymmetric membranes. There are two embodiments of the HTI membranes, involving a thin mesh embedded within a CTA rejection layer (Figure 2-8(a)) or a loose non-woven fabric attached on the back of the CTA layer (Figure 2-8(b)) (Herron, 2005). To prepare these membranes, casting solution is applied onto the surface of a rotating drum to form a casting solution layer, followed by pulling an open woven mesh or a non-woven fabric on the drum surface so that the fabric is attached to the casting solution layer. The resulting membrane is immersed into a coagulant bath and forms an asymmetric FO membrane (Herron, 2005). The HTI FO membranes have been used in many osmosis-related research (Cath et al., 2005b; McCutcheon et al., 2005b; Cartinella et al., 2006; Gray et al., 2006; McCutcheon and Elimelech, 2006; McCutcheon et al., 2006; Ng et al., 2006; Achilli et al., 2009a;

Achilli et al., 2009b; Hancock and Cath, 2009; Mi and Elimelech, 2010a; Tang et al., 2010; Hancock et al., 2011; Zhao and Zou, 2011a; Boo et al., 2012; Chanukya et al., 2012; Li et al., 2012) as well as in industry (Cohen, 2004; Gourley, 2006; Hutchings et al., 2010; Schultz, 2010). Unlike commercial RO membranes, the structures of the HTI FO membranes have been optimized to have a high porosity in the support layer (both the cellulose triacetate layer and the reinforcing fabric), as well as a small overall thickness (Tang et al., 2010). These properties can significantly reduce the structural parameter of the support layer and thus minimize the effect of ICP. Thereby, substantially higher FO water flux can be obtained by the HTI FO membranes compared to that of the RO membranes (McCutcheon et al., 2005b; Ng et al., 2006; Tang and Ng, 2008; Garcia-Castello et al., 2009). Improved fouling resistance was also observed for the HTI membranes, probably owing to their smooth hydrophilic surface (Lay et al., 2010; Mi and Elimelech, 2010b). Nevertheless, the water permeability and salt rejection of these membranes still need to be enhanced. From a material point of view, cellulose triacetate membranes are susceptible to chemical, biological and thermal degradation, which may limit their applications under harsh conditions.

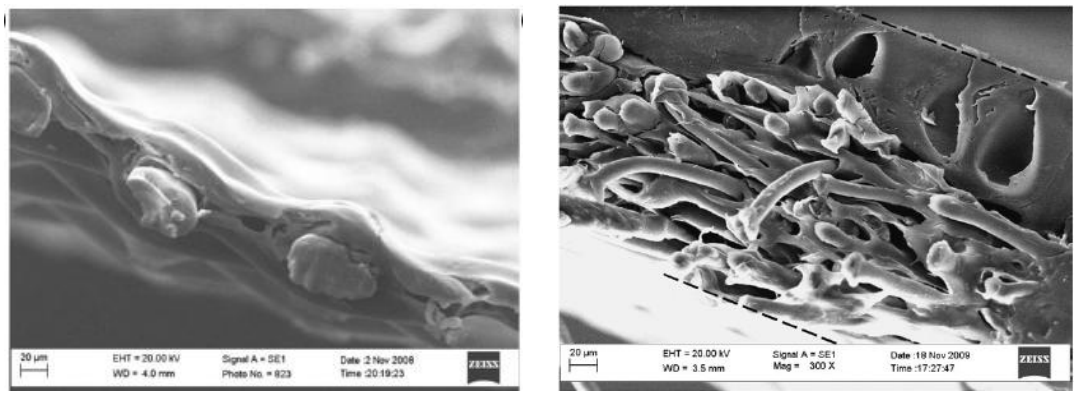

(a) (b)

Figure 2-8 Cross-sectional SEM images of commercial cellulose triacetate FO membranes (HTI, Albany, OR) with (a) embedded mesh (Tang et al., 2010) and (b) non-woven fabric (Wang et al., 2010b). Figures are reproduced from references with copyright permission.

2.4.2 Promising technologies for FO membrane fabrication

Presently, fabrication of FO membranes is still under development; consequently

commercial membranes are quite limited in types and materials. There is a significant gap between the demand and supply of high performance FO membranes. To meet the development of FO technology, a few studies have been carried out to fabricate membranes with improved FO performance. In this section, promising technologies of FO membrane fabrication are reviewed to gain insight for this study.

2.4.2.1 Integral asymmetric FO membranes

The development of integral asymmetric membranes by phase inversion was an important milestone in the field of membrane fabrication (Strathmann and Kock, 1977; Lonsdale, 1987). High performance polymeric membranes with various materials and separation properties (from MF to RO) as well as substrates for composite membranes have been prepared via this method since its invention. Phase inversion is a process whereby a polymer is transformed from a liquid state to a solid state in a controlled manner (Mulder, 1996). In this method, water-insoluble polymers (cellulose triacetate, polysulfone, polyacrylonitrile (PAN), etc.) are dissolved in a suitable solvent system to prepare a casting solution. The resulting dope is cast onto a support (e.g., glass plate, fabric, etc.) to form a liquid film (for flat-sheet membranes) or dispensed through a spinneret (for hollow fiber membranes); and liquid-liquid demixing is induced whereby the polymer solution separates into two phases. The polymer-rich phase solidifies and becomes the solid matrix, while the polymer-lean phase becomes the membrane pores (Strathmann and Kock, 1977). Phase separation can be induced by several mechanisms, e.g., non-solvent induced phase separation, solvent evaporation induced phase separation, vapor induced phase separation and thermally induced phase separation, etc. (Mulder, 1996; Van De Witte et al., 1996; Ulbricht, 2006). A large number of commercial membranes are prepared via non-solvent induced phase separation (Mulder, 1996). In this method, the polymer solution film is immersed into a coagulant bath that contains nonsolvent such as water or a mixture of solvent and water. Due to the exchange between solvent and nonsolvent, the polymer precipitates and becomes a membrane with a porous structure. The membranes prepared by phase inversion usually have an anisotropic structure comprising a thin

and dense skin on one surface or both surfaces, while the rest of the membrane is a porous matrix that serves as the support. The morphologies and pore structure of the membranes can be tuned by controlling the phase transition stage.

Integral asymmetric FO membranes prepared by phase inversion have been reported in a few studies. These membranes were typically prepared by a one-step process. The semi-permeable skin layer and porous support layer had identical chemical composition. Due to the limitations of the phase inversion method, the asymmetric membranes are typically prepared using linear and soluble polymers (Petersen, 1993). In particularly, cellulose esters are widely used among the reported asymmetric FO membranes (Su et al., 2010a; Su et al., 2010b; Zhang et al., 2010; Sairam et al., 2011; Su and Chung, 2011; Zhang et al., 2011b; Ong and Chung, 2012; Zhang et al., 2012c). Examples of these cellulose ester FO membranes are shown in Figure 2-9 (a) and (b). Several studies have been carried out to understand the formation and optimization of cellulose ester FO membranes. Su (Su et al., 2010b; Su and Chung, 2011) studied the effects of thermal annealing and bore fluid composition on the cellulose acetate (CA) hollow fiber microstructure and performance. Zhang (Zhang et al., 2010; Zhang et al., 2011b) studied the fundamentals of flat-sheet cellulose ester membrane formation via phase inversion by systematically changing the preparation conditions such as the casting substrates (Teflon and glass), non-solvent composition, annealing, etc. Ong (Ong and Chung, 2012) studied the influence of the solvent system on the CTA membrane pore structure and separation properties. Sairam (Sairam et al., 2011) studied fabrication of CA membranes with reinforcing nylon woven fabric. Other investigations on water and salt transport of cellulose ester polymers, as well as the correlation with hydrated free volume were carried out as well (Zhang et al., 2012c).

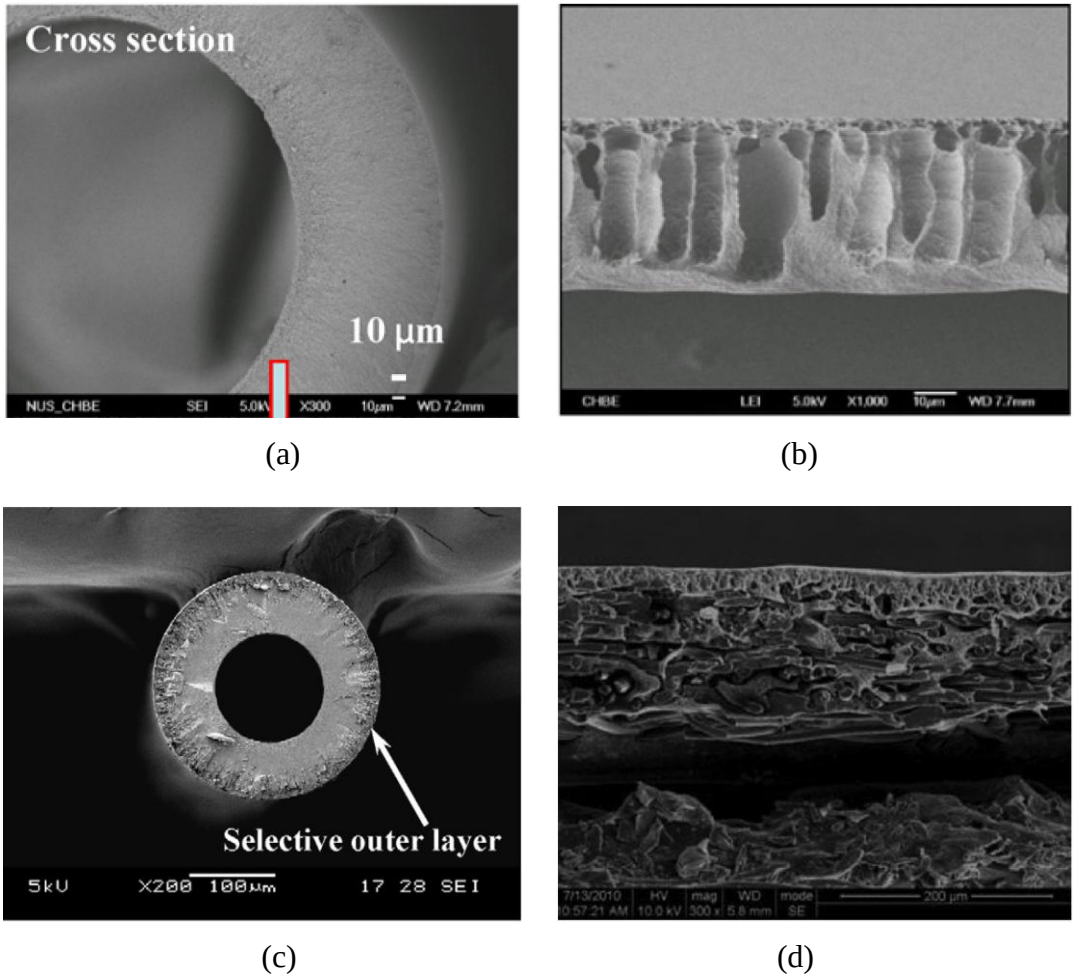

Figure 2-9 Cross-sectional images of integral asymmetric FO membranes. (a) CA hollow fiber (Su et al., 2010a). (b) Flat-sheet CTA membrane (Ong and Chung, 2012). (c) PBI hollow fiber (Wang et al., 2007). (d) Flat-sheet polyethersulfone (PES) membrane with a polyester fabric (Yu et al., 2011). Figures are reproduced from references with copyright permission.

A disadvantage of the cellulose ester membranes is their low resistance to biological, chemical and thermal degradation. Thus, operation with these membranes should be at ambient temperature within a pH range of 4-6.5 (Mulder, 1996). Their applications in bioprocesses such as the OMBR are limited as well. Therefore, attention was also paid to asymmetric membranes using high stability polymeric materials. Wang (Wang et al., 2007; Wang et al., 2009; Wang et al., 2011) reported polybenzimidazole (PBI) FO membranes with NF-like separation properties developed via phase inversion (Figure 2-9(c)). PBI is a class of heterocyclic polymers with high chemical and thermal stability. Nevertheless, the reported PBI

hollow fibers showed relatively low FO water flux (e.g., 36.5 L/(m^2 h) using 5 M $MgCl_2$ DS and pure water feed in the AL-DS orientation), probably due to the dense support structure. Yu (Yu et al., 2011) reported asymmetric polyethersulfone (PES) FO membranes with a polyester non-woven fabric. The polymer layer showed a dense top layer and a sublayer with finger-like pores (Figure 2-9(d)). A higher water flux of around 35 L/(m^2 h) was achieved by the membrane using 3 M NaCl DS and pure water feed.

Generally, preparation of integral asymmetric FO membranes is relatively simpler than other methods, which is beneficial to reduce the production cost. In some cases, post-treatments such as annealing (Su et al., 2010b) or crosslinking (Wang et al., 2009) may be performed to modify the membrane permeability. Nevertheless, there are several limitations of the asymmetric FO membranes. Firstly, only a few of the polymers used in phase inversion have a suitable combination of water permeability and salt rejection, such as cellulose acetate and cellulose triacetate (Petersen, 1993). Secondly, the support layer and rejection layer of the asymmetric membranes cannot be individually optimized during the one-step fabrication approach. Therefore, it will be challenging for asymmetric FO membranes to achieve a high water flux while maintaining high salt rejection (especially for NaCl) under FO conditions.

2.4.2.2 Thin film composite FO membranes

A TFC membrane typically comprises an ultrathin active layer that determines the membrane permeability and selectivity, supported by a porous substrate (e.g., a UF-like membrane) for mechanical strength. In contrast to asymmetric membranes prepared via a one-step phase inversion method, the two layers of TFC membranes are prepared by two successive steps using different materials (Petersen, 1993). For example, the porous substrate can be prepared by phase inversion. Then a polyamide rejection layer can be formed on top of the substrate by an interfacial polymerization reaction between a polyamine (e.g., m-phenylenediamine (MPD), p-phenylenediamine (PPDA), and piperazine) and a polyfunctional acyl chloride (e.g., trimesoyl chloride (TMC)). The fabrication of TFC membranes expands the choice

of materials and preparation methods to customize membrane properties. Thus, TFC membranes are widely used in RO and NF today and exhibit superior water permeability and salt rejection.

As FO membranes have similar separation mechanisms as RO membranes, it would be of great value to adapt the TFC structure to FO membrane fabrication. An early attempt by Wang et al. (Chou et al., 2010; Wang et al., 2010b; Shi et al., 2011) reported TFC FO hollow fibers that consisted of a PES hollow fiber substrate and a polyamide rejection layer. The resulting FO hollow fibers showed decent water permeability as well as high NaCl rejection. Meanwhile, the substrate was optimized to be highly porous with long needle-like pores penetrating through the cross-section (Figure2-10(a)), which was beneficial to reduce pore tortuosity and to increase porosity. The correspondingly small structural parameter greatly reduced the ICP propensity of the membrane. Due to the optimized rejection layer and support properties, these hollow fibers showed a high FO water flux and a small salt flux/water flux ratio. Flat-sheet TFC FO membranes were reported in the literature as well. Yip and Tiraferri (Yip et al., 2010; Tiraferri et al., 2011; Yip et al., 2011) reported TFC FO membranes consisting of a polyamide rejection layer and a polysulfone substrate, which were reinforced by a loose and thin non-woven fabric (Figure 2-10(b)). The membranes showed good resistance to ammonium bicarbonate and a much higher FO water flux than a commercial FO membrane.

Owing to the flexibility in TFC membrane preparation, more advanced TFC FO membranes, in terms of rejection layer modification and innovative substrate materials, have been reported recently. For example, Ma (Ma et al., 2012) reported mixed matrix TFC FO membranes which had NaY zeolite nanoparticles embedded in the polyamide rejection layer. The zeolite nanoparticles were super-hydrophilic, with sub-nanometer pores acting as flow paths for only water while solutes such as hydrated sodium ions were rejected due to a size sieving effect. With an optimal zeolite dosage, the membrane water permeability could be increased by about 80%. Correspondingly, a much higher FO water flux was exhibited by the zeolite-polyamide thin film nanocomposite (TFN) membranes, in both the AL-DS and AL-

FS orientations. Other advanced development for high-performance TFC FO membranes also include TFN membranes with carbon nanotubes (Jia et al., 2010), biomimetic membranes with aquaporin (Wang et al., 2012a), etc. In terms of the FO substrates, modification on the hydrophilicity of the support layer was carried out by Wang (Wang et al., 2012b) and Widjojo (Widjojo et al., 2011) by blending sulphonated polymers. Advanced substrates such as electrospun polymeric nanofibers were also incorporated into TFC FO membranes (Bui et al., 2011; Song et al., 2011). The structure of the nanofiber matrix showed a high porosity and good pore interconnectivity (Figure 2-10(c)), which are advantageous to minimize the ICP potential of membranes.

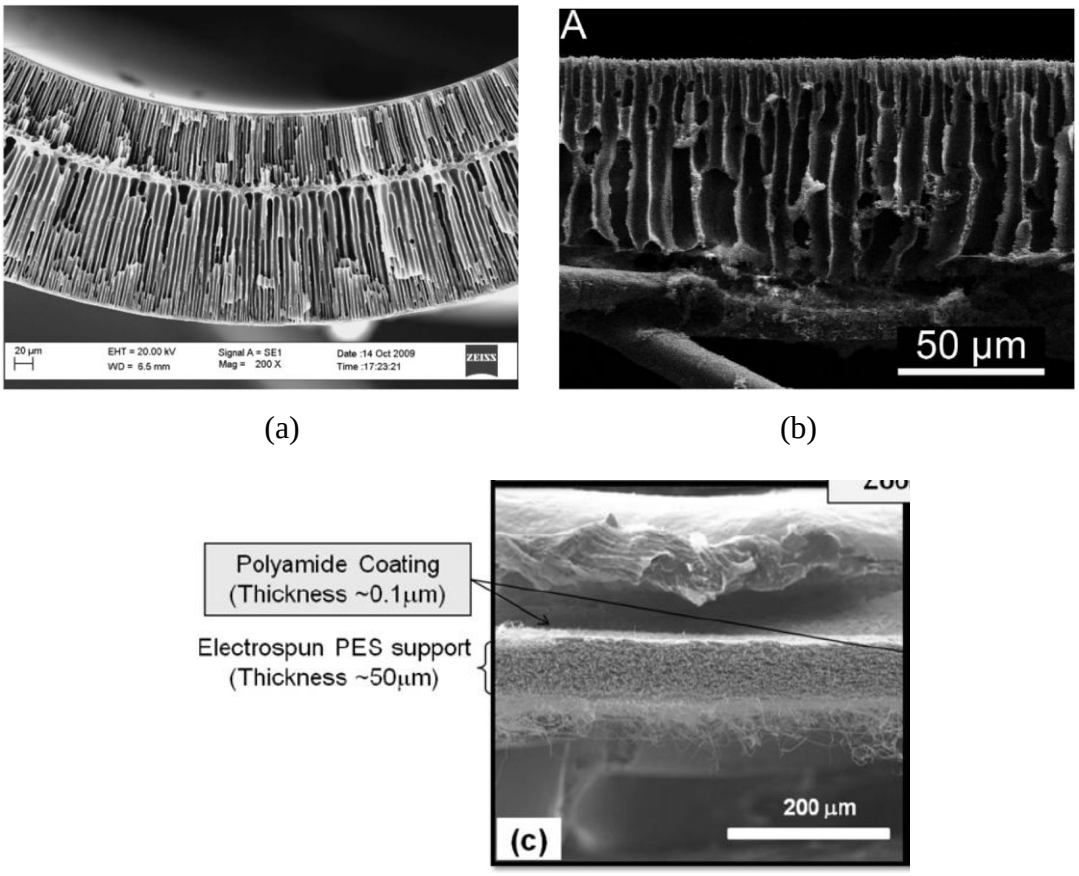

Figure 2-10 Cross-sectional images of TFC FO membranes. (a) FO hollow fiber substrate (Wang et al., 2010b). (b) Flat-sheet TFC FO membrane (Yip et al., 2010). (c) Electrospun nanofiber supported TFC FO membrane (Bui et al., 2011). Figures are adapted from references with copyright permission.

According to a prior comparison study between the asymmetric FO membranes and TFC FO membranes (Jin et al., 2012a), superior FO performance in terms of water permeability, contaminant rejection and pH stability was exhibited by the TFC FO membranes. A common characteristic of the TFC FO membranes as well as other composite membranes is that they can have different chemical compositions for the rejection layer and substrate. Thus, the preparation methods are very flexible. This is a very important advantage over asymmetric membranes for FO membrane fabrication. More specifically, the support layer can be first tailored for minimal ICP propensity, and then the physical and chemical properties of the membrane skin layer, e.g., intrinsic separation properties, surface morphologies and hydrophilicity, can be customized for specific applications.

Knowledge of TFC FO membrane optimization is still lacking currently. According to the studies in pressure-driven membranes, properties of TFC membranes are tunable via adjusting the synthesis conditions such as monomer concentrations (Khare et al., 2003; 2004; Roh et al., 2006), reactive monomer structure (Roh et al., 1998; Verássimo et al., 2006), reaction and post-treatment conditions (Prakash Rao et al., 1997), substrates (Kosaraju and Sirkar, 2008), etc. The kinetics of interfacial polymerization reaction was investigated in prior research (Chai and Krantz, 1994; Khare et al., 2003; 2004) using a pendant drop mechanical analysis (PDMA) approach. During the reaction, a solid polyamide film is formed at the interface between the aqueous solution and an immiscible organic solution. Due to the low partition coefficient of acyl chloride (e.g. TMC) in water, interfacial polymerization usually occurs on the organic side. A crosslinked polyamide network is formed as a result of the trifunctional nature of TMC. Meanwhile, a portion of the reacting trifunctional groups of TMC will form unconnected segments and result in dangling end and branches. As TMC concentration increases, a maximum degree of crosslinking will be reached while the degree of branching increasing monotonically. It is also reported that a maximum crosslinking density can be obtained with a particular combination of the diamine and acyl chloride concentrations. The above PDMA studies have important implications for the TFC FO membrane synthesis. By varying the monomer concentrations, TFC membranes

with different crosslinking density and permeability can be achieved. It will be interesting to investigate the influence of these factors on FO performance, considering the significantly different mass transport mechanisms in osmotically driven membrane processes and pressure-driven membrane processes.

2.4.2.3 Layer-by-layer assembly FO membranes

Layer-by-layer (LBL) assembly is an approach to form multilayer films on a substrate by depositing different charged species, in a sequence of alternating charge or other complementary interactions (Decher, 1997; Hammond, 2011) (Figure 2-11). So far, LBL assembly has been employed in the fabrication of high permeability NF and pervaporation membranes. FO membrane preparation via LBL were also reported recently (Qiu et al., 2011b; Saren et al., 2011; Qi et al., 2012a; Qi et al., 2012b). To prepare the LBL FO membranes, substrates with charged functional groups on the surface are required. In the studies carried out by Qi and Qiu (Qiu et al., 2011b; Saren et al., 2011; Qi et al., 2012a; Qi et al., 2012b), polyacrylonitrile substrates with weak negative charge were first partially hydrolyzed in NaOH solution to enhance the surface charge as well as hydrophilicity. The resulting negatively charged substrates were alternatively soaked in poly(allylamine hydrochloride) (PAH) polycation solution and poly(sodium 4-styrene-sulfonate) (PSS) polyanion solution. Thereby, multiple PAH/PSS polyelectrolyte layers were formed on the PAN substrates. The water permeability and selectivity of the resulting membranes can be adjusted by changing the number of polyelectrolyte layers. Generally, increasing the polyelectrolyte layers improves the membrane selectivity but reduces the water permeability. With an optimal number of layers, membranes can have a high FO water flux and selectivity. Crosslinking with glutaraldehyde solution was used in Qiu's study (Qiu et al., 2011a) to enhance the membrane stability under high ionic strength conditions. The LBL FO membranes mostly had NF-like separation properties, which could be potentially used in applications involving multivalent ions or large molecules.

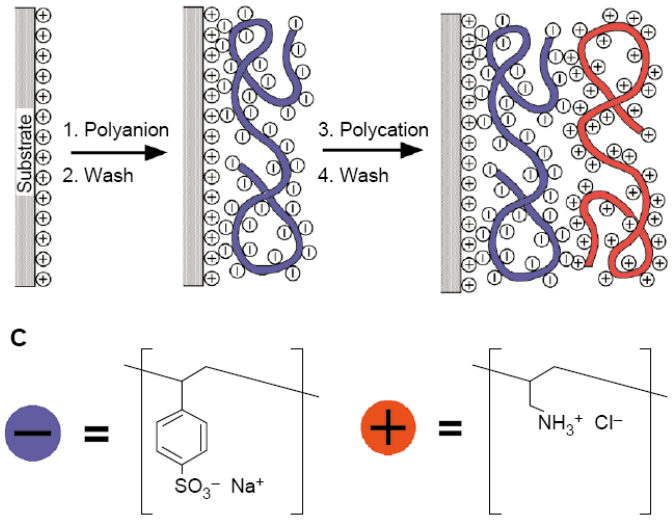

Figure 2-11 Schematic of a layer-by-layer assembly membrane using sodium salt of poly(styrene sulfonate) (polyanion) and poly(allylamine hydrochloride) (polycation) (reproduced from Ref. (Decher, 1997) with copyright permission).

The major advantages of LBL membranes are their high water permeability and a rejection layer where architecture can be easily controlled by the deposition route of polyelectrolyte layer. The substrate structures of these membranes can also be tailored for FO applications as can be done for other composite FO membranes. These advantages make it very promising to fabricate high-flux double-skinned FO membranes by the LBL method. To date only a handful of double-skinned FO membranes have been developed. In early studies, cellulose acetate double-skinned flat-sheet and hollow fiber membranes prepared by the phase inversion method were reported (Wang et al., 2010a; Su et al., 2012). However, these membranes generally showed low water permeability (< 1.0 L/(m^2 h bar)) and thus low FO water flux. The sponge-like support layer may also contribute to their low FO performance due to a high mass diffusion resistance. Recently, double-skinned crosslinked LBL FO membranes were reported (Qi et al., 2012b). These membranes showed improved anti-fouling performance relative to single-skinned membranes, without a significant compromise in the FO water flux. Nevertheless, these double-skinned membranes had NF-like separation properties on both surfaces that limited the NaCl based applications. Future work has yet to be done to increase the NaCl rejection of the draw skin, possibly by increasing the polyelectrolyte layers.

2.4.2.4 Chemically modified FO membranes

In membrane fabrication, chemical modification can introduce functional groups into the membrane and effectively change its intrinsic properties (Mulder, 1996). FO membranes prepared by chemically modifying porous membranes have been developed recently, mostly to formed a charged rejection layer with NF-like separation properties on the porous substrates. Setiawan and Qiu et al. (Qiu et al., 2011b; Setiawan et al., 2011) described a method to prepare positively charged NF-like FO hollow fibers and flat-sheet membranes via chemical modification. In this method, phase inversion formed UF-like poly(amide-imide) (PAI, Torlon®) membranes were subjected to polyethyleneimine (PEI) soaking. The imide groups in the PAI reacted with the amine-functionalized PEI and formed a positively charged NF-like diamine layer on the membrane surface (Figure 2-12). A disadvantage of the positively charged membrane is potential fouling by negatively charged foulants. Less positively charged NF-like hollow fibers were studied by Setiawan (Setiawan et al., 2012b) as well by deposition of a negatively charged PSS layer on the PEI-crosslinked PAI hollow fibers. The rejection layer was then crosslinked with glutaraldehyde. Compared to the positively charged membranes, the modified membranes showed improved fouling resistance to bovine serum albumin (BSA).

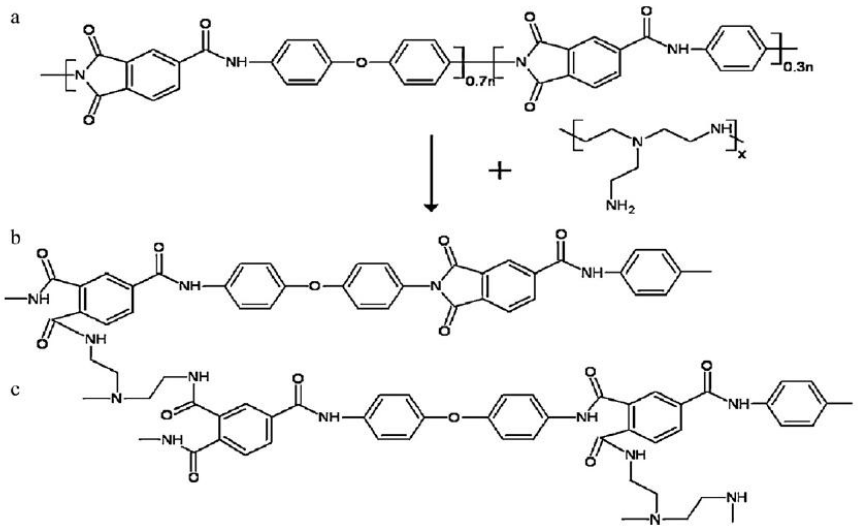

Figure 2-12 Reaction scheme between PAI and PEI (reproduced from Ref. (Setiawan et al., 2011) with copyright permission).

Similar to other types of composite membranes, the chemically modified FO membranes allow relatively independent optimization of the support structure and rejection layer. Moreover, membrane preparation via chemical modification is simple and thus it is possible to combine with other methods to produce a double-skinned FO membrane. Fang (Fang et al., 2012) reported a method to form a secondary rejection layer on a single-skinned FO hollow fiber via chemical modification. In the Fang's study, a RO-like rejection layer was synthesized by interfacial polymerization on the lumen surface of PAI hollow fiber substrates. Then the outer surface of the hollow fibers was cross-linked with PEI to form a positively charged NF-like rejection layer. This would be a promising protocol for future double-skinned FO membrane design.

2.4.2.5 Dual-layer FO membranes

FO membranes with a dual-layer structure have been reported in several studies (Yang et al., 2009a; b; Setiawan et al., 2012a). Yang (Yang et al., 2009a; b) reported NF-like dual-layer FO hollow fibers consisting of a sponge-like PES supporting inner layer and a semi-permeable PBI outer layer (Figure 2-13(a)). However, the membranes showed relatively low water permeability, probably due to the dense pore structure of the support layer. Recently, Setiawan (Setiawan et al., 2012c) reported dual-layer FO hollow fibers (Figure 2-13(b)), which had a PES inner support layer with an elongated finger-like pore structure and a crosslinked PAI outer rejection layer. The membranes prepared by this modified method showed much better FO performance. The effects of spinning conditions on the membrane morphology were also investigated (Setiawan et al., 2012a).

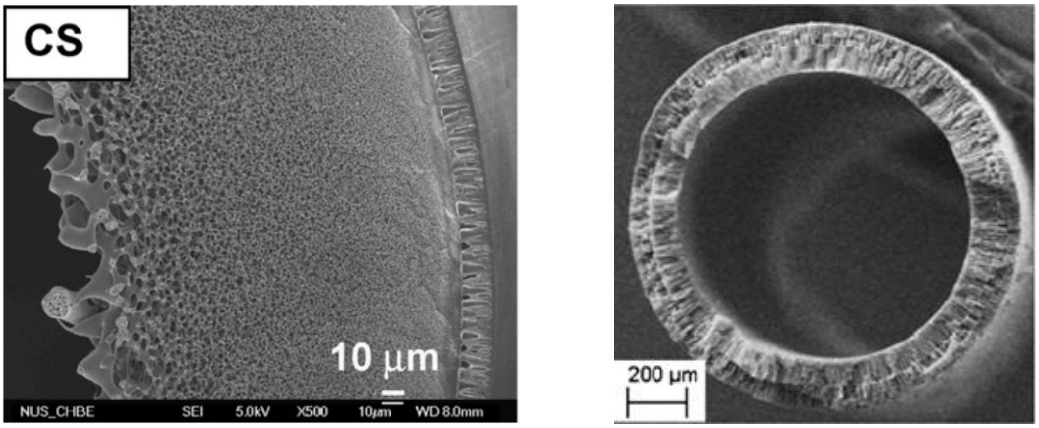

(a) (b)

Figure 2-13 Cross-sectional images of dual-layer FO membranes. (a) Dual-layer PBI-PES/PVP FO hollow fiber (Yang et al., 2009b). (b) Dual-layer PES/PAI FO hollow fiber (Setiawan et al., 2012c). Figures are reproduced from references with copyright permission.

In contrast to other investigated composite membranes, the dual-layer membranes can be fabricated in a single step that reduces the cost of production. Yet unlike the conventional integral asymmetric membranes, high-performance or functional membrane materials can be used for the rejection layer of dual-layer membranes, while low-cost materials can be used for the support layer. However, the dual-layer FO membranes reported so far were typically fabricated via coextrusion, and thus will be challenging to be adapted in other configurations such as flat-sheet membranes.

2.5 Summary

A comprehensive literature review is presented in this chapter to look into the fundamentals, opportunities and challenges of FO technology, as well as the importance and status of FO membrane fabrication. By utilizing the osmotic pressure difference instead of hydraulic pressure as the driving force, FO technology can achieve comparable separation efficiency to that of conventional pressure-driven membrane processes (e.g., NF and RO) with potentially lower energy consumption and less environmental impact. The mild operating conditions of FO are also beneficial for better preservation of the processing components. Due to these advantages, more FO research has been conducted over the last ten years, to

employ this technology in osmotic membrane bioreactors, desalination, water purification, osmotic power generation, water recovery, liquid food processing, and microbial fuel cells, etc.

Although FO is an advantageous technology, most of the research activities are still at the bench-scale due to the limited FO water flux achieved, which is mainly due to the ICP phenomenon. According to the literature, several factors are revealed to contribute to ICP and constrain the FO performance, including the membrane characteristics, draw solution properties and operating conditions. Moreover, the influence of the draw solution and operating conditions is correlated with the membrane properties. Thus, efficient membranes are of critical importance for exploitation of FO technology.

Attempts to use conventional semi-permeable membranes, such as RO membranes, have failed in FO applications, due to their severe ICP propensity and correspondingly low FO water flux. Emerging studies on the FO membrane fabrication have been reported recently. The reported membranes had various separation properties (e.g., NF-like and RO-like), structures (e.g., integral asymmetric, thin film composite and dual-layer) and chemistry (e.g., cellulose esters, polyamide based and polyelectrolyte layer-by-layer assembly). Most of these membranes showed improved FO performance compared to the RO membranes. It is suggested by this prior work that high-performance FO membranes should have a small structural parameter, high water permeability, high solute rejection, as well as membrane stability and mechanical strength for practical use. In comparison, composite membranes appear to be superior over integral asymmetric membranes under FO conditions, as the former can be easier optimized in terms of the structural parameter, permeability, chemistry, etc. In particular, TFC FO membranes are very promising among the composite FO membranes in view of their superior water permeability, salt rejection, membrane stability and low production cost. On the other hand, the main challenges in FO membrane fabrication are the complicated trade-off between the membrane properties and the fact that these parameters tend to affect the FO performance non-linearly. Yet there is a relatively poor

understanding of their competing effects, especially with respect to different operating conditions. As increasing attention is paid to FO technology, the demand for high-performance FO membranes for various applications has become a pressing issue. Therefore, not only the fabrication technology but also systematic knowledge concerning the influence of membrane properties on FO performance as well as the criteria for membrane optimization will be necessary in future research.

Chapter 3
Materials and methodology

3.1 Chemicals and materials

3.1.1 Chemicals

Unless otherwise specified, all chemicals were of analytical grade and were used as received. Ultrapure water with a resistivity of 18.2 MΩ.cm was obtained from a Milli-Q water system (Millipore Singapore Pte. Ltd.), and was used throughout this study unless specified otherwise.

Polysulfone (molecular weight 75,000-81,000 Da, Solvay Advanced Polymers, LLC) was used to prepare the substrates of the TFC FO membranes. Polysulfone is a widely used material for thin film composite membranes (Petersen, 1993). This polymer can be dissolved in suitable organic solvents and processed to form porous membranes. The resulting membranes have good chemical resistance as well as high mechanical strength even when they are dry. Due to these properties, the UF-like polysulfone membranes can be used as the substrates for TFC membranes that are prepared by interfacial polymerization. N-Methyl-2-pyrrolidone (NMP, Merck Schuchardt OHG) was used as the solvent for the casting solution. Polyvinyl pyrrolidone (PVP, average molecular weight 1,300,000 Da, Alfa Aesar), polyethylene glycol (PEG, molecular weight 600 Da, Samchun Pure Chemical Ind. Co., Ltd.) and lithium chloride (LiCl, Sinopharm Chemical Reagent Co. Ltd.) were used as additives in the casting solutions.

Chemicals used to synthesize the rejection layer of the TFC FO membranes included m-phenylenediamine (MPD, Sigma-Aldrich Inc.), ε-caprolactam (Merck Schuchardt OHG), sodium dodecyl sulfate (SDS, Scientific Apparatus), piperazine (PIP, Sigma-Aldrich Inc.), triethylamine (TEA, Alfa Aesar), trimesoyl chloride (TMC, Sigma-Aldrich Inc.) and n-hexane (Merck KGaA).

Sodium chloride (NaCl, Merck Schuchardt OHG), sodium sulfate (Na_2SO_4, Merck

Schuchardt OHG) and trisodium citrate ($Na_3C_6H_5O_7$, Wako Pure Chemical Industries Ltd.) were used to evaluate the membrane intrinsic separation properties and FO performance.

Alginic acid sodium salt extracted from brown algae (referred to as alginate, A2158, Sigma-Aldrich Inc.) was used as a model foulant in the FO fouling tests. The feed solution pH and ionic composition in the fouling tests were adjusted using hydrochloric acid (HCl, Merck Schuchardt OHG), sodium hydroxide (NaOH, Merck Schuchardt OHG) and calcium chloride ($CaCl_2$, Unichem Inc.).

3.1.2 Membrane materials

Three commercial FO membranes obtained from Hydration Technology Innovations (Albany, OR) and one commercial RO membrane obtained from Dow FilmTec (Minneapolis, MN) were used for comparison purposes. The HTI FO membranes were all based on cellulose triacetate. One of the FO membranes was cut from a Hydrowell® module (denoted as CTA-HW). This membrane is formed by casting cellulose triacetate onto a polyester woven fabric (Wang et al., 2010c). The other two membranes were received as flat-sheet coupons, either supported by a polyester woven fabric (denoted as CTA-W) or a non-woven fabric (denoted as CTA-NW). The RO membrane BW30 was a TFC polyamide membrane supported by a non-woven fabric (Tang et al., 2007c; Tang et al., 2009b). In some experiments, the non-woven fabric of the BW30 membrane was manually peeled off with care before characterizations (denoted as BW30-o in this study).

3.2 Preparation of flat-sheet TFC FO membranes

The TFC FO membranes were prepared via a two-step process: (1) a phase inversion step to form a porous membrane substrate (Section 3.2.1), and (2) an interfacial polymerization step to form the active rejection layer on the substrate (Section 3.2.2). The preparation methods are described in this section while recipes for different membranes will be provided in corresponding chapters (Chapter 4-6).

3.2.1 Preparation of substrate

To prepare a casting solution for the FO substrates, polymer (e.g., polysulfone) and additives (e.g., PVP and PEG, LiCl) were dissolved in NMP and stirred by magnetic stirrers at 70 ℃ until the solution became homogeneous. After cooling to room temperature (23 ℃), the polymer solution was filtered with a stainless steel filter connected to compressed nitrogen gas. The filtered dope was then degassed in air-tight bottles for 24 h before use. To prepare a membrane substrate, the casting solution was spread onto a clean glass plate to form a uniform film using an Elcometer 4340 motorised film applicator (Elcometer Asia Pte. Ltd.). The film was then quickly and smoothly immersed with the glass plate into a coagulant bath where 23 ℃ tap water was used as the coagulant to induce phase separation, for which a polymer-rich phase forms the membrane structure and a solvent-rich phase forms the membrane pores (Strathmann and Kock, 1977). Additives such as PVP, PEG, and LiCl were dissolved in the casting solution for some substrates to tailor the pore structure of the substrate (the recipes see Chapter 4-6). The solidified substrate was moved to a flowing water bath to remove the residual solvent and was stored in ultrapure water before use.

3.2.2 Preparation of membrane rejection layer

The active rejection layer of the TFC FO membrane was prepared by interfacial polymerization on the surface of a precast substrate. The preparation was carried out at room temperature (23 °C) unless otherwise specified. Before interfacial polymerization, a substrate was heated in a 70 °C water bath for 2 min and then quenched in a 23 °C water bath. This was to make the substrate pore structure more compact and stable. The substrate was then soaked in an aqueous solution of diamine (MPD or PIP) for 2 min. After removing the excess diamine solution on the substrate surface with compressed nitrogen gas, the substrate was brought into contact with an n-hexane solution of TMC for 1 min. A polymerization reaction between the two monomers (i.e., diamine and TMC) can take place instantaneously at the interface between the aqueous phase and organic phase (n-hexane), forming an ultrathin polyamide rejection layer on the surface of the substrate. Additives (e.g., SDS, ε-caprolactam and TEA) were added into the diamine solution in some

experiments to improve the membrane permeability. The residual TMC solution on the membrane was drained and the membrane was thoroughly washed in a flowing water bath. The nascent composite membrane was stored in ultrapure water before further use.

3.3 Membrane characterization

3.3.1 Characterization of membrane structure and surface properties

The surface morphologies and cross-sections of the membranes were observed with a scanning electron microscope (SEM). Membrane samples were dried in vacuum at room temperature. Samples were then fractured in liquid nitrogen and coated with a thin layer of gold using an EMITECH SC7620 sputter coater (Quorum Technologies Ltd.). SEM images of the membrane surface and cross-section were obtained using a Zeiss EVO 50 Scanning Electron Microscope (Carl Zeiss Pte. Ltd.). The thicknesses of the membranes were measured from the SEM cross-section images and were further verified by measurement using a micrometer. The surface roughness of membranes was examined using atomic force microscopy (AFM, XE-100, Park Systems).

Membrane contact angles were measured by the sessile drop method, using a goniometer (Contact Angle System OCA, DataPhysics Instruments GmbH). The membrane samples were vacuum dried at room temperature for 24 h. Small water droplets were applied onto a leveled membrane surface and allowed to stabilize without vibration. The profiles of the water drops were captured by an optical system to determine the contact angles.

Attenuated total reflection-Fourier transform infrared spectroscopy (ATR-FTIR) was used to examine the surface chemistry of the substrate and rejection layer of the TFC FO membranes. ATR-FTIR spectra of the substrate and TFC membranes were obtained using a Spectrum 2000 FTIR spectrometer (PerkinElmer).

The porosity (ε) of a membrane was determined by gravimetric measurement of the wet and dry membrane, according to the following equation (Sukitpaneenit and

Chung, 2009; Wang et al., 2010b):

$$\varepsilon = \frac{(m_{wet} - m_{dry})/\rho_w}{(m_{wet} - m_{dry})/\rho_w + m_{dry}/\rho_m} \times 100\% \quad (3\text{-}1)$$

where m_{wet} and m_{dry} are the wet and dry masses of the membrane samples, respectively; ρ_w and ρ_m are the densities of the wetting solvent (water in the current study) and polymer, respectively. The specific gravity of the polysulfone used in this study is 1.24. The m_{wet} was obtained by measuring the wet membrane samples after carefully removing the water on the surface. The samples were subsequently dried in vacuum oven and then measured the m_{dry}.

3.3.2 Measurement of membrane intrinsic separation properties

The intrinsic separation properties (water and salt permeability) of the membranes were evaluated in a customized cross-flow filtration setup in the RO testing mode (i.e., pressurized mode). A schematic of the setup is shown in Figure 3-1. The membrane was loaded in a plate-frame-mode membrane cell (effective membrane area of 42 cm^2) with the rejection layer facing the feed solution. A diamond-patterned spacer was placed on the feed side to create turbulence and reduce the effect of ECP. The feed solution under constant pressure flowed against the membrane; permeate water through the membrane was collected to measure the flux and salt rejection. Before sample collection, compaction of membrane was conducted until a steady-state permeate flux was reached. In this study, ultrapure water was used as the feed to measure the membrane pure water permeability (*A* value) while salt solutions were used as the feed to measure salt rejection (*R*) of the membranes. The system temperature was controlled at 23 ℃ by a chiller.

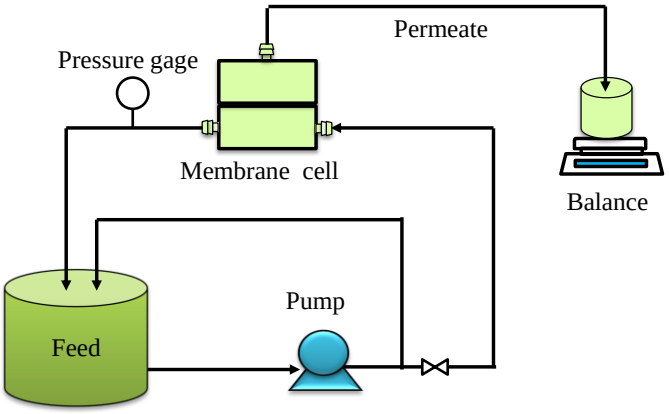

Figure 3-1 Schematic of the cross-flow RO setup for determining the membrane intrinsic separation properties.

The membrane water permeability *A* was calculated according to:

$$A = \frac{J_v}{\Delta p} \tag{3-2}$$

where Δp is the applied pressure and J_v is the permeate water flux.

The membrane salt rejection *R* was determined based on conductivity measurements (Ultra Meter II^{TM} 4P, Myron L Company, CA) of the feed and the permeate:

$$R = 1 - \frac{C_p}{C_{feed}} \tag{3-3}$$

where C_{feed} and C_p are the salt concentrations of the feed and the permeate, respectively. The salt permeability *B* of the membrane was calculated according to the following equation:

$$B = J_v \left(\frac{1}{R} - 1 \right) \tag{3-4}$$

where J_v is the permeate water flux and *R* is the salt rejection.

3.3.3 Evaluation of FO performance

The FO performance (water flux and salt flux) of each membrane was evaluated with a bench-scale cross-flow FO setup. A schematic of the setup is illustrated in Figure 3-2. The setup consisted of two loops with feed and draw solution circulated on each side of the membrane. The membrane coupon was mounted in a cell with a plate-frame configuration. The effective membrane area was 60 cm^2. Identical diamond-patterned spacers were placed on both sides of the membrane to minimize the ECP. A co-current flow pattern was used to reduce strain on the membrane. A cross-flow velocity was 23.2 cm/s for both the feed and draw solutions. The temperature was held constant at 23 ℃.

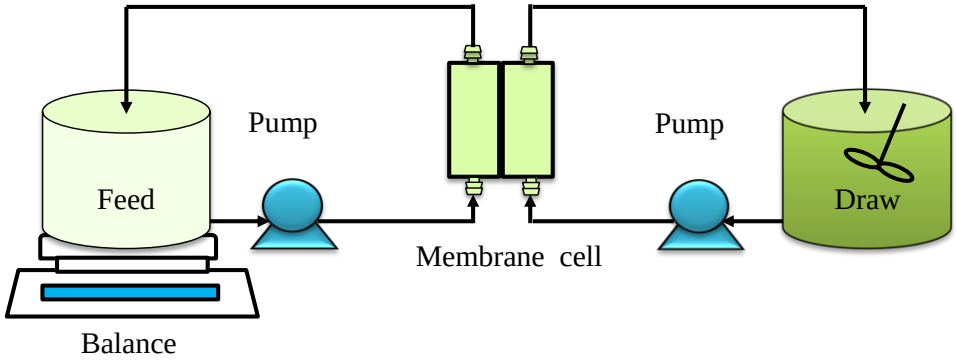

Figure 3-2 Schematic of the cross-flow FO setup for membrane testing.

The FO water flux J_v was determined by measuring the weight change of the feed solution:

$$J_v = \frac{\Delta V_{feed}}{A_m \Delta t} = \frac{\Delta m_{feed} / \rho_{feed}}{A_m \Delta t} \tag{3-5}$$

where ΔV_{feed} and Δm_{feed} are the volume and weight changes of the feed solution, respectively; A_m is the effective membrane area; ρ_{feed} is the density of the feed solution and Δt is the sampling time interval.

The FO solute flux J_s was determined by calculating the change in the salt mass in the feed solution based on conductivity measurements:

$$J_s = \frac{V_t C_t - V_0 C_0}{A_m \Delta t} \tag{3-6}$$

where V_0 and V_t are the initial and real-time volumes of the feed solution, respectively; C_0 and C_t are the initial and real-time salt concentrations of the feed solution, respectively.

3.3.4 Determining membrane structural parameter

The structural parameter S is one of the critical properties of FO membranes. It is defined as the product of the support layer thickness (l) and tortuosity (τ) divided by the porosity (ε) (Loeb et al., 1997; Tang et al., 2010):

$$S = \frac{l\tau}{\varepsilon} \tag{3-7}$$

A large S value inevitably leads to severe ICP. According to the classical ICP model developed by Loeb et al. (Loeb et al., 1997), the FO water flux can be predicted by the following equations:

AL-DS: $$J_v = \frac{D}{S} \ln \frac{A\pi_{draw} - J_v + B}{A\pi_{feed} + B} \tag{3-8}$$

AL-FS: $$J_v = \frac{D}{S} \ln \frac{A\pi_{draw} + B}{A\pi_{feed} + J_v + B} \tag{3-9}$$

where D is the solute diffusion coefficient; π_{draw} and π_{feed} are the osmotic pressures of the draw solution and feed solution, respectively. Thus, the structural parameter S can be determined experimentally from Equations (3-8) and (3-9).

3.3.5 FO fouling tests

The fouling performance of the TFC FO membranes was evaluated in the AL-FS orientation using alginate as a model foulant. The fouling tests were performed in

the cross-flow FO setup as Figure 3-2. Before each fouling test, the membranes were stabilized for 30 min with the background electrolyte solutions, for which the compositions were identical to that under the subsequent fouling test except that no foulant was added. To be specific, the FS contained 1 mM $CaCl_2$ and 7 mM NaCl. The calcium concentration and ionic strength (10 mM) were similar to that in the wastewater. According to prior studies (Mi and Elimelech, 2008; She et al., 2012a), the presence of $CaCl_2$ is also able to enhance the alginate fouling in the FO process and thus one can better observe the foulant deposition. 1.5 M Na_2SO_4 was used as DS to reduce the reverse diffusion of draw solute for the NF-like FO membranes and to achieve a practicable water flux for fouling occurrence. Alginate was added to the FS at 30 min after the FO test; the duration of fouling tests was 14 h. The water flux right before adding foulant was taken as the initial flux. Baseline tests (without foulant addition) were similarly conducted. The experimental conditions for fouling tests were as follows:

- FS: 100 mg/L alginate, 7 mM NaCl and 1 mM $CaCl_2$, pH 6.0 $\pm$0.1;
- DS: 1.5 M Na_2SO_4;
- cross-flow velocities of both the FS and DS: 23.2 cm/s;
- temperature: 23 ℃.

After each fouling test, the membrane coupons (area ~15 cm^2) were cut from the fouled membranes and were gently rinsed with pure water and then soaked in 0.001 M NaOH for foulant extraction (Wang and Tang, 2011b). Mild sonication (20 min) was applied. Clean membrane coupons were similarly treated with NaOH soaking and sonication, for which the resulting extract was used as control. The extract was examined by the phenol-sulfuric acid method using UV wavelength of 485 nm. The foulant mass on the fouled membranes was determined after deducting the contribution of the membrane itself. SEM analysis was conducted on the fouled membranes to check the foulant deposition.

Chapter 4
Synthesis and characterization of flat-sheet thin film composite forward osmosis membranes

4.1 Introduction

FO is an osmotically-driven membrane process in which water diffuses through a semi-permeable membrane under an osmotic pressure difference across the membrane (Cath et al., 2006). An essential element in this process is the semi-permeable membrane, which acts as the barrier for solute transport thus enabling build-up of an osmotic pressure difference between the draw solution and the feed solution. Theoretically, any membrane with sufficient rejection to solutes could be used in osmotically driven membrane processes. Nevertheless, prior studies have proved that conventional RO membranes had poor performance in the FO process (McCutcheon et al., 2005b), due to internal concentration polarization occurring inside the porous support layer of the membrane. A concentrative ICP occurs when the membrane rejection layer is placed against the draw solution, where solutes from the feed solution accumulate in the porous support layer as a result of their retention by the rejection layer (McCutcheon and Elimelech, 2006). On the other hand, a dilutive ICP occurs due to the dilution of draw solution concentration in the support layer when the active rejection layer faces feed solution (McCutcheon and Elimelech, 2006). Both concentrative and dilutive ICP can cause a dramatic reduction in the osmotic pressure difference across the active rejection layer and thus reduce the available water flux (Loeb et al., 1997; McCutcheon and Elimelech, 2006; Tang et al., 2010).

Exploitation of FO technologies has been studied for a few decades (Kessler and Moody, 1976; Loeb, 1976; Loeb et al., 1976; Moody and Kessler, 1976); however, lack of an efficient membrane to overcome the problem of internal concentration polarization greatly hindered further development of these technologies in the earlier years (Cath et al., 2006). Although many researchers have investigated the mechanisms of ICP (Lee et al., 1981; Loeb et al., 1997; McCutcheon and Elimelech,

2006; Ng et al., 2006; McCutcheon and Elimelech, 2008; Tang et al., 2010; Wang et al., 2010b; Xiao et al., 2011), there are just a few studies focusing on FO membrane fabrication (Herron, 2005; Wang et al., 2007; Wang et al., 2009; Yang et al., 2009b; a; Chou et al., 2010; Su et al., 2010a; Wang et al., 2010a; Wang et al., 2010b; Yip et al., 2010; Zhang et al., 2010; Setiawan et al., 2011; Tiraferri et al., 2011). Meanwhile the only FO membranes available commercially are the cellulose triacetate asymmetric membranes from Hydration Technologies Innovations (McCutcheon and Elimelech, 2006; Tang et al., 2010; Wang et al., 2010c). The HTI membranes have been highly optimized in terms of the support structure to allow these membranes to achieve a decent FO water flux (McCutcheon and Elimelech, 2006; Tang et al., 2010). On the other hand, the water permeability and salt rejection of these membranes appear to be relatively low (Tang et al., 2010; Xiao et al., 2011; Zou et al., 2011). Therefore, there are still significant opportunities for the improvement of FO membrane fabrication technology. According to experience in the reverse osmosis field (Petersen, 1993; Tang et al., 2009a), the TFC-based membranes generally have superior separation properties and more freedom in membrane optimization than integral asymmetric FO membranes prepared via phase inversion. Thus, it is expected that TFC-based membranes can play an important role in FO applications, which deserves further investigation (Kwon et al., 2008).

The objective of this chapter is to fabricate efficient TFC FO membranes, and to determine the effect of the substrate and rejection layer properties on the FO performance. Thin film composite polyamide membranes with tailored support and rejection layers were developed. The morphologies and physical characteristics of the resulting FO membranes were investigated and compared to commercial FO as well as RO membranes to illustrate the importance of both the support layer structure as well as the active rejection layer separation properties.

4.2 Materials and methods

4.2.1 Chemicals and membrane materials

Polysulfone beads (molecular weight 75,000-81,000 Da, Solvay Advanced

Polymers, LLC), polyvinyl pyrrolidone (PVP, average molecular weight 1,300,000 Da, Alfa Aesar), lithium chloride (LiCl, Sinopharm Chemical Reagent Co. Ltd.), and n-Methyl-2-pyrrolidone (NMP, Merck Schuchardt OHG) were used to prepare the membrane substrates. M-phenylenediamine (MPD, Sigma-Aldrich Inc.), sodium dodecyl sulfate (SDS, Scientific Apparatus), trimesoyl chloride (TMC, Sinopharm Chemical Reagent Co. Ltd.) and n-hexane (Fisher Scientific) were used to synthesize the rejection layer of the TFC FO membranes. Sodium chloride (NaCl, Merck Schuchardt OHG) was used to evaluate the membrane intrinsic separation properties and FO performance. All chemicals were of analytical grade and were used as received unless otherwise specified. Ultrapure water was supplied from a Milli-Q water system (Millipore Singapore Pte. Ltd.) with a resistivity of 18.2 MΩ.cm.

Three commercial cellulose triacetate FO membranes (CTA-HW, CTA-W and CTA-NW) obtained from HTI (Albany, OR) and one commercial TFC polyamide RO membrane (BW30) obtained from Dow FilmTec (Minneapolis, MN) were used for the purpose of comparison. In addition, membrane coupons of BW30-o were prepared for this study by carefully removing the non-woven fabric of BW30. The details of these membranes refer to Section 3.1.2.

4.2.2 Synthesis of flat-sheet TFC FO membranes

4.2.2.1 Preparation of substrate

The TFC FO membranes were prepared via two steps: (1) a phase inversion step to form the membrane substrate (this section), and (2) an interfacial polymerization step to form the active rejection layer (Section 4.2.2.2). To prepare a casting solution for the FO substrate, a certain amount of polysulfone and additives (PVP and LiCl) were dissolved in organic solvent NMP (Table 4-1). The functions of the reagents can be referred to Section 3.2.1. The casting solution was stirred by a magnetic stirrer at 70 ℃ until the solution became homogeneous and transparent. After cooling to room temperature (23 ℃), the polymer solution was filtered with a stainless steel filter connected to compressed nitrogen gas. The filtered dope was then degassed in air-tight bottles for 24 h before use. To prepare a polysulfone

substrate, the casting solution was spread onto a clean glass plate to form a uniform film using an Elcometer 4340 motorised film applicator (Elcometer Asia Pte. Ltd.). The film was then quickly and smoothly immersed with the glass plate into a coagulant bath where 23 ℃ tap water was used as coagulant. The time between casting the film and immersing it in the coagulant bath was 10 ± 1 s. The relative humidity in the air was 64 ± 4%. Exposure of the casting solution film to the air may affect the formation of the substrate due to the water vapor absorption; however, the effect would be constant in this study since the preparation conditions were well-controlled and consistent. The resulting substrate was kept in flowing water bath to remove residual solvent and stored in ultrapure water before use.

Table 4-1 Synthesis conditions for TFC FO membranes

Membrane ID	TFC-1	TFC-2
Substrate via phase inversion		
Casting solution	Polysulfone 17.5 wt.%, PVP 0.5 wt.%, NMP 82.0 wt.%	Polysulfone 15.5 wt.%, PVP 0.5 wt.%, LiCl 3.0 wt.%, NMP 81.0 wt.%
Thickness of casting solution	175 μm	150 μm
Rejection layer via interfacial polymerization [a]		
Diamine solution (in water)	MPD 1.0 wt.%	MPD 1.5 wt.%, SDS 0.1 wt.%
TMC solution (in n-hexane) [b]	0.5 mg/ml	1 mg/ml

a. Compositions of monomer solutions (MPD dissolved in water and TMC dissolved in n-hexane) are listed.

b. The unit of TMC solution concentration (mg/ml) in this study represents the ratio of TMC mass over the volume of solvent (n-hexane).

4.2.2.2 Preparation of polyamide rejection layer

The active rejection layer of the TFC FO membrane was prepared by interfacial polymerization on the surface of a polysulfone substrate (see Section 3.2.2). Two types of TFC FO membranes were synthesized (denoted as TFC-1 and TFC-2); their preparation conditions are summarized in Table 4-1. In this study, MPD

performed as the reactive monomers in the aqueous phase while TMC performed as the reactive monomer in the organic phase. SDS was dissolved in the aqueous solution for TFC-2 to improve the permeability of the membrane. The preparation was carried out at room temperature unless otherwise specified. The substrate was heated in a 70 °C water bath for 2 min before cooling down in ultrapure water at room temperature. This substrate was then soaked in an aqueous solution of MPD for 2 min, and the excessive MPD solution on the substrate surface was removed. Subsequently, an n-hexane solution of TMC was gently poured onto the surface of the MPD-soaked substrate and was allowed to react with the residual MPD for 1 min to form the polyamide rejection layer. The resulting TFC membrane was rinsed with tap water to remove the residual reagents and was stored in ultrapure water before characterization.

4.2.3 Membrane characterization

4.2.3.1 Characterization of membrane morphology, porosity, and contact angle

The morphologies of the membranes were observed with a scanning electron microscope (SEM). Membrane samples were dried in vacuum at room temperature for 24 h. Samples were then fractured in liquid nitrogen and coated with a thin layer of gold using an EMITECH SC7620 sputter coater (Quorum Technologies Ltd., UK). SEM images of the membrane surface and cross-section were obtained using a Zeiss EVO 50 Scanning Electron Microscope (Carl Zeiss Pte. Ltd.).

The membrane porosity (ε) was determined by measuring the dry mass (m_{dry}) and wet mass (m_{wet}) of membrane samples according to Equation (3-1).

The contact angles of the membranes were measured via the sessile drop method, using a goniometer (Contact Angle System OCA, DataPhysics Instruments GmbH (Tang et al., 2010)). The membrane samples were dried in vacuum at room temperature for 24 h before measurement. Small water droplets were applied onto a leveled membrane surface and profiles of the water drops were captured by an optical system to determine the contact angles.

4.2.3.2 Measurement of membrane intrinsic separation properties

The intrinsic separation properties of FO membranes were evaluated in a cross-flow RO filtration setup in the pressurized mode (Figure 3-1). The water permeability *A* of a membrane was evaluated by RO tests over an applied pressure range of 1-5 bar with ultrapure water as the feed. The *A* value was calculated according to Equation (3-2). The pure water flux of the polysulfone substrate was determined similarly using pure water feed at an applied pressure of 1 bar.

The NaCl rejection and permeability of a membrane were measured in the same RO setup over 1-5 bar, using a 20 mM NaCl solution as the feed. External concentration polarization was minimized by using a diamond-patterned feed spacer and a relatively high cross-flow (22.3 cm/s). The salt rejection of the membrane was determined based on conductivity measurements (Ultra Meter II™ 4P, Myron L Company) of the feed and permeate. The NaCl rejection *R* and permeability *B* can be calculated using Equations (3-3) and (3-4), respectively.

4.2.3.3 FO performance evaluation

The FO water flux and salt flux were evaluated with the bench-scale FO setup (Figure 3-2). Both the feed solution and draw solution were circulated at a fixed cross-flow rate of 23.2 cm/s. 0.5 M NaCl solution was used as one of the draw solutions to represent the seawater. Moreover, another draw solution containing 2.0 M NaCl was used to evaluate the potential FO water flux when more concentrated DS was available. The feed solution contained 10 mM NaCl to represent the salinity in wastewater. Both the AL-DS and AL-FS orientations were tested. The FO water flux J_v was determined by measuring the weight change of the feed solution (Equation (3-5)) while the salt flux J_s was determined by calculating the change in salt mass in the feed solution based on conductivity measurements (Equation (3-6)).

The structural parameter *S* of an FO membrane is defined as the product of the support layer thickness (l) and tortuosity (τ) divided by its porosity (ε) (Loeb et al., 1997; Tang et al., 2010), as in Equation (3-7). In this study, the structural parameters were determined experimentally based on the achieved FO water flux

and Equations (3-8) and (3-9).

4.3 Results and discussion

4.3.1 Characterization of membrane substrates

Two TFC FO membranes, TFC-1 and TFC-2, were fabricated (Table 4-1) for which the substrates are denoted as S-1 and S-2, respectively. The structures of these two substrates are shown in Figures 4-1(a)-(d) for S-1 and Figures 4-2(a)-(d) for S-2. From the SEM micrographs, both substrates had overall thickness ~75 μm (Figures 4-1(a) and 4-2(a), and Table 4-2). These substrates had highly porous structures with long finger-like pores formed under a thin sponge-like skin layer (thickness < 2 μm, see Figures 4-1(b) and 4-2(b)). The finger-like pores are preferred for FO membranes to minimize the structural parameter, since such pores have a tortuosity of nearly unity (see Equation (3-7)). Gravimetric measurements confirmed that both substrates had high porosities (77 ± 3% for S-1 and 82 ± 2% for S-2, Table 4-2). Corresponding to the high porosity and the finger-like pore structures, relatively small *S* values were achieved for both substrates (0.71 ± 0.14 mm for S-1 and 0.67 ± 0.17 mm for S-2, Table 4-2).

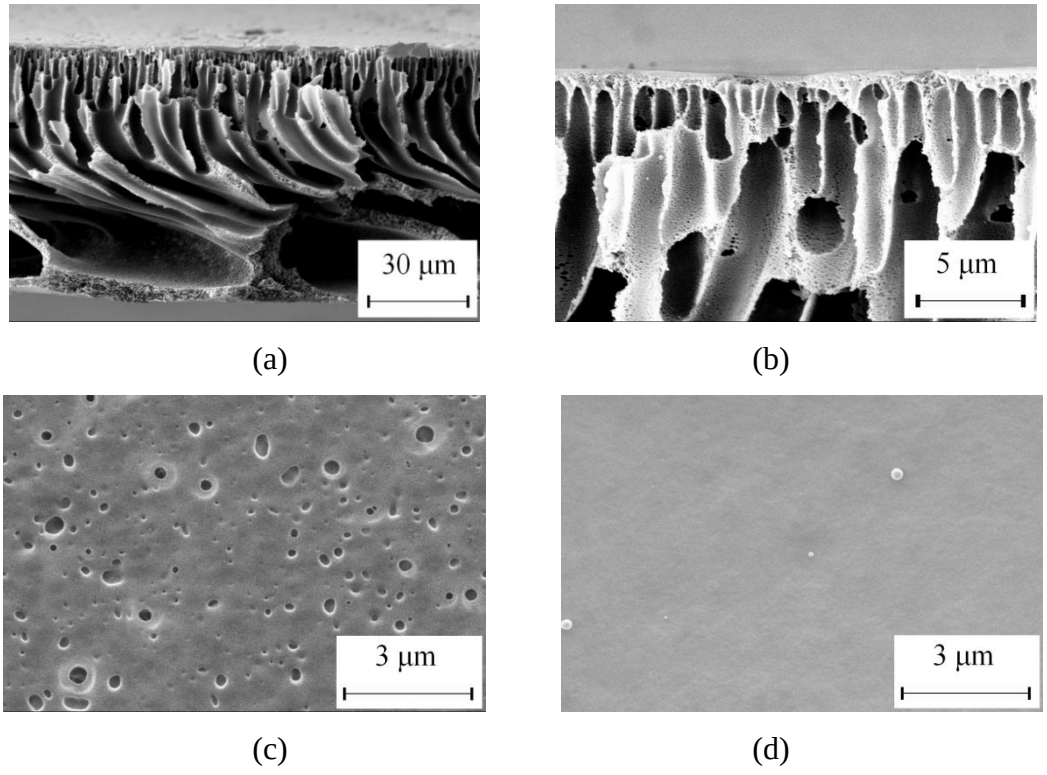

Figure 4-1 SEM micrographs of substrate S-1. (a) and (b) Cross-sections. (c) Bottom surface. (d) Top surface.

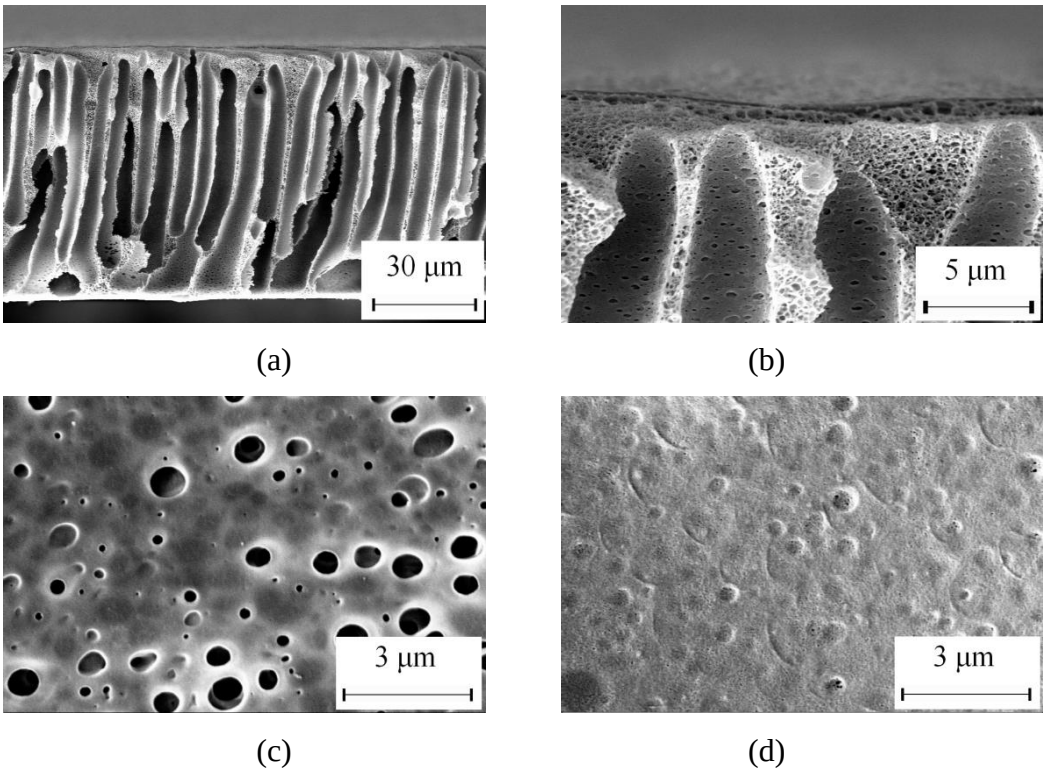

Figure 4-2 SEM micrographs of substrate S-2. (a) and (b) Cross-sections. (c) Bottom surface. (d) Top surface.

Table 4-2 Characteristics of FO membrane substrates [a]

Sample	Thickness [c] (μm)	Porosity [d] (%)	*S* value [e] (mm)	Pure water flux [f] (L/(m^2 h))	Contact angle (°)
S-1 (TFC-1)	76.1 ± 3.0	77 ± 3	0.71 ± 0.14	107 ± 10	56 ± 1
S-2 (TFC-2)	72.8 ± 0.7	82 ± 2	0.67 ± 0.17	190 ± 15	53 ± 3
CTA-HW [b]	90.0 ± 6.0 (60 [b])	64 ± 1	0.72 ± 0.15	-	74 ± 2 [g]
CTA-W [b]	44.7 ± 14.1 (20 [b])	46 ± 1	1.00 ± 0.54	-	69 ± 2 [g]
CTA-NW	144 ± 24	50 ± 2	1.38 ± 0.26	-	74 ± 3 [h]
BW30	152 ± 4	35 ± 1	37.5 ± 19.6	-	92 ± 2 [i]
BW30-o	58.1 ± 5.1	49 ± 1	14.0 ± 1.6	-	92 ± 2 [i]

a. The polysulfone substrates were examined for the TFC FO membranes while the integral membrane coupons were used for the commercial membranes. The experimental errors are reported as the standard deviation of at least 3 repeated measurements.

b. The cross-sections of CTA-HW and CTA-W are highly non-uniform due to their woven support. The thickness values given in parentheses are the minimum cross-section thickness at the thinnest part of the cross-section.

c. The thickness measured for commercial membranes includes the contribution from rejection layer. The thickness of the polyamide rejection layer for the BW30 is on the order of 200 nm (Tang et al., 2007c). The thickness of the skin layer for CTA membranes is on the order of a few micrometers (Figure 4-3) (Wang et al., 2012c).

d. The porosity values shall be taken as nominal values since the membranes may be slightly swelled by water during measurements. In addition, for measuring the porosity of commercial FO and RO membranes, the rejection layers were not removed.

e. Determined from FO water flux results using Equations (3-8) and (3-9).

f. Tested at an applied pressure of 1 bar using pure water feed.

g. Measured for the bottom surface of the membranes.

h. Measured for the bottom surface of the cellulose triacetate layer after the removal of the non-woven fabric.

i. Measured for the polysulfone substrate after the removal of the non-woven fabric layer.

The slightly higher porosity for S-2 is consistent with the lower polysulfone concentration used to cast this substrate. In addition, while some macrovoids were developed at the bottom of S-1 (Figure 4-1(a)), substrate S-2 had more uniform and better defined pores with pore diameters on the order of a few micrometers (Figure 4-2(a)). The improved pore structure of S-2 was likely due to the use of LiCl, a commonly used pore former to promote the development of the finger-like pores (Shi et al., 2008; Setiawan et al., 2012a). Further studies on the formation of such finger-like pores are recommended with regard to the substrate optimization. The bottom surfaces of S-1 and S-2 are shown in Figures 4-1(c) and 4-2(c), respectively. Sub-micrometer pores were observed for both substrates, although the pores for S-2 were larger. Similarly, the top surface (i.e., the spongy skin layer) of S-2 also appeared more porous than S-1 (Figures 4-1(d) and 4-2(d)). As a result of its higher bulk and surface porosity as well as the improved pore structure, S-2 had a relatively high pure water permeability of 190 L/(m^2 h bar), nearly double of that for S-1.

Based on Equation (3-7) and assuming a tortuosity of 1.0, the contribution of the finger-like pores to the overall structural parameter can be estimated (0.1 mm for S-1 and 0.09 mm for S-2). The large difference between the measured overall *S* values and the estimated values for the finger-like pores can be attributed to (1) the termination of some finger-like pores before they reached the back surface of the substrates (i.e., dead-end pores), and (2) the presence of the sponge-like skin layer (see Figures 4-1(b) and 4-2(b)). The porosity of this skin layer was likely much lower compared to the bulk porosity of the substrate. While the skin layer thickness was less than 2 μm, it nevertheless can make a significant contribution to the overall structural parameter as a result of its tortuous nature and low porosity. From a membrane fabrication point of view, there is a critical need to optimize this spongy skin layer. An overly porous skin layer with large surface pores may result in more defects in the polyamide rejection layer during interfacial polymerization and thus compromise the membrane rejection (Petersen, 1993). On the other hand, an overall thick spongy skin layer with low porosity and high tortuosity may unnecessarily compromise the structural parameter. In view of the critical importance of this skin

layer, further studies on the skin layer optimization are warranted.

In order to better understand the role of the support structure on the structural parameter *S* (the current section) and that on the FO performance (Section 4.3.3), four commercial membranes (CTA-HW, CTA-W, CTA-NW, and BW30) were also characterized. In addition, samples of the BW30 with its non-woven fabric support removed (denoted as BW30-o) were also studied. The properties of these membranes are summarized in Table 4-2, with their SEM cross-section micrographs shown in Figures 4-3(a)-(e). As shown in the micrographs, the CTA-HW (Figure 4-3(a)) and CTA-W (Figure 4-3(b)) membranes had a unique structure - both membranes had woven polyester meshes embedded in the asymmetric CTA membranes. These meshes had a fiber size ~30-40 μm and a fiber-to-fiber distance ~130-170 μm, in good agreement with microscopic observations in the literature (Wang et al., 2010c). Due to the presence of this woven mesh, the thickness of the membranes was highly non-uniform such that regions away from the mesh fibers were thinner than regions where fibers were located. Based on our current microscopic observations of multiple locations, the CTA-HW membrane had a thickness ranging from ~60 μm at the thinnest location to ~90 μm at the thickest location. The support layer of this membrane was highly porous (ε = 64%, Table 4-2), which was also confirmed by the SEM cross-section image (Figure 4-3(a)) that shows numerous large finger-like pores (10-40 μm in diameter, also see Ref. (Wang et al., 2010c)). The measured *S* value was ~0.72 mm, comparable to the substrates developed (S-1 and S-2, Table 4-2). Compared to the CTA-HW, the membrane CTA-W had a much less porous structure - large-sized pores were only observed near the fabric fibers (Figure 4-3(b)). As a result, its porosity was only ~46%. Correspondingly, the structural parameter for the CTA-W was higher than that for the CTA-HW, despite the thinner cross-section for the CTA-W (only ~20 μm at the thinnest location, Figure 4-3(b) and Table 4-2). This confirms the critical importance of the substrate porosity in determining the *S* value - large porosity is preferred to achieve a lower *S* value, agreeing well with Equation (3-7).

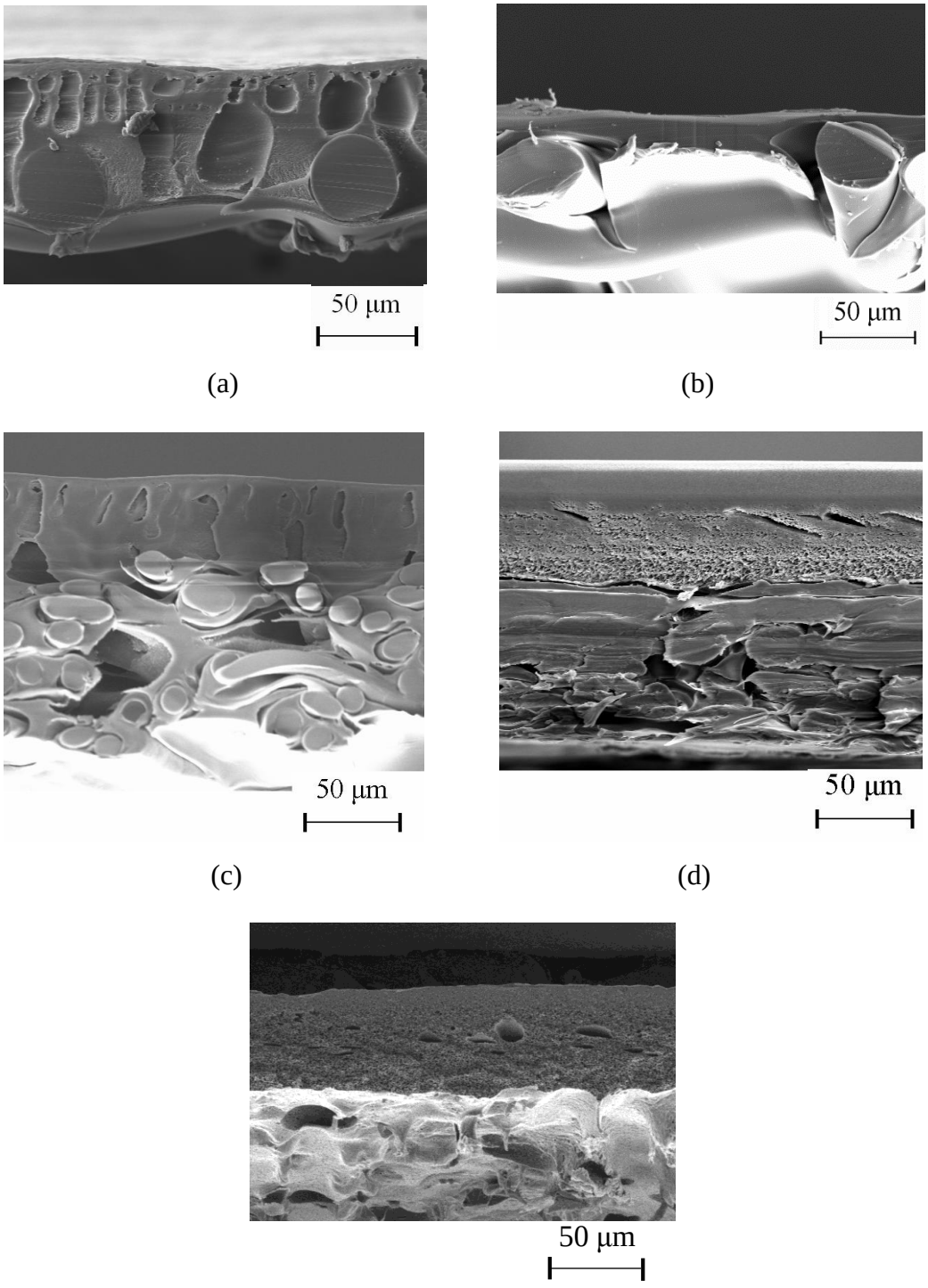

Figure 4-3 SEM cross-section micrographs of commercial FO and RO membranes. (a) CTA-HW FO membrane. (b) CTA-W FO membrane. (c) CTA-NW FO membrane. (d) BW30 RO membrane. (e) BW30 membrane without reinforcing fabric (BW30-o).

The structure of the CTA-NW is shown in Figure 4-3(c). Unlike the woven-

supported CTA-HW and CTA-W, the membrane CTA-NW had an asymmetric cellulose triacetate layer supported by a non-woven fabric. The cellulose triacetate layer was ~60 μm in thickness, and the non-woven fabric layer had a thickness ~80 μm. Consequently, the overall thickness of the CTA-NW was much greater than the other two CTA FO membranes (Table 4-2). The cellulose triacetate layer of the CTA-NW had a comparable thickness to that of the CTA-HW (Figures 4-3(a) and 4-3(c)). In addition, these two membranes also had similar pore structures, although the CTA-NW was slightly less porous (Table 4-2). The *S* value of the CTA-NW was ~1.38 mm, larger than that of CTA-HW (0.72 mm). The larger *S* value for the CTA-NW is consistent with its lower porosity and larger overall thickness due to the presence of the non-woven fabric layer.

Membrane BW30 is a typical commercial TFC polyamide membrane (Tang et al., 2007c; Tang et al., 2009b). This membrane comprises an ultrathin polyamide rejection layer, a polysulfone substrate, together with a non-woven fabric layer (see Figure 4-3(d) and Refs. (Tang et al., 2007c; b)). The thickness of the polysulfone layer and non-woven fabric layer were ~60 μm and ~90 μm, respectively. As shown in Table 4-2, the BW30 had the largest overall thickness among all the membranes evaluated. In addition, its non-woven fabric layer also appeared more compact and less porous than that of the CTA-NW (Figures 4-3(c) and 4-3(d)), presumably due to the need to withstand significantly higher applied pressure for typical RO applications. Thus, it is not surprising to see that the *S* value for the BW30 (~37.5 mm) was the largest among the various membranes in Table 4-2, partially due to the thick and compact non-woven fabric layer. However, the large *S* value cannot be solely attributed to the fabric layer. Upon removing the non-woven fabric layer, the resulting membrane (BW30-o, see Figure 4-3(e)) still had a very large *S* value of ~14.0 mm. Compared to the other membranes, the BW30 and BW30-o had a spongy pore structure for the polysulfone substrate instead of the straight finger-like pore structure. Despite its significant porosity (~50%, see Table 4-2), this spongy structure will likely result in a high tortuosity value. This explains why the *S* value of the BW30-o was an order of magnitude higher than the other membranes, even though its thickness and porosity were comparable to the other membranes. This

result is also consistent with the previous discussion that the *S* values of the membranes TFC-1 and TFC-2 were mainly contributed by the sponge-like skin layer despite its small thickness (< 2 μm).

The hydrophobicity of the polysulfone substrates prepared in the current studies was also characterized using contact angle measurements (Table 4-2). Both S-1 and S-2 had contact angles ~55 º, lower than that of the polysulfone layer of BW30 (~92 º) as well as those of the CTA membranes. The relatively small contact angles for S-1 and S-2 can be attributed to the addition of PVP in the membrane casting solutions. According to McCutcheon et al. (McCutcheon and Elimelech, 2008), hydrophilic substrates tend to have better FO flux performance as a result of improved wetting.

4.3.2 Characterization of membrane rejection layers

The active rejection layer of the TFC FO membranes was synthesized on top of the polysulfone substrate via interfacial polymerization, where the sponge-like skin layer of the substrate was responsible for providing a smooth surface and sufficient mechanical cushion for the polyamide rejection layer. As shown in the SEM images (Figures 4-4(a) for TFC-1 and 4-4(b) for TFC-2), the polyamide layers formed in the current study had a ridge-and-valley structure that is typical for TFC polyamide membranes formed by TMC and MPD monomers (Petersen, 1993; Tang et al., 2007a; Tang et al., 2009b). The contact angles of the polyamide rejection layers synthesized were ~45 º, comparable to that measured for the BW30 but lower than those of the CTA FO membranes (Table 4-3). The separation properties (water permeability *A*, NaCl rejection *R*, and NaCl permeability *B*) of membranes TFC-1 and TFC-2 were characterized and compared to commercial FO and RO membranes in the current section (Table 4-3).

Table 4-3 Properties of synthesized TFC FO membranes and commercial membranes [a]

Sample	Contact angle (°)	Surface morphology	Water permeability [b]		NaCl rejection [c] (%)	Salt permeability B [d] (10^{-8} m/s)	B/A [d] (bar)
			(L/(m^2 h bar))	(10^{-12} m/(s Pa))			
TFC-1	43 ± 4	Ridge-and-valley	1.15 ± 0.16	3.2 ± 0.5	94.5	4.7 ± 1.4	0.16 ± 0.06
TFC-2	45 ± 4	Ridge-and-valley	1.78 ± 0.23	5.0 ± 0.7	93.4	9.4 ± 1.9	0.20 ± 0.06
CTA-HW	63 ± 3	Smooth	1.19 ± 0.19	3.3 ± 0.5	78.5	25.6 ± 1.4	0.84 ± 0.08
CTA-W	73 ± 2	Smooth	0.33 ± 0.04	0.9 ± 0.1	81.9	4.0 ± 0.9	0.47 ± 0.12
CTA-NW	64 ± 2	Smooth	0.46 ± 0.07	1.3 ± 0.2	92.4	2.7 ± 0.2	0.22 ± 0.03
BW30	42 ± 2	Ridge-and-valley	3.04 ± 0.44	8.4 ± 1.2	92.2	18.9 ± 1.4	0.24 ± 0.03
BW30-o	42 ± 2	Ridge-and-valley	2.79 ± 0.40	7.8 ± 1.1	86.9	33.4 ± 4.3	0.47 ± 0.09

a. The experimental errors are reported as the standard deviation of at least 3 repeated measurements.

b. Evaluated in the RO testing mode over an applied pressure range of 1-5 bar with ultrapure water as the feed.

c. Evaluated in the RO testing mode at 3.75 bar with 20 mM NaCl as feed.

d. Evaluated in the RO testing mode over an applied pressure range of 1-5 bar for a feed water containing 20 mM NaCl.

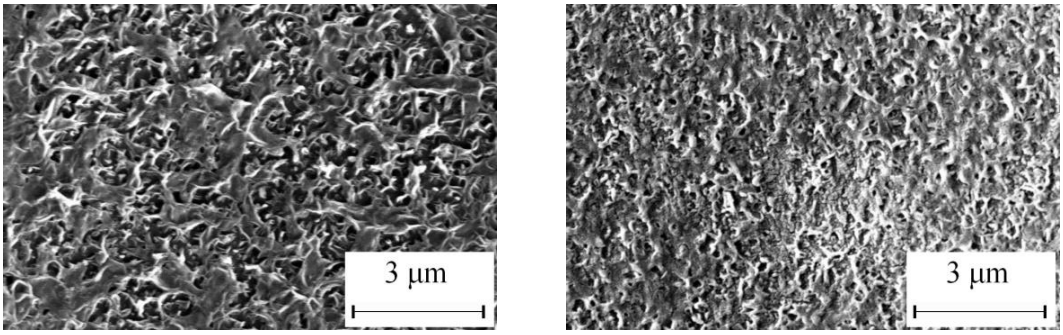

(a) (b)

Figure 4-4 SEM micrographs of the polyamide rejection layer of (a) TFC-1 and (b) TFC-2.

Both the TFC-1 and TFC-2 exhibited comparable or even higher water permeability and better NaCl rejection compared to the commercial CTA FO membranes (Table 4-3). For example, the TFC-2 had a pure water permeability of ~5.0×10^{-12} m/(s Pa), approximately 50% higher than that of the CTA-HW membrane. At an applied pressure of 3.75 bar in the RO testing mode, both the TFC-1 and TFC-2 had decent NaCl rejections of 94.5% and 93.4%, respectively. It is worthwhile to note that the solute rejection of an FO membrane can increase significantly at higher testing pressures (Tang et al., 2010). The TFC-2 had improved water permeability over the TFC-1, partially due to the use of the surfactant SDS in its recipe to improve the interfacial polymerization process (Table 4-1 and also see Ref. (Petersen, 1993)). The commercial BW30 membrane (with or without fabric) also had a high water permeability (~8×10^{-12} m/(s Pa)) while maintaining acceptable NaCl rejection of ~92% at 3.75 bar. At 13.8 bar, the BW30 had a rejection of ~98% (Tang et al., 2009b).

Figure 4-5 shows a plot of the NaCl permeability *B* versus the water permeability *A* for both TFC polyamide membranes as well as the CTA based membranes. In general, data points with a higher water permeability and lower NaCl permeability (corresponding to the lower right corner of Figure 4-5) are preferred. Compared to the CTA membranes that had relatively low *A* values, the TFC polyamide membranes (TFC-1, TFC-2, and BW30) showed superior separation properties of the rejection layers. Historically in the RO field, TFC membranes have replaced

cellulose acetate based membranes due to their superior separation properties and excellent pH stability (stable over pH 3-10) (Petersen, 1993). An added advantage of TFC membranes is that the rejection layer and the substrate can be individually optimized via the two-step fabrication method (phase inversion followed by interfacial polymerization) (Petersen, 1993). Such flexibility is especially valuable for FO membrane synthesis, due to the critical importance of both the support layer structure (Section 4.3.1) and the rejection layer separation properties. With a tailored support structure to minimize the *S* value and ICP, TFC polyamide based membranes can be promising alternatives to existing CTA based FO membranes (Section 4.3.3 and Refs. (Chou et al., 2010; Wang et al., 2010b; Yip et al., 2010)).

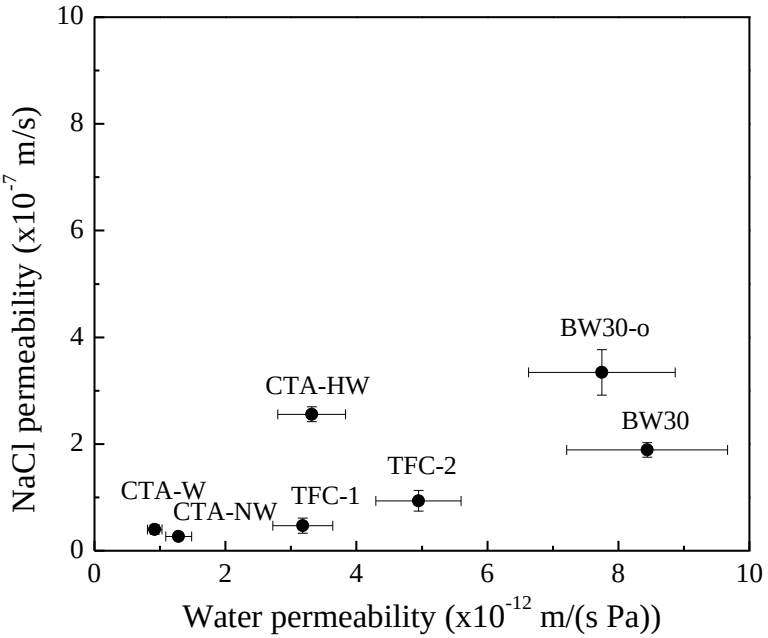

Figure 4-5 NaCl permeability versus water permeability for the synthesized TFC FO membranes and commercial membranes. Cross-flow RO testing conditions: 20 mM NaCl as feed, applied pressure over 1-5 bar, 23 ℃. The error bars represent standard deviations of at least three repeated measurements.

The *B/A* values of the various membranes are also tabulated in Table 4-3. As discussed by Tang and coworkers (Tang et al., 2010; Xiao et al., 2011; Zou et al., 2011), the *B/A* ratio is a direct indicator of the selectivity of an FO membrane. A larger *B/A* ratio (i.e., lower selectivity) is likely to cause more severe solute reverse

diffusion from the draw solution into the feed water (Tang et al., 2010; Xiao et al., 2011; Zou et al., 2011), which can lead to undesirable solute accumulation in FO systems (Xiao et al., 2011) as well as accelerated FO membrane fouling (Zou et al., 2011). In addition, the rejection of contaminants (such as micropollutants) by a dense membrane is also affected by the *B/A* ratio, with a lower *B/A* ratio (improved selectivity) generally preferred (Jin et al., 2011). In the current study, both the TFC-1 and TFC-2 had relatively low *B/A* ratios, once again indicating their superior separation properties.

4.3.3 FO performance evaluation

The FO water flux of the synthesized TFC FO membranes as well as the commercial membranes is shown in Table 4-4, where the feed solution contained 10 mM NaCl and the draw solution contained either 0.5 M or 2.0 M NaCl. Among all the membranes evaluated, the commercial RO membrane BW30 had the poorest FO water flux despite its superior water permeability ($A = 8.4 \times 10^{-12}$ m/(s Pa) or 3.04 L/(m^2 h bar)). A water flux of merely 3.20 L/(m^2 h) was obtained in the AL-DS FO testing mode using a 2.0 M NaCl draw solution (osmotic pressure ~100 bar). In contrast, an applied pressure of only 1.0 bar would be needed to achieve the same water flux in the RO mode. Compared to the pressure-driven RO mode, the osmotically-driven FO mode suffers from severe ICP. For the BW30 under the above mentioned testing conditions, ~99% of the overall osmotic driven force was lost due to ICP. Such FO flux inefficiency for the BW30 was the direct result of its sponge-like polysulfone substrate and the thick and compact non-woven support that hindered the mass transfer within its support (see Section 4.3.1). A previous study has also attributed the lower FO water flux of conventional TFC membranes with sponge-like supports to their support layer hydrophobicity (McCutcheon and Elimelech, 2008). Upon peeling away the non-woven fabric, the resulting membrane BW30-o still had an unacceptably low water flux (Table 4-4). The above results clearly suggest that the sponge-like substrate, which tends to have large tortuosity value thus promoting severe ICP, is highly undesirable for FO applications.

Table 4-4 FO water flux of synthesized TFC FO membranes and commercial membranes

Membrane orientation	AL-DS		AL-FS	
DS concentration	0.5 M	2.0 M	0.5 M	2.0 M
TFC-1	17.3 ± 1.1	41.3 ± 5.0	9.27 ± 0.37	17.4 ± 1.0
TFC-2	20.0 ± 0.7	53.7 ± 0.8	13.4 ± 2.0	25.1 ± 4.1
CTA-HW	16.2 ± 1.1	36.1 ± 0.3	9.03 ± 0.00	20.6 ± 3.3
CTA-W	7.10 ± 0.49	23.0 ± 0.4	5.36 ± 0.33	12.2 ± 0.2
CTA-NW	8.01 ± 0.16	19.7 ± 1.8	4.12 ± 0.26	7.64 ± 0.80
BW30	1.77 ± 1.15	3.20 ± 1.44	1.56 ± 0.69	1.96 ± 1.30
BW30-o	2.89 ± 1.35	4.46 ± 1.97	2.21 ± 0.98	3.34 ± 1.27

Testing conditions: 0.5 M or 2.0 M NaCl DS; 10 mM NaCl FS. FO water flux reported in units of L/(m^2 h). The experimental errors are reported as the standard deviation of at least three repeated measurements.

Both the commercial CTA FO membranes and the fabricated TFC FO membranes had relatively low *S* values. Compared to the BW30, these membranes achieved much higher FO water fluxes (Table 4-4). Among the three commercial FO membranes obtained from HTI, the membrane CTA-HW had the highest FO water flux. This can be explained by (1) its higher water permeability ($A = 3.3 \times 10^{-12}$ m/(s Pa), see Table 4-3) compared to the other two membranes, as well as (2) its higher porosity (Table 4-2). The TFC FO membranes fabricated in the current study (TFC-1 and TFC-2) had the highest FO water flux among all the membranes evaluated. With a 2.0 M NaCl draw solution and using the AL-DS orientation, the TFC-2 had a flux of ~54 L/(m^2 h), which was 50% higher compared to that of the CTA-HW, the best performing commercial FO membrane. The TFC-1 and TFC-2 had an *S* value in the range of 0.67-0.71 mm, similar to that of the CTA-HW. Thus, their better FO water flux over the CTA-HW was mainly due to their superior separation properties (Table 4-3). As predicted by Equations (3-8) and (3-9), a higher *A* value can result in improved water flux under otherwise identical test conditions (Appendix Section C). Consistent with this explanation, the more permeable TFC-2 had a higher FO flux compared to the TFC-1 and CTA-HW. The current study convincingly demonstrates that both a low *S* value and high *A* value

are needed to achieve an excellent FO water flux. While the commercial CTA-HW membrane was optimized in terms of its substrate to achieve a low *S* value (Section 4.3.1), its rejection layer was far from optimal (Section 4.3.2). On the other hand, the conventional RO membrane BW30 had superior water permeability but an unacceptably large *S* value.

The FO solute flux is plotted against the water flux for both membrane orientations (see Figure 4-6(a) for AL-DS and Figure 4-6(b) for AL-FS using a 0.5 M NaCl draw solution). An ideal FO membrane shall possess high water flux J_v and low solute flux J_s. A large J_s, indicating a severe leakage of draw solutes into the feed solution (i.e., solute reverse diffusion), is detrimental to FO operation. Increased solute reverse diffusion can promote severe ICP as well as membrane fouling (Xiao et al., 2011; Zou et al., 2011). The J_s/J_v ratio (i.e., the effective solute concentration reverse-diffused through the FO membrane (Tang et al., 2010; Xiao et al., 2011; Zou et al., 2011)) is represented by the slope between a data point and the origin. Thus, data points located in the lower right corner of the figures indicate preferred FO performance (higher J_v, lower J_s, and lower J_s/J_v ratio). The synthesized TFC FO membranes showed superior J_v and J_s combinations. Both the TFC-1 and TFC-2 achieved high water flux while maintaining relatively low J_s/J_v ratios. As discussed previously, the high water flux was due to their optimized substrate structure and superior water permeability of the rejection layer. On the other hand, the low J_s/J_v ratios can be attributed to their excellent selectivity (i.e., their low B/A ratios, see Section 4.3.2 and Table 4-3). The FO performance of the synthesized TFC FO membranes and those reported in literature is also tabulated in Table 4-5. In comparison, the TFC FO membranes generally performed better than the asymmetric membranes in terms of FO water flux and selectivity, for which the TFC membranes can achieve decent J_v and low J_s even when NaCl was used as draw solute. The current study suggests that thin film composite membranes offer significant advantages over integral asymmetric membranes – (1) the TFC approach allows flexibility for independent optimization of the substrate and the rejection layer, and (2) the polyamide rejection layer formed by interfacial polymerization also tends to have better water permeability and solute rejection (Petersen, 1993;

Tang et al., 2009b).

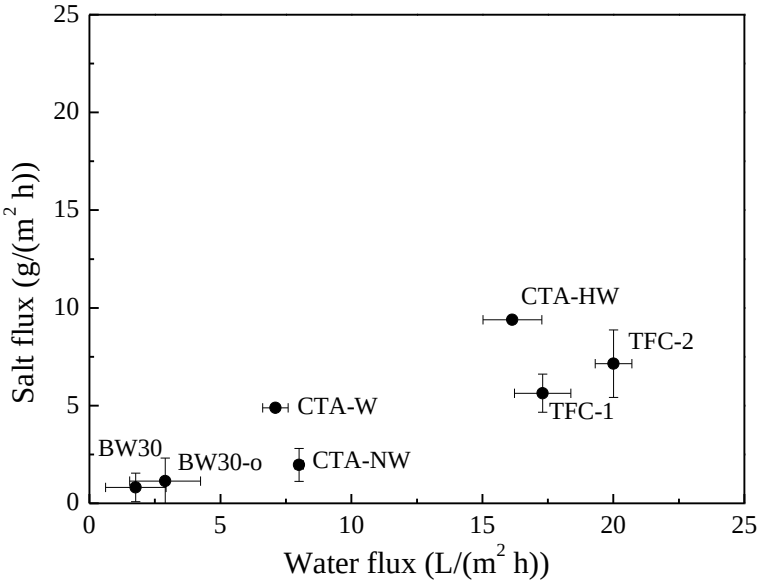

(a)

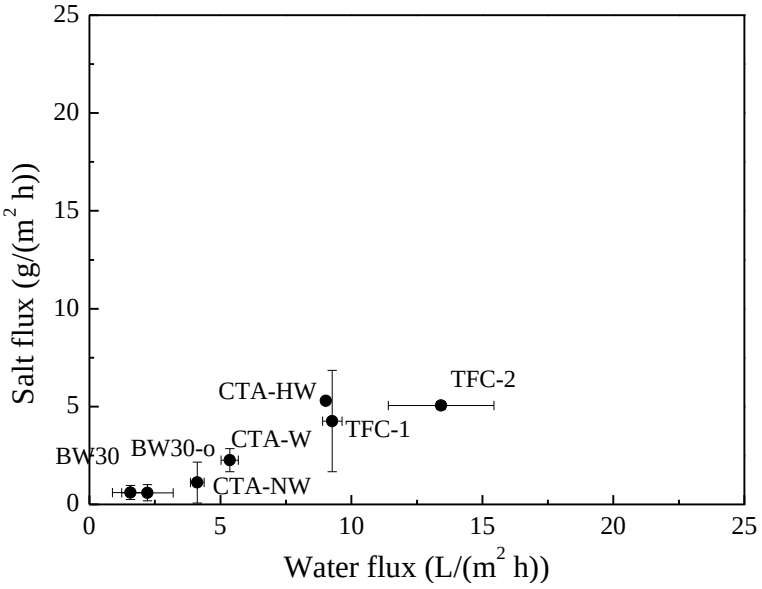

(b)

Figure 4-6 FO water flux and solute flux of synthesized TFC FO membranes and commercial membranes. Testing conditions: 10 mM NaCl as feed solution; 0.5 M NaCl as draw solution; with both membrane orientations: (a) AL-DS and (b) AL-FS. The error bars represent standard deviations of at least three repeated measurements.

Table 4-5 Comparison of FO performance with literature data

Structure	Material	FO performance			Testing conditions			References
		J_v (L/(m^2 h))	J_s (g/(m^2 h))	Membrane orientation	Feed solution	Draw solution	Temperature (℃)	
TFC flat-sheet membrane	Polyamide-polysulfone	17.3 ± 1.1	5.63 ± 0.98	AL-DS	10 mM NaCl	0.5 M NaCl	23	Present work
		9.27 ± 0.37	4.26 ± 2.59	AL-FS	10 mM NaCl	0.5 M NaCl	23	
TFC flat-sheet membrane	Polyamide-polysulfone	20.0 ± 0.7	7.15 ± 1.73	AL-DS	10 mM NaCl	0.5 M NaCl	23	
		13.4 ± 2.0	5.05 ± 0.20	AL-FS	10 mM NaCl	0.5 M NaCl	23	
Commercial asymmetric flat-sheet membrane (CTA-HW)	Cellulose triacetate	16.2 ± 1.1	9.39 ± 0.00	AL-DS	10 mM NaCl	0.5 M NaCl	23	
		9.03 ± 0.00	5.29 ± 0.00	AL-FS	10 mM NaCl	0.5 M NaCl	23	
Commercial asymmetric flat-sheet membrane (CTA-W)	Cellulose triacetate	7.10 ± 0.49	4.88 ± 0.13	AL-DS	10 mM NaCl	0.5 M NaCl	23	
		5.36 ± 0.33	2.26 ± 0.59	AL-FS	10 mM NaCl	0.5 M NaCl	23	
Commercial asymmetric flat-sheet membrane (CTA-NW)	Cellulose triacetate	8.01 ± 0.16	1.96 ± 0.84	AL-DS	10 mM NaCl	0.5 M NaCl	23	
		4.12 ± 0.26	1.12 ± 1.05	AL-FS	10 mM NaCl	0.5 M NaCl	23	
TFC flat-sheet membranes	Polyamide-polysulfone	18.16 ± 0.96	-	AL-FS	DI water	1.5 M NaCl	25 ± 0.5	(Yip et al., 2010)
TFC flat-sheet membranes	Polyamide-polysulfone	20.5 ± 3.8	-	AL-FS	DI water	1.0 M NaCl	25 ± 0.5	(Tiraferri et al., 2011)
TFC flat-sheet membranes	Polyamide-polysulfone	13.9 ± 1.0	-	AL-FS	DI water	1.0 M NaCl	25 ± 0.5	
TFC flat-sheet membranes	Polyamide-polysulfone	9.2 ± 0.2	-	AL-FS	DI water	1.0 M NaCl	25 ± 0.5	
TFC flat-sheet membranes	Polyamide-polysulfone	6.2 ± 2.8	-	AL-FS	DI water	1.0 M NaCl	25 ± 0.5	

Structure	Material	FO performance			Testing conditions			References
		J_v (L/(m^2 h))	J_s (g/(m^2 h))	Membrane orientation	Feed solution	Draw solution	Temperature (℃)	
TFC flat-sheet membranes	Polyamide-polysulfone	10.8 ±2.4	-	AL-FS	DI water	1.0 M NaCl	25 ±0.5	
TFC flat-sheet membranes	Polyamide-polysulfone	12.5 ±1.0	-	AL-FS	DI water	1.0 M NaCl	25 ±0.5	
TFC flat-sheet membranes	Polyamide-polysulfone	14.3 ±2.5	-	AL-FS	DI water	1.0 M NaCl	25 ±0.5	
TFC flat-sheet membranes	Polyamide-polysulfone	25.0 ±4.1	-	AL-FS	DI water	1.0 M NaCl	25 ±0.5	
TFC flat-sheet membranes	Polyamide-polysulfone	17.6 ±0.4	-	AL-FS	DI water	1.0 M NaCl	25 ±0.5	
TFC flat-sheet membranes	Polyamide-polysulfone	5.6 ±1.6	-	AL-FS	DI water	1.0 M NaCl	25 ±0.5	
TFC flat-sheet membranes	Polyamide-polysulfone	0.5 ±0.1	-	AL-FS	DI water	1.0 M NaCl	25 ±0.5	
TFC flat-sheet membranes	Polyamide-polysulfone	5.4 ±0.6	-	AL-FS	DI water	1.0 M NaCl	25 ±0.5	
TFC flat-sheet membranes	Polyamide-polysulfone	5.6	-	AL-FS	DI water	1.0 M NaCl	25 ±0.5	
Double-skinned flat-sheet membrane	Cellulose acetate	48.2	6.5	$MgCl_2$-Bottom	DI water	5.0 M $MgCl_2$	22 ±0.5	(Wang et al., 2010a)
		27.4	3.9	$MgCl_2$-Top	DI water	5.0 M $MgCl_2$	22 ±0.5	
Double-skinned flat-sheet membrane	Cellulose acetate	17.3 ±0.4	1.2 ±0.2	AL-DS	DI water	2.0 M $MgCl_2$	22 ±0.5	(Zhang et al., 2010)
		10.3 ±0.3	0.8 ±0.1	AL-FS	DI water	2.0 M $MgCl_2$	22 ±0.5	
Double-skinned flat-sheet membrane	Cellulose acetate	14.7 ±1.0	2.2 ±0.4	AL-DS	DI water	2.0 M $MgCl_2$	22 ±0.5	
		9.8 ±0.7	1.2 ±0.3	AL-FS	DI water	2.0 M $MgCl_2$	22 ±0.5	
Double-skinned flat-sheet membrane	Cellulose acetate	9.5 ±0.4	698.6 ±14.8	AL-DS	DI water	2.0 M $MgCl_2$	22 ±0.5	
		7.9 ±0.5	824.8 ±15.0	AL-FS	DI water	2.0 M $MgCl_2$	22 ±0.5	

Structure	Material	FO performance			Testing conditions			References
		J_v (L/(m^2 h))	J_s (g/(m^2 h))	Membrane orientation	Feed solution	Draw solution	Temperature (℃)	
TFC hollow fiber	Polyamide-polyethersulfone	12.9	5.0	AL-DS	DI water	0.5M NaCl	23	(Wang et al., 2010b)
		5	2.12	AL-FS	DI water	0.5M NaCl	23	
TFC hollow fiber	Polyamide-polyethersulfone	32.2	3.5	AL-DS	DI water	0.5M NaCl	23	
		14	1.75	AL-FS	DI water	0.5M NaCl	23	
TFC hollow fiber	Polyamide-polyethersulfone	32.9	2.9	AL-DS	500 ppm (8.6 mM) NaCl	0.5M NaCl	20-25	(Chou et al., 2010)
Positively charged hollow fiber	Poly(amide-imide)-polyethyleneimine	6.34	3.0	AL-DS	DI water	1.5 M $MgCl_2$	23	(Setiawan et al., 2011)
		4.15	1.9	AL-FS	DI water	1.5 M $MgCl_2$	23	
Positively charged hollow fiber	Poly(amide-imide)-polyethyleneimine	17.3	16.6	AL-DS	DI water	1.5 M $MgCl_2$	23	
		11.7	3.9	AL-FS	DI water	1.5 M $MgCl_2$	23	
Positively charged hollow fiber	Poly(amide-imide)-polyethyleneimine	17.2	37.7	AL-DS	DI water	1.5 M $MgCl_2$	23	
		12.9	4.8	AL-FS	DI water	1.5 M $MgCl_2$	23	
Asymmetric hollow fiber	Cellulose acetate	7.3	-	AL-DS	DI water	2.0M $MgCl_2$	-	(Su et al., 2010a)
		5.0	-	AL-FS	DI water	2.0M $MgCl_2$	-	
Asymmetric hollow fiber	Polybenzimidazole	3.84	-	AL-DS	DI water	2.0 M NaCl	22.5	(Wang et al., 2007)
Asymmetric hollow fiber	Polybenzimidazole	5.65	-	AL-DS	DI water	2.0 M $MgSO_4$	22.5	
Asymmetric hollow fiber	Polybenzimidazole	7.74	-	AL-DS	DI water	2.0 M Na_2SO_4	22.5	
Asymmetric hollow fiber	Polybenzimidazole	9.02	-	AL-DS	DI water	2.0 M $MgCl_2$	22.5	

Structure	Material	FO performance			Testing conditions			References
		J_v (L/(m^2 h))	J_s (g/(m^2 h))	Membrane orientation	Feed solution	Draw solution	Temperature (℃)	
Asymmetric hollow fiber	Polybenzimidazole	36.5	-	AL-DS	DI water	5.0 M $MgCl_2$	23	(Wang et al., 2009)
Asymmetric hollow fiber	Polybenzimidazole	32.4	-	AL-DS	DI water	5.0 M $MgCl_2$	23	
Dual-layer hollow fiber	polybenzimidazole-polyethersulfone/polyvinyl pyrrolidone	17.1	-	AL-DS	0.1 g/L lysozyme aqueous solution	3.125 M $MgCl_2$	-	(Yang et al., 2009b)
		12.7	-	AL-FS	0.1 g/L lysozyme aqueous solution	3.125 M $MgCl_2$	-	
Dual-layer hollow fiber	polybenzimidazole-polyethersulfone/ polyvinyl pyrrolidone	24.2	-	AL-FS	DI water	5.0 M $MgCl_2$	23	(Yang et al., 2009a)
Dual-layer hollow fiber	polybenzimidazole-polyethersulfone/ polyvinyl pyrrolidone	33.8	-	AL-DS	DI water	5.0 M $MgCl_2$	23	
Dual-layer hollow fiber	polybenzimidazole-polyethersulfone/ polyvinyl pyrrolidone	45.6	-	AL-DS	DI water	5.0 M $MgCl_2$	38.5	

4.4 Conclusions

In this chapter, thin film composite FO membranes were synthesized. The polysulfone substrates, prepared by phase inversion, had long finger-like pores under a thin sponge-like skin layer. The polyamide rejection layers were then formed by interfacial polymerization of TMC and MPD. The resulting FO membranes (TFC-1 and TFC-2) had small structural parameters (S = 0.67-0.71 mm) as a result of the thin cross-section, low tortuosity, and high porosity of the membrane substrates. In addition, these membranes had a high water permeability and selectivity. In comparison to commercial CTA-based asymmetric FO membranes as well as the brackish water RO membrane BW30, both the TFC-1 and TFC-2 exhibited superior FO performance. With a 2.0 M NaCl draw solution in the AL-DS orientation, the TFC-2 achieved a flux of ~54 L/(m^2 h), which was 50% higher than the commercial FO membrane CTA-HW. This was attributed to the combination of its high permeability rejection layer and its high-porosity substrate with a finger-like pore structure. Meanwhile, the TFC FO membranes had relatively low J_s/J_v ratios as a result of their excellent rejection layer selectivity.

Chapter 5
Influence of monomer concentrations on the performance of polyamide-based thin film composite forward osmosis membranes

5.1 Introduction

The optimal features of high-performance FO membranes include a support layer with a small structural parameter and an active rejection layer with high water permeability and excellent solute rejection. In this study, TFC FO membranes were fabricated by a two-step approach: (1) the porous substrates are formed by phase inversion, and then (2) a thin polyamide rejection layer is prepared by interfacial polymerization of diamine and trimesoyl chloride. Therefore, the structural parameter of the support layer can be individually reduced by optimizing the phase inversion step. In parallel, the separation properties of the membranes are also allowed to be customized by changing the interfacial polymerization conditions. (Petersen, 1993).

Among the handful of existing studies on TFC FO membranes, a few studies (Wang et al., 2010b; Tiraferri et al., 2011; Wei et al., 2011b) have focused on the effect of the membrane substrate on FO performance. On the other hand, systematic studies on the role of the polyamide rejection layer on FO performance are still lacking. It is generally understood in the RO literature that there is a strong trade-off between the water permeability and salt rejection of TFC-based RO membranes- a polyamide rejection layer with higher water permeability typically has a lower salt rejection (Tang et al., 2009b; Geise et al., 2011). Unlike pressure-driven membrane processes, the FO water flux is highly non-linear with respect to the membrane water permeability and solute rejection, as well as the osmotic driving force (see Equations 3-8 and 3-9) (Tang et al., 2010). This is mainly due to the presence of internal concentration polarization in FO processes (Loeb et al., 1997; McCutcheon and Elimelech, 2006; Tang et al., 2010). The trade-off between the membrane water

permeability and solute rejection imposes a critical and complicated constraint for optimizing FO membrane performance, which deserves further attention.

The objective of this chapter was to investigate the effect of the TFC polyamide layer fabrication conditions on FO performance. In this chapter, the TFC polyamide membranes were prepared by interfacial polymerization of MPD and TMC in view of the superior salt rejection of the resulting membranes (Petersen, 1993; Roh et al., 1998). The reaction scheme is shown in Figure 5-1. The resulting polyamide rejection film has a three-dimensionally crosslinked structure, with *n* being the crosslinking density (Tang et al., 2007c). The influence of the monomer concentration used in the interfacial polymerization and the resulting polyamide rejection layer separation properties on FO performance was systematically studied. This investigation may provide important insights into TFC FO membrane synthesis and optimization. In addition, it may help membrane users to select the most suitable membranes for a given FO application.

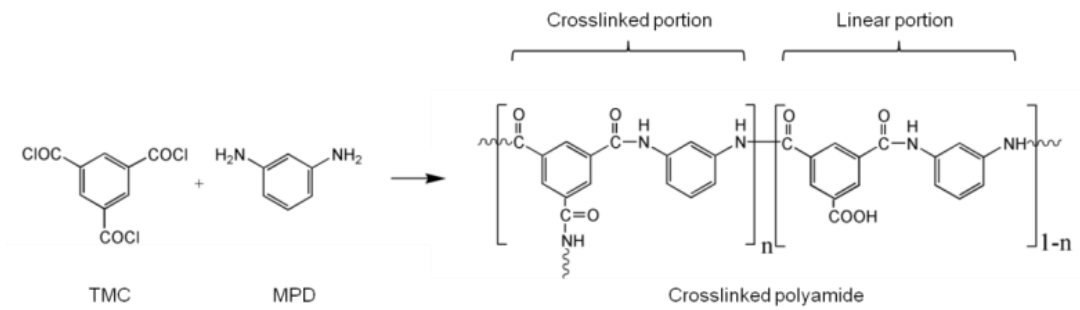

Figure 5-1 Schematic of interfacial polymerization (Tang et al., 2007c).

5.2 Materials and methods

5.2.1 Chemicals

All reagents used in this chapter were of analytical grade and were used as received. Polysulfone beads (molecular weight 75,000-81,000 Da, Solvay Advanced Polymers, LLC), n-Methyl-2-pyrrolidone (NMP, Merck Schuchardt OHG), and polyvinyl pyrrolidone (PVP, average molecular weight 1,300,000 Da, Alfa Aesar) were used to prepare the membrane substrates. M-phenylenediamine (MPD, Sigma-Aldrich Inc.), trimesoyl chloride (TMC, Sinopharm Chemical Reagent Co. Ltd),

and n-hexane (Fisher Scientific) were used to synthesize the rejection layer of the TFC FO membranes. Sodium chloride (NaCl, Merck KGaA) solutions were used to evaluate both the membrane intrinsic separation properties and the FO performance. Ultrapure water with a resistivity of 18.2 MΩ.cm was obtained from a Milli-Q water system (Millipore Singapore Pte. Ltd.), and was used throughout this study unless specified otherwise.

5.2.2 Preparation of TFC FO membranes

5.2.2.1 Preparation of substrate

The TFC FO membrane was prepared by synthesizing a polyamide rejection layer on the surface of a porous polysulfone substrate. For substrate preparation, a casting solution composed of 17.5 wt.% polysulfone, 0.5 wt.% PVP and 82.0 wt.% NMP (identical composition to substrate S-1 in Chapter 4) was prepared by continuous stirring at 70 °C. The function of each reagent can be referred to Section 3.2.1. After cooling to room temperature (23 ℃), the polymer solution was filtered and then degassed for 24 h. An Elcometer 4340 motorised film applicator (Elcometer Asia Pte. Ltd.) was used to cast the polymer solution onto a clean glass plate at a gate height of 175 μm. The glass plate was then smoothly immersed into a coagulant bath filled with tap water (23 ℃) to induce phase separation. The time between casting the film and immersing it in the coagulant bath was controlled within 10 ± 1 s. The relative humidity in the ambient air was 64 ± 4%. The resulting polysulfone substrate was washed thoroughly in a flowing water bath for 24 h to remove the excess solvent and additives. The clean substrate was then stored in ultrapure water before use.

5.2.2.2 Preparation of polyamide rejection layer

The rejection layer of the TFC FO membrane was formed by interfacial polymerization of MPD and TMC (see reaction schematic in Figure 5-1). The function of each monomer can see Section 3.2.2. Interfacial polymerization is an instantaneous reaction, which would be quickly inhibited by the growing film at the interface between the aqueous and organic phases. The resulting polyamide rejection layer typically has a thickness of several hundred nanometers (Khare et al.,

2003; Tang et al., 2007c). Due to the fast reaction, interfacial polymerization is diffusion-controlled, for which the resulting polyamide crosslinking density is determined by the ratio and magnitude of the instantaneous monomer flux to the reaction front (Khare et al., 2003; 2004). Therefore, membranes with different separation properties would be obtained by varying the concentration driving force, i.e., the monomer concentrations. However, the influence of monomer concentrations on the polyamide properties and the corresponding FO performance has yet to be studied. Therefore, two series of FO membranes were prepared in this Chapter, as shown in Table 5-1. In the first series (the MPD series), the aqueous solutions (MPD in water) contained MPD concentrations ranging from 0.5 wt.% to 2.0 wt.%, while the organic solutions (TMC in n-hexane) had a fixed concentration of 5.0 mg/ml. In the second series (the TMC series), the MPD concentration was held constant at 1.0 wt.%, and the TMC concentration varied from 0.5 mg/ml to 10.0 mg/ml.

Table 5-1 Preparation conditions for TFC FO membranes

S/N		Casting solution for substrate	Reagents for interfacial polymerization	
			MPD in water (wt.%)	TMC in n-hexane [a] (mg/ml)
MPD series	1	17.5 wt.% polysulfone, 0.5 wt.% PVP, 82.0 wt.% NMP	0.5	5.0
	2		1.0	5.0
	3		1.5	5.0
	4		2.0	5.0
TMC series	1	17.5 wt.% polysulfone, 0.5 wt.% PVP, 82.0 wt.% NMP	1.0	0.5
	2		1.0	1.0
	3		1.0	5.0
	4		1.0	10.0

a. The unit of TMC solution concentration (mg/ml) represents the ratio of TMC mass over the volume of solvent (n-hexane).

Before interfacial polymerization, the polysulfone substrates were heated in a 70 °C water bath for 2 min and then quenched in a 23 °C water bath. The substrates were

then soaked in an MPD solution for 2 min. After removing the excess MPD solution on the substrate surface with compressed nitrogen gas, a TMC solution was gently poured onto the substrate surface. TMC was allowed to react with MPD for 1 min to form the polyamide rejection layer, followed by draining off the excess TMC solution from the membrane surface. The nascent composite membrane was washed with fresh tap water and stored in ultrapure water before further use.

5.2.3 Membrane characterization

5.2.3.1 Characterization of membrane substrates

Images of the polysulfone substrates were obtained with a Zeiss EVO 50 Scanning Electron Microscope (SEM, Carl Zeiss Pte. Ltd.). Vacuum dried membrane samples were fractured in liquid nitrogen and were sputter-coated with a uniform layer of gold using an EMITECH SC7620 sputter coater (Quorum Technologies Ltd., UK) before SEM imaging. The thicknesses of membranes were measured from the SEM cross-section images and were further verified by measurement using a micrometer. The membrane porosity (ε) was determined by gravimetric measurement of dry and wetted membrane samples (Equation 3-1). The S value of the substrate was determined by fitting experimental FO water flux data using Equations (3-8) and (3-9), where the rejection layer water permeability A and solute permeability B were measured independently from cross-flow RO tests (Section 5.2.3.2). Sessile drop contact angle measurements were performed using an OCA Contact Angle System (DataPhysics Instruments GmbH).

5.2.3.2 Measurement of membrane intrinsic separation properties

The intrinsic separation properties of the synthesized TFC FO membranes were evaluated using the cross-flow RO filtration setup (Figure 3-1). All the RO tests were performed at 23 °C at an applied pressure of 1 bar using a feed water containing 100 ppm NaCl. The water permeability was determined based on gravimetric measurement of the permeate water flux (Equation 3-2), and the salt rejection was determined based on feed and permeate water conductivity measurements (Ultrameter II^{TM} 4P, Myron L Company) (Equation 3-3).

5.2.3.3 Measurement of FO performance

The FO performance of the TFC FO membranes was evaluated using the bench-scale cross-flow FO setup (Figure 3-2). All the FO tests were performed at room temperature (23 °C). The feed solution and draw solution were circulated at a fixed cross-flow rate of 23.2 cm/s. Diamond-pattern spacers were placed on both sides of the membrane to minimize the effect of external concentration polarization (Wang et al., 2010c). An aqueous solution containing 10 mM NaCl was used as the feed. Concentrated NaCl solutions (0.5 M and 2.0 M) were used as draw solutions. The FO tests were performed in both the AL-DS and AL-FS orientations. The FO water flux J_v and salt flux J_s were determined by measuring the weight and concentration change of the feed solution at predetermined time intervals (Equation 3-5 and 3-6).

5.3 Results and discussion

5.3.1 Properties of membrane substrates

Substrates prepared in this part of the work had the same composition as the substrate S-1 reported in Chapter 4. SEM examination of the cross-sections (micrographs not shown) revealed identical structural features: thin and highly porous cross-sections with finger-like pores. For completeness, the substrate properties are summarized below (data obtained from Table 4-2):

- Thickness: 76.1 ± 3.0 μm
- Porosity: $77 \pm 3\%$
- *S* value: 0.71 ± 0.14 mm
- contact angle: $56 \pm 1°$

The small structural parameter (as a result of the thin cross-section, large porosity, and long finger-like pores) and relatively low contact angle tend to reduce internal concentration polarization (McCutcheon and Elimelech, 2008; Wei et al., 2011b). McCutcheon et al. (McCutcheon and Elimelech, 2008) reported that the FO water flux can be significantly improved at increased substrate hydrophilicity as a result of improved substrate wetting. The contact angle of the polysulfone substrate was significantly lower than the commercial HTI FO membranes (contact angle ~70°,

Table 4-3). On the other hand, its structural parameter is comparable or slightly lower than the HTI membranes (*S* ranging from 0.72 - 1.38, Table 4-2).

5.3.2 Intrinsic separation properties of TFC FO membranes

The active rejection layer of the TFC FO membranes was prepared by interfacial polymerization of MPD and TMC. The monomer concentrations were systematically changed to obtain membranes with different separation properties (Table 5-1).

Figure 5-2 shows the influence of the MPD concentration on the membrane separation properties, where the TMC concentration was fixed at 5 mg/ml. The water permeability was reduced drastically from 5.7 to 1.3 L/(m^2 h bar) when the MPD concentration increased from 0.5 wt.% to 1.0 wt.%. Further increase in the MPD concentration from 1.0 wt.% to 2.0 wt.% resulted in another 1/3 reduction in the water permeability. Correspondingly, the salt rejection was increased from 45% to 75% and the *B/A* value was reduced from 1.14 bar to 0.31 bar over the MPD concentration range of 0.5 wt.% to 2.0 wt.%. Under FO conditions, the salt flux/water flux ratio is proportional to the *B/A* value. Thus, the MPD concentration would have significant influence on the FO performance of the membranes, which will be discussed in Section 5.3.3. The current results suggest the formation of denser and less permeable rejection layers at the higher MPD concentrations. Similar results have been reported by other researchers (Song et al., 2005; Roh et al., 2006). Due to the instantaneous reaction, interfacial polymerization is strongly controlled by the diffusion of MPD and TMC to the reaction front. In particular, the MPD monomer has to diffuse through the growing film because the reaction with TMC occurs on the organic side. The crosslinking density of the resulting polyamide film is significantly determined by the ratio and magnitude of the monomer fluxes to the reaction front (Khare et al., 2003; 2004). A low monomer concentration would lead to low concentration driving force and thus a "loose" polyamide film was formed. Increasing the MPD concentration can monotonically enhance the degree of crosslinking and form a denser film. With increasing TMC concentration, however, the degree of cross-linking will reach a maximum while the

degree of branching increasing monotonically. An increased MPD/TMC ratio tended to promote a higher degree of crosslinking, which was likely responsible for the simultaneous decrease in water permeability and increase in salt rejection.

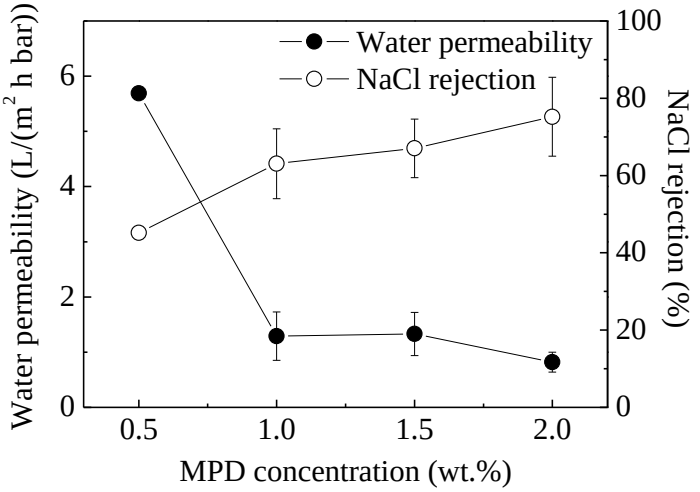

Figure 5-2 Intrinsic separation properties of TFC membranes prepared with varied MPD concentrations and fixed TMC concentration (5 mg/ml). Cross-flow RO testing conditions: 100 ppm NaCl as feed, applied pressure of 1 bar, 23 ℃. The error bars represent the standard deviation among three membrane coupons tested.

Figure 5-3 shows the effect of the TMC concentration on the membrane water permeability and NaCl rejection, where the MPD concentration was kept constant at 1.0 wt.%. Increasing the TMC concentration from 0.5 mg/ml to 10.0 mg/ml resulted in a ~50% enhancement of the water permeability. Meanwhile, the membrane rejection was also very sensitive to the change in TMC concentration since it decreased from 83% to 51%. At the moderate MPD concentration (1.0 wt.%) used in the current study, a higher TMC concentration might result in a deficiency of MPD at the reaction front. The lower MPD/TMC ratio tends to result in more unreacted acyl chloride groups and thus a reduced degree of crosslinking of the polyamide rejection layer (Roh et al., 2006; Jin and Su, 2009), which explains the higher water permeability and lower salt rejection.

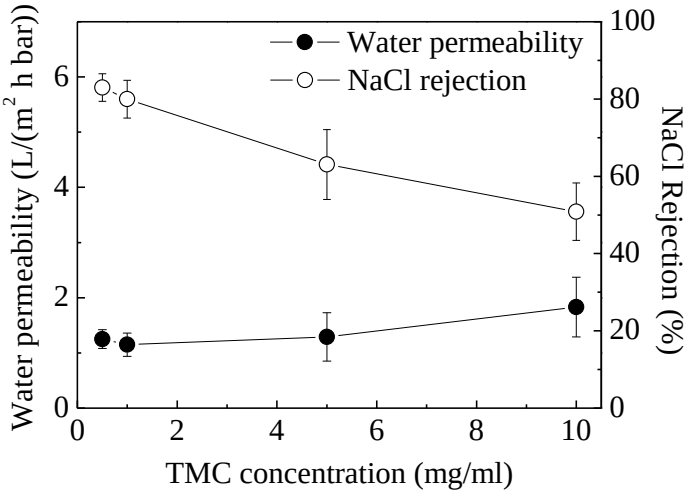

Figure 5-3 Intrinsic separation properties of TFC membranes prepared with varied TMC concentrations and fixed MPD concentration (1.0 wt.%). Cross-flow RO testing conditions: 100 ppm NaCl as feed, applied pressure of 1 bar, 23 ℃. The error bars represent the standard deviation among three membrane coupons tested.

The above results demonstrated a strong trade-off between membrane water permeability and salt rejection, which is in good agreement with the literature (Tang et al., 2009b). This has important implications for TFC FO membrane optimization. While the higher water permeability of a "looser" (i.e., less crosslinked) membrane tends to enhance the FO water flux due to reduced membrane resistance (Tang et al., 2011; Wei et al., 2011b), its lower salt rejection may simultaneously cause a more severe ICP due to the solute reverse diffusion (which has the opposite effect of decreasing the FO water flux (Saren et al., 2011; Tang et al., 2011)). This poses a strong constraint on the available FO water flux, which will be further discussed in Section 5.3.3.

5.3.3 Influence of monomer concentrations on FO performance

5.3.3.1 Influence of MPD concentration on FO performance

The FO water flux and salt flux of the TFC membranes were evaluated using a 10 mM NaCl feed solution in both the AL-DS and AL-FS orientations. The draw solution contained either 0.5 M or 2.0 M NaCl. The dependence of the FO performance on interfacial polymerization conditions (i.e., monomer concentrations) is shown in Figure 5-4 and Figure 5-5.

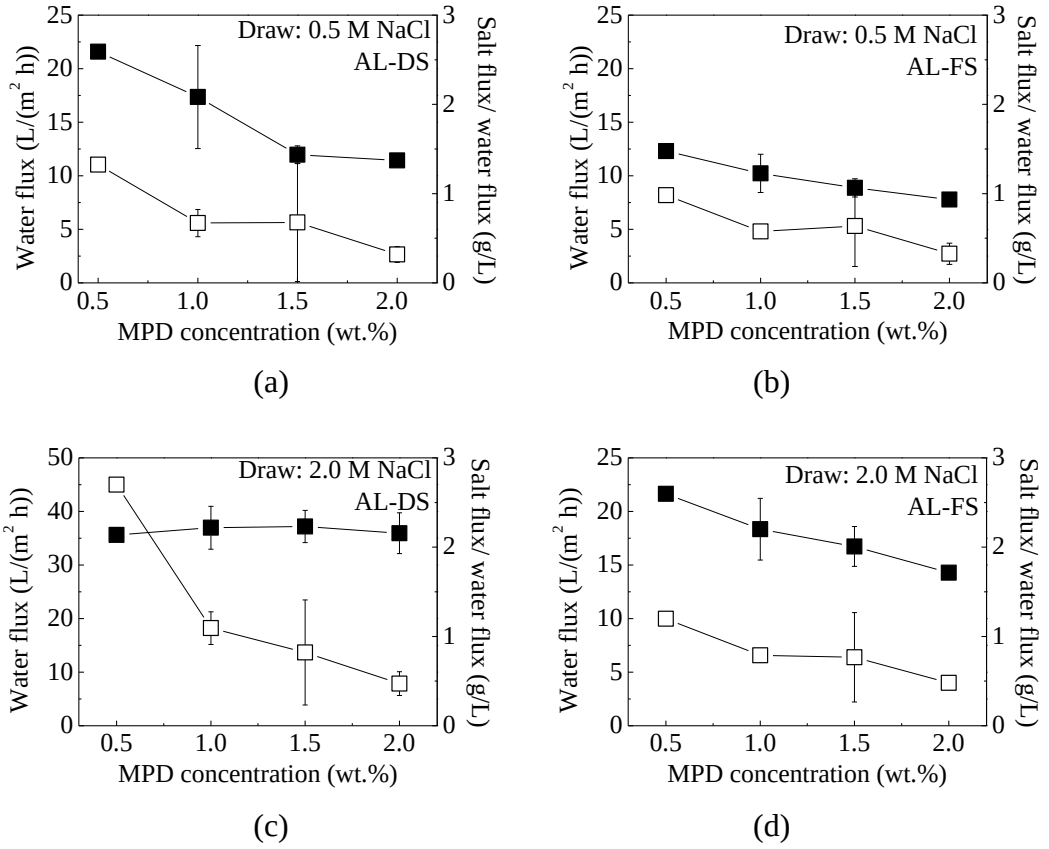

Figure 5-4 FO performance of TFC membranes prepared with varied MPD concentrations and fixed TMC concentration of 5 mg/ml (-■- water flux; -□- salt flux/water flux). (a) AL-DS and (b) AL-FS orientations for a 0.5 M NaCl draw solution. (c) AL-DS and (d) AL-FS orientations for a 2.0 M NaCl draw solution. The feed solutions contained 10 mM NaCl. The error bars represent the standard deviation among three membrane coupons tested.

Figure 5-4 shows the effect of the MPD concentration on both the FO water flux J_v and the salt flux/water flux ratio J_s/J_v. Using a 0.5 M NaCl draw solution in the AL-DS orientation, J_v decreased from 22 to 11 L/(m^2 h) as the MPD concentration increased from 0.5 wt.% to 2.0 wt.% (Figure 5-4 (a)). This can be attributed to the reduced water permeability of the membranes at higher MPD concentrations (Figure 5-2), since a lower water permeability generally means a greater decrease in the osmotic driven force due to the membrane hydraulic resistance (see Appendix Section C and Refs. (Chou et al., 2010; Tang et al., 2011)). Meanwhile, the J_s/J_v ratio, an important performance parameter in the FO process (Achilli et al., 2010; Saren et al., 2011; Xiao et al., 2011; Zou et al., 2011), was also significantly reduced with increasing MPD concentration. Previous studies demonstrated that the

J_s/J_v ratio is directly related to the membrane selectivity (Phillip et al., 2010; Tang et al., 2010; Tang et al., 2011; Wei et al., 2011b; Xiao et al., 2011; Zou et al., 2011). Thus, the reduced solute reverse diffusion for membranes formed at higher MPD concentrations is readily explained by their better membrane rejection (Figure 5-2). An excessively large J_s/J_v ratio is undesirable due to (1) the severe solute accumulation on the feed side arising from solute reverse diffusion (Lay et al., 2011; Xiao et al., 2011), (2) the increased risk of reverse-diffusion-induced membrane fouling (Zou et al., 2011), (3) the poor retention against contaminants in the feed solution (Jin et al., 2011), and (4) the higher draw solution replenishment cost (Achilli et al., 2010). A similar trend was also observed for the AL-FS orientation using a 0.5 M NaCl draw solution (i.e., both J_v and J_s/J_v decreased at higher MPD concentrations, see Figure 5-4(b)), although the FO water flux in AL-FS was generally lower due to its more severe internal concentration polarization (McCutcheon and Elimelech, 2006; Tang et al., 2010; Li et al., 2011c; Tang et al., 2011).

Figures 5-4(c) and (d) show the effect of MPD concentration on FO performance using a 2.0 M NaCl draw solution for the AL-DS and AL-FS orientations, respectively. In both cases, the J_s/J_v ratio decreased at higher MPD concentrations. Once again, this confirms that membranes with a better rejection tend to have a lower J_s/J_v ratio (Tang et al., 2010; Tang et al., 2011). However, it is interesting to compare the FO water flux trends in the AL-DS orientation for the 0.5 M and 2.0 M draw solutions. While increasing the MPD concentration from 0.5 wt.% to 2.0 wt.% led to a ~50% reduction in the water flux for a 0.5 M DS (Figure 5-4(a)), J_v was only marginally affected by the MPD concentration for a 2.0 M DS (Figure 5-4(c)). Despite the fact that the water permeability of the membrane formed for a 0.5 wt.% MPD was an order of magnitude higher than that for a 2.0 wt.% MPD, this did not translate into any obvious enhancement in the FO water flux. This can be explained by the more severe solute reverse diffusion for the 0.5 wt.% MPD case- while its higher water permeability tends to promote a greater FO water flux due to the lower membrane resistance loss, its poor solute retention has the tendency to promote a more severe ICP and thus to reduce the water flux (Saren et al., 2011). As an

extreme case, a membrane that has a very high water flux but no rejection against the draw solution will perform badly in terms of the FO water flux since the osmotic pressure difference cannot be effectively established across the membrane. Here, the net effect of the membrane separation properties on J_v is likely to be governed by the competition between the frictional loss mechanism and the solute-reverse-diffusion-induced-ICP mechanism. For the 0.5 M NaCl draw solution in the current study, the J_s-induced-ICP mechanism was likely less important due to its relatively low water flux levels (~ or < 20 L/(m^2 h)) noting that the ICP increases exponentially with the water flux, which supports the experimental observation that increasing water permeability had a net positive effect on the FO water flux at this lower DS concentration. At higher water flux levels (for the 2.0 M NaCl DS), the J_s-induced-ICP mechanism became more important, such that it counter-balanced the positive effect of higher water permeability. Finally, the FO water flux in the AL-FS orientation for the 2.0 M NaCl DS is shown in Figure 5-4(d). In this particular case, J_v decreased at higher MPD concentrations (lower water permeability). Once again, this suggests that J_s-induced-ICP was less important, most likely as a result of the relatively low water flux level in this orientation.

It is also worthwhile to note that the ICP is strongly affected by the membrane structural parameter S (McCutcheon and Elimelech, 2006; Li et al., 2011c; Tang et al., 2011; Wei et al., 2011b). For substrates with very small S values, the J_s-induced-ICP mechanism is probably less important and the membrane frictional loss tends to be more critical. In this case, a high A value (i.e., less crosslinked TFC membranes) may be more important in order to enhance the FO water flux. For membranes with larger S values, the role of solute rejection may become increasingly more important due to the more severe ICP. Furthermore, a small S value can increase both the water flux and solute flux, but the J_s/J_v ratio will not be affected (Tang et al., 2010; Tang et al., 2011). According to prior studies (Tang et al., 2010; Tang et al., 2011), this ratio is mainly governed by the membrane selectivity.

5.3.3.2 Influence of TMC concentration on FO performance

The effect of TMC concentration on TFC FO performance is shown in Figure 5-5. In all cases, increasing the TMC concentration resulted in higher J_s/J_v ratios (Figures 5-5(a)-(d)), which is consistent with the reduced membrane solute rejection (Figure 5-3). On the other hand, the dependence of the FO water flux on the TMC concentration was more complicated (also refer to Section 5.3.3.1). For the 0.5 M NaCl draw solution, the FO water flux increased at higher TMC concentrations in both the AL-DS (Figure 5-5(a)) and AL-FS (Figure 5-5(b)) orientations. This trend matched well with that of the water permeability (Figure 5-3), i.e., higher J_v was obtained for the more permeable membranes. A similar trend was also observed for the 2.0 M DS in the AL-FS membrane orientation (Figure 5-5(d)). In these three series of tests, membranes prepared with 10.0 mg/ml TMC during interfacial polymerization exhibited the highest water flux. This supports our previous discussion (Section 5.3.3.1) that increasing membrane water permeability tends to improve the FO water flux. The solute reverse diffusion effect on J_v was likely less important in these cases due to their relatively low water flux levels (< 25 L/(m^2 h)).

However, with a 2.0 M NaCl draw solution in the AL-DS orientation, the opposite trend for the FO water flux was observed- J_v decreased at higher TMC concentration (Figure 5-5(c)) despite the increased water permeability. As discussed in Section 5.3.3.1, increasing water permeability does not necessarily lead to a better FO water flux, especially when J_s-induced-ICP plays a dominant role. In these tests, the FO water flux (35-45 L/(m^2 h)) was relatively high and thus would be less sensitive to the increased water permeability at higher TMC concentrations. In addition, the salt rejection of the membranes was greatly reduced at higher TMC concentrations. For example, the NaCl rejections were 83% and 51% for the membranes prepared with 0.5 mg/ml and 10.0 mg/ml TMC, respectively (Figure 5-3). The 10.0 mg/ml TMC membrane suffered serious salt leakage when it was exposed to the high-concentration draw solution (2.0 M NaCl), which was compounded with a relatively high water flux level to result in a severe solute-reverse-diffusion-induced ICP (see Section 5.3.3.1 and Ref. (Saren et al., 2011)). Thus, the reduction in FO water flux at higher TMC concentrations was likely due

to the dominance of J_s-induced-ICP mechanism over the membrane-resistance-loss mechanism.

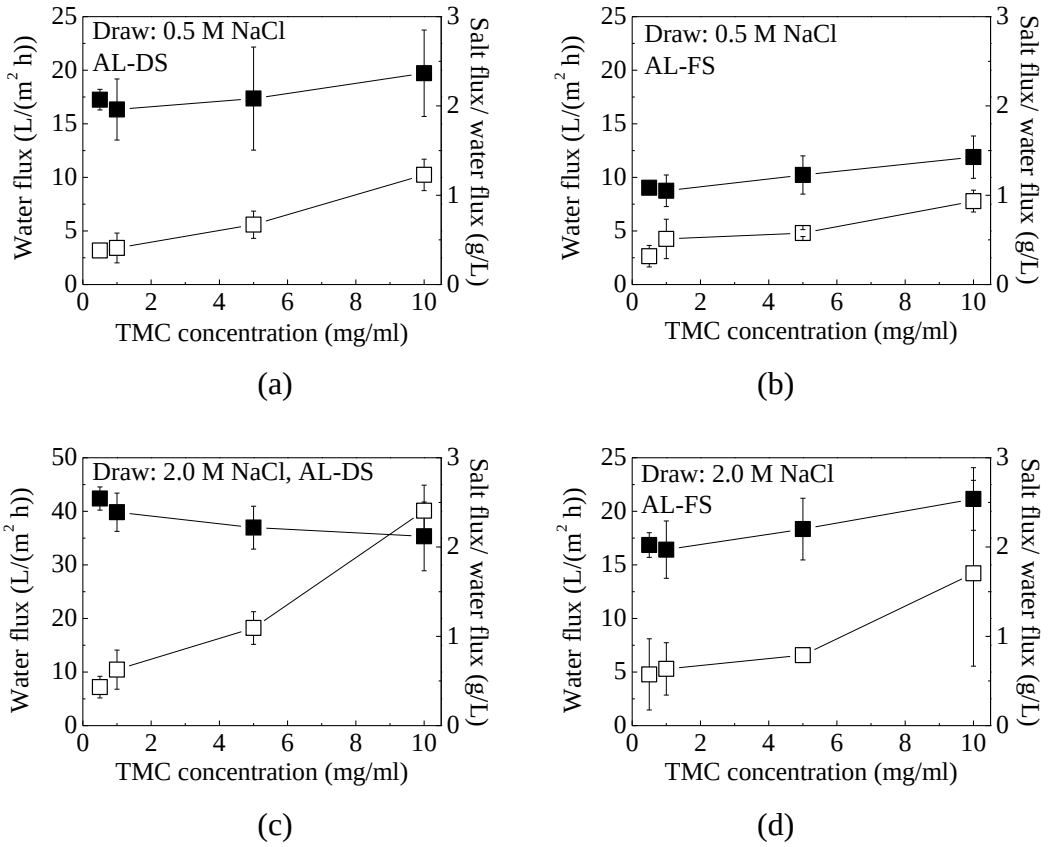

Figure 5-5 FO performance of TFC membranes prepared with varied TMC concentrations and fixed MPD concentration of 1.0 wt.% (-■- water flux; -□- salt flux/water flux). (a) AL-DS and (b) AL-FS orientations for a 0.5 M NaCl draw solution. (c) AL-DS and (d) AL-FS orientations for a 2.0 M NaCl draw solution. The feed solutions contained 10 mM NaCl. The error bars represent the standard deviation among three membrane coupons tested.

5.3.4 Implications for FO membrane optimization

Unlike pressure-driven RO membranes whose water flux generally increases with increased water permeability, the current study reveals that the FO water flux is governed by both the membrane water permeability and its solute retention in a highly non-linear manner. Thus, the optimization of the FO water flux calls for careful consideration of the various competing mechanisms. Under conditions where solute reverse diffusion may cause a severe J_s-induced ICP (e.g., higher draw solution concentration and higher water flux level), membranes should be optimized

to achieve a high salt rejection even if this is at the expense of lower water permeability (see Figures 5-4(c) and 5-5(c) and Refs. (Saren et al., 2011; Tang et al., 2011)). Furthermore, the reverse-diffused solutes may also accumulate in the feed solution (Lay et al., 2011; Xiao et al., 2011) or even interact with the foulants in the feed solution to cause severe membrane fouling (Zou et al., 2011), which further underscores the importance of the membrane rejection on the optimized and stable FO water flux. On contrast, membranes with a very low water permeability are likely to be dominated by the frictional loss due to their high hydraulic resistance (Saren et al., 2011; Tang et al., 2011). In such cases, improving the water permeability will likely improve the FO water flux. The current study seems to support the notion that both excessively low water permeability and excessively high water permeability are not desirable for FO optimization based on a previous modeling study (Tang et al., 2011). A balance between water permeability and salt rejection is especially important in the development of high-flux FO membranes where a relatively high ICP level may be encountered.

The current study also reveals that the optimization of an FO membrane will depend on its specific application conditions (e.g., membrane orientation and draw solution concentration). As a result of the highly non-linear dependence of FO on operating conditions and membrane properties, an optimized membrane for one specific application does not necessarily guarantee a good performance under other operating conditions. For example, while the membrane for a 10.0 mg/ml TMC had the highest water flux for a 0.5 M NaCl draw solution in AL-DS (Figure 5-5(a)), it had the lowest water flux for a 2.0 M NaCl DS in the same membrane orientation (Figure 5-5(c)). Future FO membrane optimization studies need to explicitly consider the constraints imposed by membrane synthesis with respect to the different competing mechanisms (frictional loss and ICP) for each given FO application.

5.4 Conclusions

In this chapter, the influence of monomer concentrations and the resulting TFC membrane separation properties on the FO performance were systematically

investigated:

- According the RO test results, a strong trade-off between membrane water permeability and salt rejection was observed. TFC membranes prepared with higher MPD concentrations or lower TMC concentrations had a lower water permeability but better salt rejection.
- The FO solute reverse diffusion was directly related to the membrane rejection (which can be obtained by RO tests); higher salt rejection was favorable for reducing the J_s/J_v ratio.
- The FO water flux was affected by both the membrane water permeability and solute rejection. Under conditions where the membrane-frictional-loss mechanism dominates (e.g., at low water flux level due to lower draw solution concentration used and/or in the AL-FS orientation), better FO water flux can be achieved by increasing the membrane water permeability. In contrast, a higher membrane rejection may be more important under conditions where solute reverse diffusion may cause enhanced ICP of the back-diffused draw solutes.
- In viewing the trade-off between membrane permeability and rejection as well as the highly non-linear dependence of FO flux on membrane properties and operating conditions, FO membranes should be optimized in according to the major mechanism (e.g., frictional loss versus solute-reverse-diffusion-induced ICP) under the specific operating conditions. Under conditions where the membrane frictional loss dominates the FO flux behavior (e.g., low DS concentration), the A value plays a more important role in determining the FO water flux. However, when ICP is severe, the membrane solute rejection can be more critical compared to its water permeability in FO optimization. In the latter case, a more densely crosslinked TFC membrane may be preferred.

Chapter 6

Comparison of NF-like and RO-like thin film composite forward osmosis membranes - Implications for membrane selection and process optimization

6.1 Introduction

The past decade has witnessed a surge of research activities on FO technology, which is accompanied by increasing attention to FO membrane fabrication (Zhao et al., 2012b). As discussed in Chapter 5, a critical property of high-performance FO membranes is a high solute rejection to prevent the solute diffusion through the membrane and to generate a sufficient osmotic pressure difference across the membrane (Hancock and Cath, 2009). With the significant interest of using seawater as either the feed solution (e.g., FO based seawater desalination (Chou et al., 2010)) or draw solution (e.g., PRO based osmotic power generation from the controlled mixing of a seawater and a river water (She et al., 2012b)), most of the existing membrane fabrication work has focused on developing FO membranes with a high sodium chloride rejection (e.g., with RO-like separation properties) (Herron, 2005; Chou et al., 2010; Wang et al., 2010b; Yip et al., 2010; Bui et al., 2011; Song et al., 2011; Tiraferri et al., 2011; Wei et al., 2011b; Yip et al., 2011; Yu et al., 2011; Wang et al., 2012b). However, high-rejection RO-like skins tend to have a relatively low water permeability (Tang et al., 2009b; Geise et al., 2011), which may limit membrane performance under certain conditions (Wei et al., 2011a).

Recently, research on FO technology has been expanded to more applications (Hoover et al., 2011). Promising examples include the forward osmosis membrane bioreactor (Cornelissen et al., 2008; Achilli et al., 2009b; Lay et al., 2010; Cornelissen et al., 2011; Alturki et al., 2012; Zhang et al., 2012a), osmotic power generation (Yip et al., 2011; Chou et al., 2012), water recovery (Cath et al., 2005a; Lutchmiah et al., 2011), desalination (Tan and Ng, 2010; Zhao et al., 2012a), liquid

food processing (Petrotos and Lazarides, 2001; Jiao et al., 2004), and microbial fuel cells (Zhang et al., 2011a). The diverse applications impose different requirements on the membrane properties. For example, water flux reduction and deterioration of biological activity in an OMBR system were observed, partly due to the build-up of salinity in the reactor (Xiao et al., 2011; Alturki et al., 2012). In this case, "loose" membranes with a lower rejection to feed solutes (e.g., NF-like FO membranes) may be able to minimize the accumulation of feed solutes in the bioreactor, provided that proper draw solutes are used. NF-like membranes also tend to have a higher water permeability than RO-like membranes (Tang et al., 2009b; Geise et al., 2011) and they may have a different fouling tendency compared to the RO-like counterparts. Until recently, there have been only a few NF-like FO membranes reported, prepared by various methods such as phase inversion (Wang et al., 2007; Yang et al., 2009a; Su et al., 2010a), chemical crosslinking (Qiu et al., 2011b; Setiawan et al., 2011; 2012b), and layer-by-layer assembly (Qiu et al., 2011a; Saren et al., 2011; Qi et al., 2012b). Nevertheless, systematic comparisons of RO-like and NF-like FO membranes (e.g., in terms of their water flux and solute rejection, fouling propensity, operational constraints, and potential applications) are still lacking.

The objective of this chapter was to systematically compare NF-like and RO-like FO membranes in terms of their flux performance and fouling behavior. Due to the growing interest in TFC FO membranes (Zhao et al., 2012b), NF-like and RO-like TFC polyamide FO membranes were prepared on identical porous substrates. The influence of membrane surface characteristics and separation properties on FO performance (water flux, solute rejection, and fouling behavior) was investigated. The results may have important implications for membrane selection and process operation for FO applications.

6.2 Materials and methods

6.2.1 Chemicals

Polysulfone (molecular weight 75,000-81,000 Da, Solvay Advanced Polymers LLC), polyethylene glycol (PEG, molecular weight 600 Da, Samchun Pure

Chemical Ind. Co., Ltd.), lithium chloride (LiCl, Merck Schuchardt OHG) and n-Methyl-2-pyrrolidone (NMP, Merck Schuchardt OHG) were used to prepare the substrates of the TFC FO membranes. Piperazine (PIP, Sigma-Aldrich Inc.), triethylamine (TEA, Alfa Aesar), m-phenylenediamine (MPD, Sigma-Aldrich Inc.), ε-caprolactam (Merck Schuchardt OHG), sodium dodecyl sulfate (SDS, Scientific Apparatus), trimesoyl chloride (TMC, Sigma-Aldrich Inc.) and n-hexane (Merck KGaA) were used to synthesize the polyamide rejection layers. Sodium chloride (NaCl, Merck Schuchardt OHG), sodium sulfate (Na_2SO_4, Merck Schuchardt OHG) and trisodium citrate ($Na_3C_6H_5O_7$, Wako Pure Chemical Industries Ltd.) were used to evaluate the membrane intrinsic separation properties and FO performance. Alginic acid sodium salt extracted from brown algae (referred to as alginate, A2158, Sigma-Aldrich Inc.) was used as a model foulant in the FO fouling tests. The feed solution pH and ionic composition in the fouling tests were adjusted by adding hydrochloric acid (HCl, Merck Schuchardt OHG), sodium hydroxide (NaOH, Merck Schuchardt OHG) and calcium chloride ($CaCl_2$, Unichem Inc.). All the chemicals were of analytical grade and were used as received. Ultrapure water supplied from a Milli-Q water system (Millipore Singapore Pte. Ltd.) with a resistivity of 18.2 MΩ.cm was used throughout this study unless specified otherwise.

6.2.2 Membrane preparation

TFC FO membranes were prepared via a two-step process, including a phase inversion step to cast a porous substrate and an interfacial polymerization step to form an NF-like or RO-like rejection layer on the substrate. Identical polysulfone substrates were used to prepare both the NF-like and the RO-like FO membranes, in order to specifically study the effect of the rejection layer properties on the FO performance. To prepare the substrate, a polymer solution containing 16.0 wt.% polysulfone, 5.0 wt.% PEG, 2.0 wt.% LiCl, and 77 wt.% NMP was prepared by continuous stirring at 70 °C. The function of each chemical can be referred to Section 3.2.1. The polymer solution was degassed at 23 °C for 24 h, and was spread onto a clean glass plate using an Elcometer 4340 film applicator (Elcometer Asia Pte. Ltd.) at a casting gate height of 150 μm. The relative humidity in the air during

casting was 64 ± 4%. The cast film was immediately immersed into a tap water bath to induce phase separation. The time between casting the film and immersing it in the coagulant bath was 10 ± 1 s. The solidified membrane was moved to a flowing water bath to remove any residual solvent and was stored in ultrapure water before use.

The rejection layers of NF-like and RO-like TFC FO membranes were synthesized using identical interfacial polymerization procedures, except that different recipes were used (Table 6-1). Precast polysulfone substrates were heated in a 70 °C water bath for 2 min before interfacial polymerization, followed by quenching in a 23 °C water bath for a compact and stable substrate structure. Recipes for the NF-like (denoted as TFC-N) and RO-like (denoted as TFC-R) rejection layer preparation are given in Table 6-1. The function of each reagent can be referred to Section 3.2.2. To prepare the rejection layer, the substrate was first soaked in a diamine (PIP or MPD) aqueous solution for 2 min. Excess solution was removed from the membrane surface using compressed nitrogen gas. Then the substrate was brought into contact with a n-hexane solution of TMC for 1 min. The interfacial polymerization reaction between diamine and TMC monomers formed a crosslinked ultrathin polyamide rejection layer on the substrate. The resulting membranes were thoroughly washed in flowing water bath, and were stored in ultrapure water before use.

Table 6-1 Monomer solutions for synthesis of the rejection layer of the NF-like (TFC-N) and RO-like (TFC-R) TFC FO membranes

	Diamine solution (in water)	TMC solution (in n-hexane) [a]
TFC-N	PIP 1.0 wt.%, TEA 1.0 wt.%, SDS 0.1 wt.%	TMC 2.0 mg/ml
TFC-R	MPD 1.5 wt.%, ε-caprolactam 1.5 wt.%, SDS 0.1 wt.%	TMC 1.0 mg/ml

a. The unit of TMC solution concentration (mg/ml) represents the ratio of TMC mass over the volume of solvent (n-hexane).

6.2.3 Membrane characterization

6.2.3.1 Membrane surface properties

Both the substrate and the TFC FO membranes were characterized by attenuated total reflection-Fourier transform infrared spectroscopy (ATR-FTIR, Spectrum 2000 FTIR Spectrometer, PerkinElmer). The surface morphology and structure of the membranes were examined using scanning electron microscopy (SEM, Zeiss EVO 50, Carl Zeiss). Before SEM observation, samples were sputter-coated with a thin layer of gold using an EMITECH SC7620 sputter coater (Quorum Technologies Ltd.). The membrane surface roughness was determined using atomic force microscopy (AFM, XE-100, Park Systems). The contact angles of the membranes were measured using the sessile drop method (Contact Angle System OCA, DataPhysics Instruments GmbH).

6.2.3.2 Membrane intrinsic separation properties

The water and salt permeabilities of the TFC FO membranes were evaluated in the cross-flow RO setup (Figure 3-1) at 23 °C with a feed pressure of 5 bar. the water permeability (A) was determined using pure water as the feed and was calculated by measuring the permeate flux through the membrane (Equation 3-2). The salt permeability (B) values for three model salts (NaCl, Na_2SO_4 and trisodium citrate) were evaluated individually using a feed salt concentration of 10 mM. Conductivities of the feed and permeate streams were measured (Ultra Meter II^{TM} 4P, Myron L Company) to calculate the membrane rejection as well as the salt permeability (Equation 3-3 and 3-4).

6.2.3.3 FO performance

The FO water flux J_v and salt flux J_s of the TFC FO membranes were evaluated using the cross-flow FO setup (Figure 3-2). Both the AL-DS and the AL-FS orientations were evaluated. The draw solutions were prepared using NaCl, Na_2SO_4 or trisodium citrate. Trisodium citrate is a safe sodium salt that is often used as a food additive and medical reagent. Its acidity constants are 3.13 (pK_{a1}), 4.76 (pK_{a2}) and 6.40 (pK_{a2}). Thus, a trisodium citrate aqueous solution has a high pH (9.3 ± 0.1) compared to typical inorganic strong electrolytes (e.g., ~6 for NaCl solution). The high solubility of trisodium citrate (42.5 g/100 ml at 25 ℃) in water enables generating sufficient osmotic pressure for FO applications. Therefore, it was chosen

as a potential draw solute in addition to the commonly used inorganic draw solutes NaCl and Na_2SO_4. A 10 mM NaCl solution was used as the FS to simulate the typical total dissolved solutes content in domestic wastewater, secondary effluent or ground water. Parallel tests with pure water as the FS were conducted to determine the reverse diffusion of draw solute. In addition, a 0.5 M NaCl FS was also tested to simulate seawater desalination conditions. The temperature of all the FO tests was maintained at 23 °C. For calculations of the FO water flux and salt flux refer to Section 3.3.3.

6.2.3.4 FO fouling tests

The fouling behavior of the TFC-N and TFC-R were evaluated in the AL-FS orientation (the more fouling resistant orientation (Tang et al., 2010)) using alginate as a model foulant. For each test, the membrane was first equilibrated with the FS (containing 7 mM NaCl and 1 mM $CaCl_2$) and DS (1.5 M Na_2SO_4) for 30 min before alginate was added to the FS to start membrane fouling. The fouling test was then continued for 14 h; the water flux right before adding foulant was taken as the initial flux. Baseline tests (without foulant addition) were similarly conducted. The experimental conditions for fouling test were as follows:

- FS: 100 mg/L alginate, 7 mM NaCl and 1 mM $CaCl_2$, pH 6.0 $\pm$ 0.1;
- DS: 1.5 M Na_2SO_4;
- Cross-flow velocities of both the FS and DS: 23.2 cm/s;
- Temperature: 23 ℃.

The fouled membranes were characterized by SEM to check the foulant deposition. In addition, membrane coupons (area ~15 cm^2) were cut from both the fouled and clean membranes and were gently rinsed with pure water. They were then soaked in 0.001 M NaOH under mild sonication for 20 min to extract the foulant from the membrane surface (Wang and Tang, 2011b). The extract was analyzed by the phenol-sulfuric acid method using UV wavelength of 485 nm to determine the deposited foulant mass.

6.3 Results and discussion

6.3.1 Membrane surface properties

In this study, NF-like and RO-like TFC FO membranes were prepared using identical polysulfone substrates, for which the cross-section was shown in Figure 6-1. The substrate had a small thickness of 74.6 ± 0.8 μm. The cross-section of the substrate showed a highly porous structure with elongated finger-like pores aligned under a sponge-like skin layer. The porosity of the substrate was as high as 77.0 ± 0.6%. Thus, a moderate structural parameter of the substrate was achieved (0.87 ± 0.18 mm). The thin and highly porous substrate structure was specially designed to achieve a lower ICP potential based on prior studies.

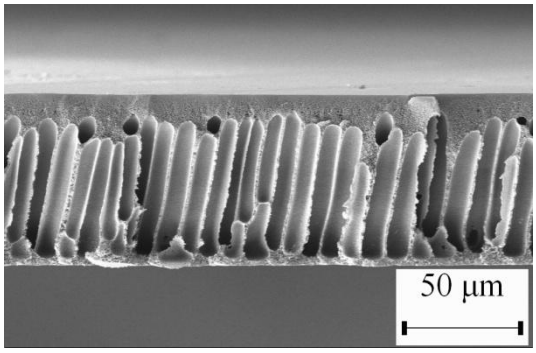

Figure 6-1 Cross-sectional SEM image of the polysulfone substrate of NF-like and RO-like TFC FO membranes.

ATR-FTIR spectra of the substrate and FO membranes are shown in Figure 6-2(a). Comparison between the spectra of the TFC-N and the substrate shows a new peak at ~1620 cm^{-1} for the TFC-N, which can be assigned to the amide I band for the semi-aromatic poly(piperazine-amide) layer (Tang et al., 2009a). The TFC-R had three characteristic peaks at 1659 cm^{-1} (amide I band), 1611 cm^{-1} (aromatic amide) and 1547 cm^{-1} (amide II band) of the fully aromatic polyamide chemistry (Tang et al., 2009a). SEM micrographs show that the TFC-N (Figure 6-2(b)) had a smoother surface compared to the TFC-R (Figure 6-2(c)). The ridge-and-valley roughness structure of the TFC-R, which was absent in the TFC-N, is characteristic of the MPD/TMC-based fully aromatic polyamide rejection layer (Tang et al., 2009a). Based on AFM characterization (Figure 6-2(d) and (e)), the root-mean-square

roughness (R_{rms}) values were 29.0 ± 4.4 nm for TFC-N and 184.9 ± 19.9 nm for TFC-R (Table 6-2). The surface contact angles of TFC-N and TFC-R were 25.7 ± 3.9 ° and 39.2 ± 5.2 °, respectively (Table 6-2), which are in good agreement with previously reported values for semi-aromatic and fully aromatic polyamide films (Tang et al., 2009b). The significantly different surface properties of the TFC-N and TFC-R may have important implications for their fouling behavior (see Section 6.3.4), since membranes with smoother and more hydrophilic surfaces tend to have better fouling resistance for pressure-driven membrane processes (Vrijenhoek et al., 2001; Li et al., 2007; Wang and Tang, 2011c).

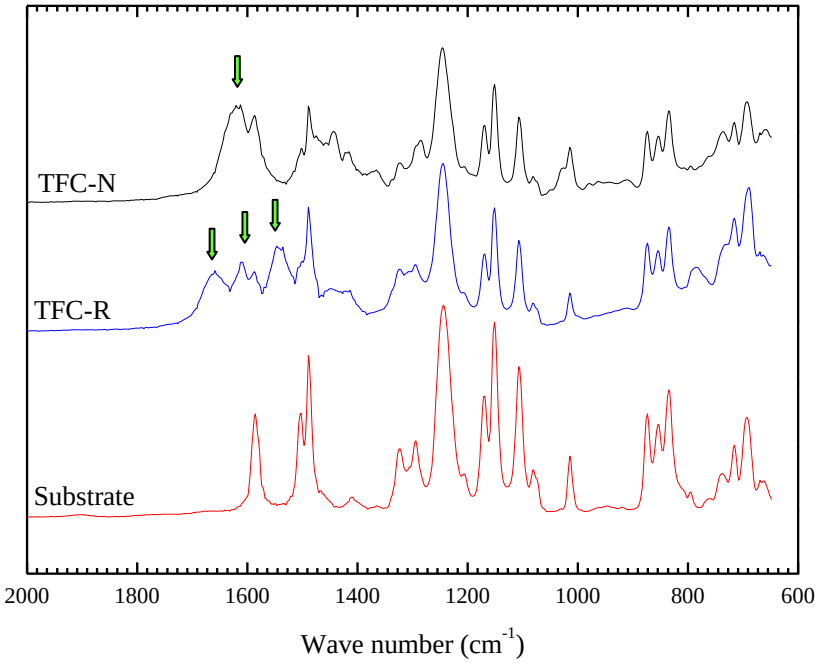

(a)

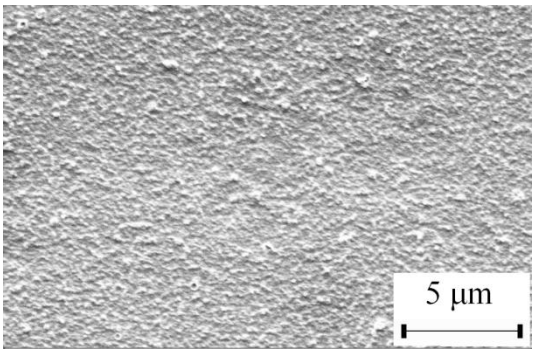

(b)

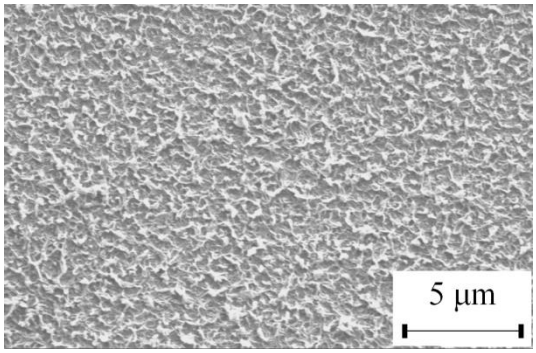

(c)

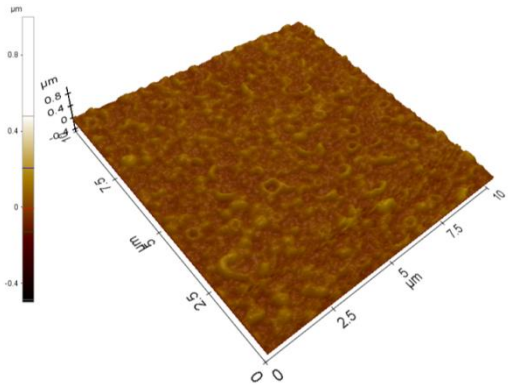

(d)

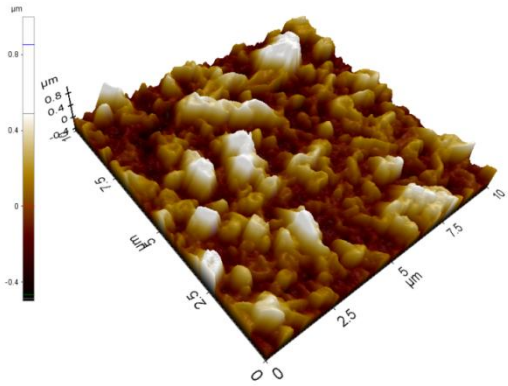

(e)

Figure 6-2 ATR-FTIR, SEM and AFM characterizations of TFC-N and TFC-R membranes: (a) ATR-FTIR spectra of the prepared polysulfone substrate and TFC FO membranes, SEM images of (b) TFC-N and (c) TFC-R, and AFM images of (d) TFC-N and (e) TFC-R.

Table 6-2 Properties of NF-like (TFC-N) and RO-like (TFC-R) TFC FO membranes

Membrane properties	TFC-N	TFC-R
Surface roughness (nm)	29.0 ± 4.4	184.9 ± 19.9
Contact angle (°)	25.7 ± 3.9	39.2 ± 5.2
Water permeability (A) [a]		
(L/(m^2 h bar))	5.01 ± 0.25	3.46 ± 0.34
($\times 10^{-12}$ m/(s Pa))	13.92 ± 0.71	9.62 ± 0.93
NaCl		
Rejection [b] (%)	33.3 ± 0.2	97.5 ± 0.2
Permeability (B_{NaCl}) [b] (m/s)	1.45 ± 0.06 $\times 10^{-5}$	1.10 ± 0.16 $\times 10^{-7}$
B_{NaCl}/A (bar)	10.41 ± 0.09	0.11 ± 0.01
Na_2SO_4		
Rejection [b] (%)	98.8 ± 0.01	99.6 ± 0.1
Permeability (B_{Na2SO4}) [b] (m/s)	7.81 ± 0.47 $\times 10^{-8}$	1.66 ± 0.42 $\times 10^{-8}$
B_{Na2SO4}/A (bar)	0.06 ± 0.001	0.02 ± 0.003
Trisodium citrate		
Rejection [b] (%)	99.4 ± 0.01	99.6 ± 0.03
Permeability ($B_{Na3C6H5O7}$) [b] (m/s)	4.72 ± 0.15 $\times 10^{-8}$	1.96 ± 0.40 $\times 10^{-8}$
$B_{Na3C6H5O7}/A$ (bar)	0.03 ± 0.001	0.02 ± 0.002

a. Determined with pure water feed in the RO mode at 5 bar and 23 °C. The experimental errors are reported as the standard deviations of at least three repeated measurements.

b. Determined with 10 mM salt in feed in the RO mode at 5 bar and 23 °C. The experimental errors are reported as the standard deviations of at least three repeated measurements.

6.3.2 Membrane intrinsic separation properties

The water and solute (NaCl, Na_2SO_4 and trisodium citrate) permeability coefficients of the TFC-N and TFC-R are summarized in Table 6-2. The TFC-N had a much higher water permeability (A = 5.01 ± 0.25 L/(m^2 h bar)) than that of the TFC-R (A = 3.46 ± 0.34 L/(m^2 h bar)). Compared to the existing commercial cellulose

triacetate (CTA) FO membranes (HTI, Albany, OR), for which the water permeability is 0.33-1.19 L/(m^2 h bar) (Section 4.3.2), both the TFC-N and TFC-R exhibited superior water permeabilities. The solute permeability (*B*) of the TFC-N followed the sequence of NaCl > Na_2SO_4 > trisodium citrate, which is consistent with the increasing molecular weights of these solutes. As typical for NF membranes, the TFC-N showed a low rejection to NaCl (33.3 ± 0.2% at 5 bar), whereas its rejection of Na_2SO_4 and trisodium citrate were significantly higher (98.8 ± 0.01% and 99.4 ± 0.01%, respectively, when tested at 5 bar). In contrast, the TFC-R had a high rejection (>97% at 5 bar) to all the three solutes.

The NaCl permeability of the TFC-N was two orders of magnitude higher than that of the TFC-R (Table 6-2). The much lower NaCl rejection of the TFC-N suggests that this type of NF-like FO membrane may not be suitable for applications where the DS is NaCl based (e.g., PRO for seawater osmotic energy recovery (She et al., 2012b)) or when NaCl in FS needs to be rejected (e.g., FO based seawater desalination (Chou et al., 2010)). For Na_2SO_4 and trisodium citrate, the TFC-N had comparable selectivity to the TFC-R, which suggests that the TFC-N may have potential applications for non-NaCl based FO applications. The FO performance of the two membranes using the three different DSs is compared in Section 6.3.3; the implications for selecting optimal FO membranes and operating conditions for given FO applications are further discussed in Section 6.3.5.

6.3.3 FO performance of NF-like and RO-like TFC FO membranes

It has been demonstrated in Chapter 5 that the FO water flux was determined by the rejection layer via a frictional loss mechanism and solute-reverse-diffusion induced ICP. In view of the contribution of the substrate, it can be concluded that the water flux during an FO process is governed by several important mechanisms: (1) the frictional resistance loss mechanism (M_R) (Wei et al., 2011a), (2) the solute reverse diffusion induced ICP ($M_{ICP\text{-}Js}$) (Wei et al., 2011a), and (3) the concentrative internal concentration polarization of feed solutes ($M_{ICP\text{-}feed}$ in AL-DS) or the dilution of draw solutes (dilutive ICP or $M_{ICP\text{-}draw}$ in AL-FS) (McCutcheon and Elimelech, 2006). In this section, the FO performance of the NF-like and RO-like

TFC FO membranes was systematically compared. The influence of the membrane separation properties (salt permeability *B* and water permeability *A*) and operating conditions on FO performance will be systematically evaluated in view of these mechanisms (Table 6-3).

Table 6-3 Major mechanisms and important parameters governing the water flux of FO membranes

Orientation	Major mechanisms	Important parameters		
		Membrane related	DS related	FS related
AL-DS (higher flux, less fouling resistant)	Frictional loss (M_R)	A	-	-
	J_s-induced ICP ($M_{ICP\text{-}Js}$)	A, B_{draw}, S	B_{draw}, D_{draw}	-
	Concentrative ICP of feed solutes ($M_{ICP\text{-}feed}$)	B_{feed}, S	-	B_{feed}, π_{feed}, D_{feed}
AL-FS (lower flux, more fouling resistant)	Frictional loss (M_R)	A	-	-
	J_s-induced ICP ($M_{ICP\text{-}Js}$)	A, B_{draw}, S	B_{draw}, D_{draw}	-
	Dilutive ICP of draw solutes ($M_{ICP\text{-}draw}$)	S	D_{draw}	-

6.3.3.1 Influence of solute permeability

The FO water flux performance of the TFC-N and TFC-R using different draw solutes (NaCl, Na_2SO_4 and trisodium citrate) are shown in Figure 6-3, and the solute reverse diffusion can be found in Figure 6-4. According to the experimental results, the TFC-R exhibited better performance than TFC-N when NaCl was used as the draw solute (Figures 6-3(a)-(d)). For example, J_v generated by the 1.5 M NaCl draw solution (osmotic pressure π_{draw} = 72.2 bar, 10 mM NaCl in FS) was 33.2 ± 4.5 L/(m^2 h) for the TFC-R (Figure 6-3(b)) but that was only 4.7 ± 1.4 L/(m^2 h) for the TFC-N (Figure 6-3(a)) in the AL-DS orientation. More than 98% of the osmotic driving force was lost for the TFC-N due to ICP. Nevertheless, $M_{ICP\text{-}feed}$ was not a dominant mechanism in this particular case - even after replacing the 10 mM NaCl FS with pure water, J_v of the TFC-N increased only marginally to 5.2 ± 1.2 L/(m^2 h) (Figure 6-5). Corresponding to its lower FO water flux using NaCl DS,

the TFC-N had a J_s/J_v ratio of 29.8 ± 4.2 g/L in the AL-DS orientation, about two orders of magnitude higher than that of the TFC-R (0.27 ± 0.03 g/L, Figure 6-4). The severe NaCl reverse diffusion of TFC-N is attributed to the large NaCl permeability (Table 6-2) (Wei et al., 2011a). The leakage of draw solutes through the low rejection membrane to the feed water reduced the effective osmotic pressure difference and increased the ICP level inside the membrane substrate (J_s-induced ICP or $M_{ICP\text{-}Js}$) (Wei et al., 2011a). The effective osmotic pressure due to solute reverse diffusion can be estimated by the *B/A* value for the selected draw solute (Tang et al., 2010; Xiao et al., 2011). For the TFC-N, the B_{NaCl}/A value was ~10.4 bar (Table 6-2), which is much larger than the osmotic pressure arising from the feed solutes (π_{feed} ~0.5 bar for 10 mM NaCl) such that $M_{ICP\text{-}Js}$ dominated over $M_{ICP\text{-}feed}$ (Figure 6-5). Only a marginal difference in J_v was observed for the TFC-N with pure water and 10 mM NaCl as feed (Figure 6-5). In comparison, the B_{NaCl}/A value for the TFC-R (0.11 ± 0.01 bar) was much smaller compared to π_{feed}, suggesting that $M_{ICP\text{-}Js}$ was much less important in the case of the TFC-R. For example, J_v of the TFC-R was very sensitive to the feed solution especially when the feed concentration was low (e.g., 0-10 mM) in the AL-DS orientation (Figure 6-5(a)). This analysis explains the much higher water flux for the TFC-R when NaCl was used as the DS.

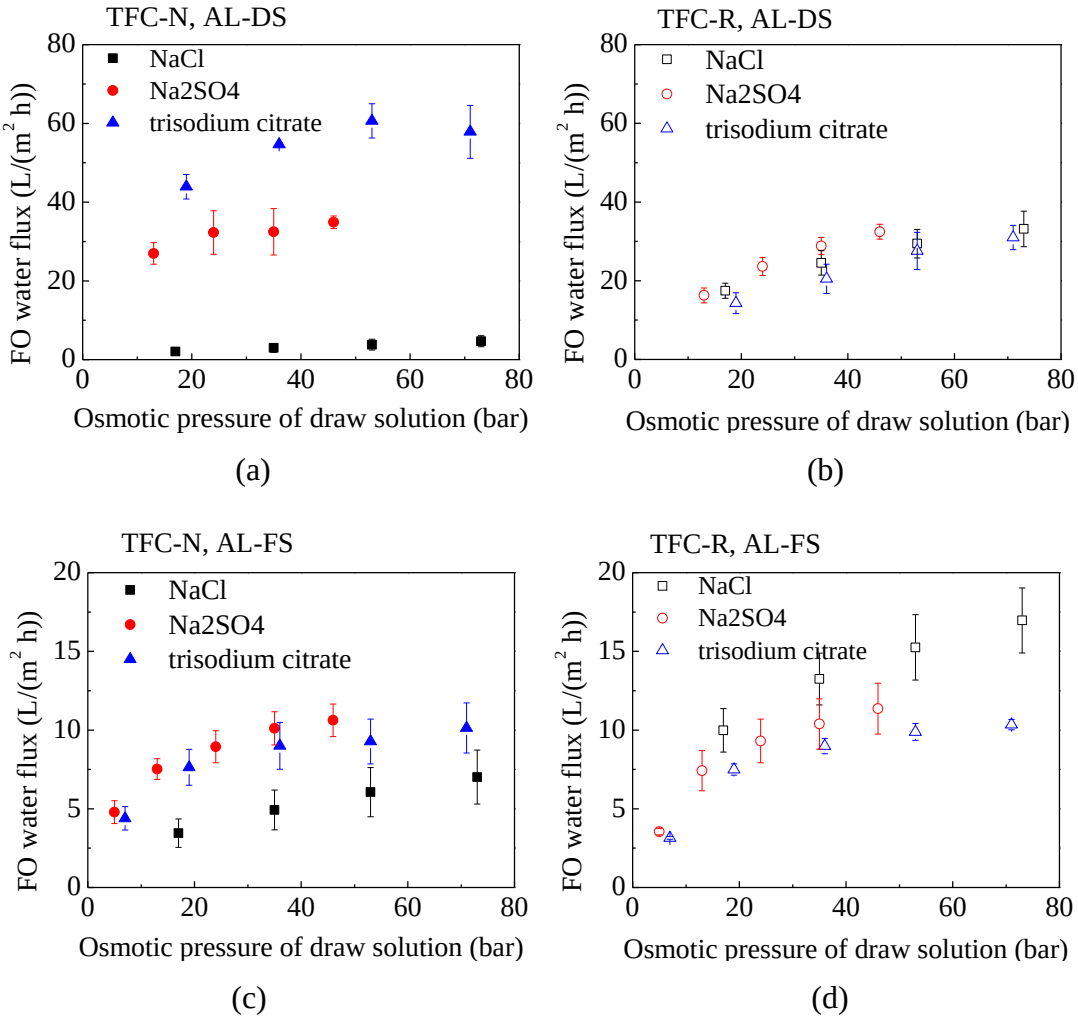

Figure 6-3 FO water flux of the NF-like and RO-like TFC FO membranes with membrane orientation of: (a) (b) AL-DS and (c) (d) AL-FS. The membranes evaluated are with an NF-like rejection layer (TFC-N) for (a) (c) and with an RO-like rejection layer (TFC-R) for (b) (d). The tests were operated using 10 mM NaCl as feed and different salts as the draw solute (as legends) at 23 °C. The osmotic pressures of draw solutions were calculated by OLI System software. Error bars represent standard deviations of at least three repeated measurements.

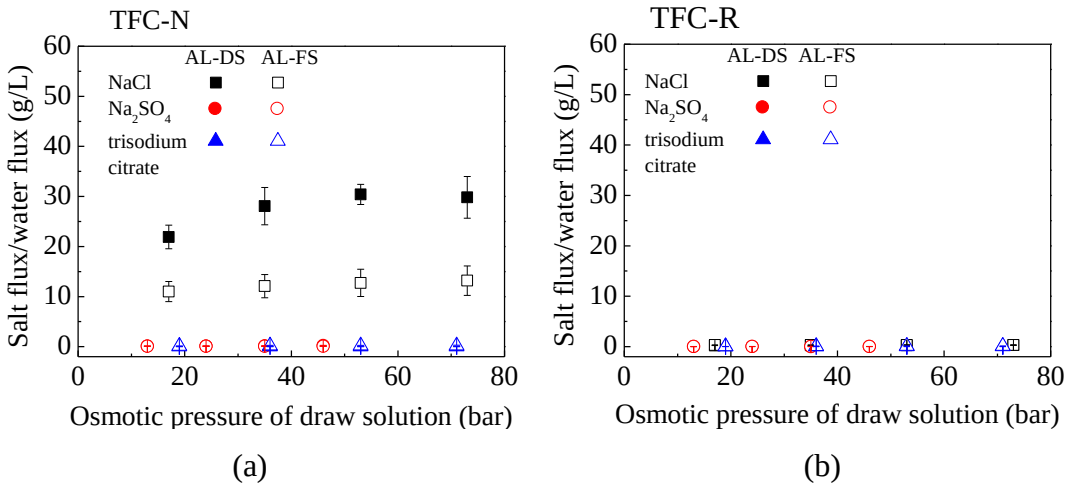

Figure 6-4 FO salt flux/water flux ratio of TFC FO membranes with (a) NF-like (TFC-N) or (b) RO-like (TFC-R) rejection layer using different draw solutes (as legends). Pure water was used as feed and the testing temperature was 23 °C. The osmotic pressures of the draw solutions were calculated by OLI System software. Error bars represent standard deviations of at least three repeated measurements.

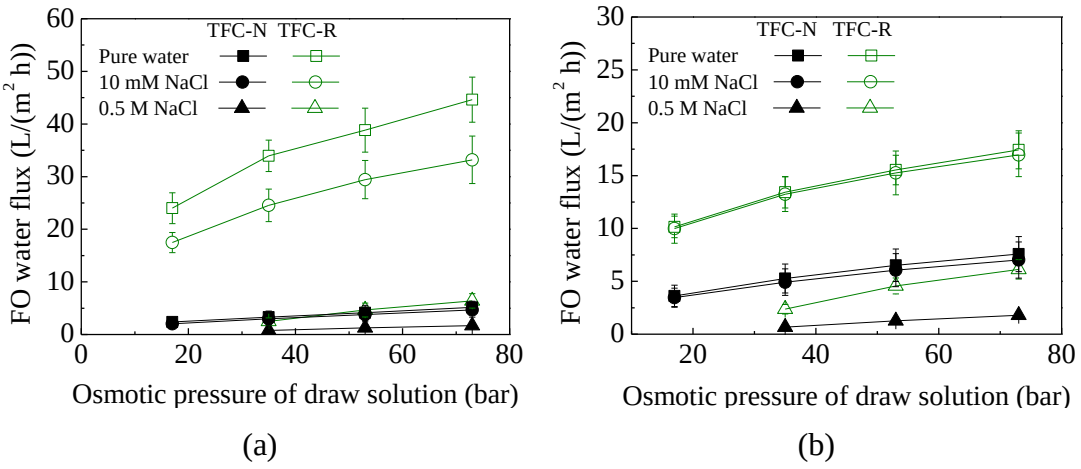

Figure 6-5 FO water flux of the NF-like (TFC-N) and RO-like (TFC-R) TFC FO membranes using different feed solutions, with membrane orientation of (a) AL-DS and (b) AL-FS. NaCl was used as the draw solute and the testing temperature was 23 °C. The osmotic pressures of the NaCl draw solutions were calculated by OLI System software. Error bars represent standard deviations of at least three repeated measurements.

When comparing the effect of different draw solutes in the AL-DS orientation, the FO water flux of the TFC-N followed the sequence of NaCl < Na_2SO_4 < trisodium

citrate (Figure 6-3(a)), which is identical to that of the solute rejection. This result is not surprising since the $M_{ICP\text{-}Js}$ mechanism can be dominant for the NF-like FO membranes as discussed above. The *B/A* values followed the order of NaCl > Na_2SO_4 > trisodium citrate (Table 6-2), which suggests that $M_{ICP\text{-}Js}$ was in decreasing importance following the same order. A high FO water flux was obtained for the case of Na_2SO_4 and trisodium citrate, where $M_{ICP\text{-}Js}$ played a less significant role (*B/A* = 0.06 and 0.03 bar, respectively). Therefore, NF-like FO membranes have a promising water flux when using draw solutes with a lower permeability coefficient. By only using a 0.3 M trisodium citrate DS (π_{draw} = 19 bar), J_v was as high as 43.9 ± 3.1 L/(m^2 h) and J_s/J_v was as low as 0.006 ± 0.002 g/L. The water flux of the TFC-R in AL-DS was much less sensitive to the DS type (Figure 6-3(b)), which is explained by the relatively low *B/A* values for the three solutes (~ or < 0.11 bar). The effect of the DS type on the FO water flux in AL-FS, where $M_{ICP\text{-}draw}$ plays a significant role, is further discussed in Section 6.3.3.3.

6.3.3.2 Influence of membrane water permeability

The membrane water permeability plays an important role since when it is low the membrane will inevitably experience severe frictional resistance loss. By comparing the water flux results of the TFC-N (Figure 6-3(a)) and the TFC-R (Figure 6-3(b)) when using Na_2SO_4 or trisodium citrate as the DS in the AL-DS orientation, it is clear that the TFC-N performed better than the TFC-R. For example, the TFC-N achieved a water flux ~37% higher than the TFC-R for a 0.5 M Na_2SO_4 DS (π_{draw} = 24 bar) and a 10 mM NaCl FS. The results for the trisodium citrate draw solution showed even a larger difference. The enhanced water flux performance for the TFC-N under these conditions is a result of its higher water permeability (~50% higher than that of the TFC-R). However, it is important to note that the beneficial effect of an increased water permeability can only be observed when M_R dominates over the other mechanisms (such as $M_{ICP\text{-}Js}$, $M_{ICP\text{-}feed}$, and $M_{ICP\text{-}draw}$). For example, when NaCl was used as the DS, the water flux of the TFC-N was an order of magnitude lower than that of the TFC-R (Figures 6-3(a) and 6-3(b)) due to the dominance of $M_{ICP\text{-}Js}$ for the low rejection TFC-N (Section 6.3.3.1).

Comparison of the water flux performance of the TFC-N and TFC-R in the AL-FS orientation using Na_2SO_4 or trisodium citrate as the DS is also interesting (Figure 6-6). The two membranes had nearly identical water fluxes in the AL-FS at π_{draw} > 10 bar, as indicated by the overlapping error bars. This may be explained by the dominant role of $M_{ICP\text{-}draw}$ in the AL-FS orientation (see more discussion in Section 6.3.3.3) relative to M_R. However, at π_{draw} < 10 bar, J_v of the TFC-N was 30%-40% higher compared to that of the TFC-R. For the latter case, ICP was less important due to the relatively low water flux level such that M_R became more significant.

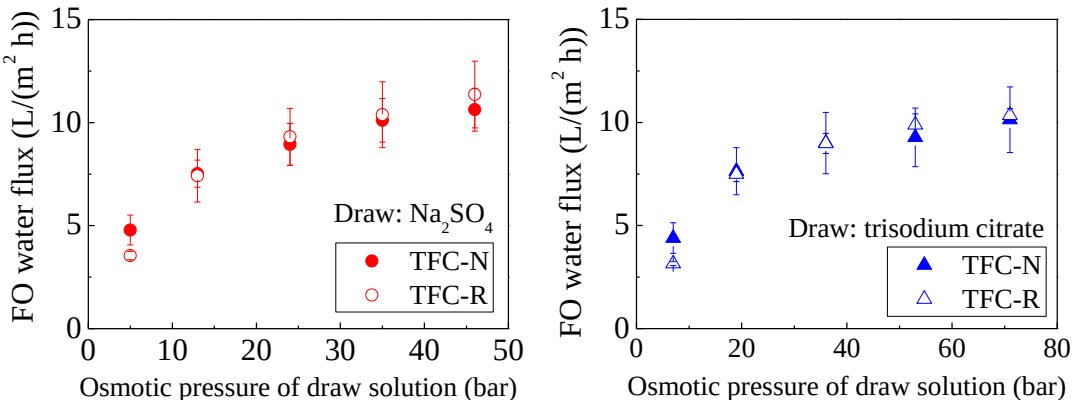

Figure 6-6 FO water flux of the TFC FO membranes with an NF-like (TFC-N) or RO-like (TFC-R) rejection layer, using (a) Na_2SO_4 and (b) trisodium citrate draw solutions. The tests were operated using 10 mM NaCl as the feed in AL-FS mode at 23 °C. The osmotic pressures of the draw solutions were calculated by OLI System software. Error bars represent standard deviations of at least three repeated measurements.

6.3.3.3 Influence of solute diffusion coefficient

In the AL-FS orientation, the dilutive ICP of the draw solutes ($M_{ICP\text{-}draw}$) can significantly reduce the effective draw solution concentration at the interface between the rejection layer and the porous support (McCutcheon and Elimelech, 2006). This mechanism is not applicable in the AL-DS orientation. Thus, the FO behavior in AL-FS can be quite different from that in AL-DS, which can be seen by comparing Figure 6-3(b) and Figure 6-3(d) for the TFC-R membrane. In the AL-FS, J_v increased in the following order: NaCl > Na_2SO_4 > trisodium citrate as the DS. In contrast, no significant difference in J_v was observed in the AL-DS among the

different draw solutes. As discussed in Sections 6.3.3.1 and 6.3.3.2, the water flux in the AL-DS is governed by three mechanisms: M_R, $M_{ICP\text{-}feed}$, and $M_{ICP\text{-}Js}$. As long as the membrane rejection against the draw solutes is sufficiently high (for the case of the TFC-R) to minimize $M_{ICP\text{-}Js}$, the FO water flux will not be strongly affected by the type of draw solute since both M_R and $M_{ICP\text{-}feed}$ are not directly dependent on the DS solute. In the AL-FS, however, the draw solutes have to diffuse into the porous support layer in a direction opposite to the permeate water flux. Previous studies have revealed that the dilutive ICP is exponentially dependent on the mass transfer rate of the draw solutes (D_{draw}/S, where D_{draw} is the draw solute diffusion coefficient and S is the structural parameter of the support layer) (Loeb et al., 1997; Cornelissen et al., 2008; Xiao et al., 2011; Zhao and Zou, 2011b). For membranes with the same structural parameter, the severity of dilutive ICP increases for draw solutes with a lower D_{draw}. The dominance of dilutive ICP means that the order of J_v for the TFC-R in the AL-FS merely follows that of the draw solute diffusion coefficients (at a concentration of 1.0 M and 23 ℃, $D_{Cl\text{-}} = 1.67 \times 10^{-9}$ m^2/s, $D_{SO42\text{-}} = 7.02 \times 10^{-10}$ m^2/s, $D_{[C6H5O7]3\text{-}} = 4.74 \times 10^{-10}$ m^2/s). Besides the diffusion coefficient, the viscosity of the draw solutes may also affect the water flux in AL-DS, with larger molecules (higher viscosity) typically reducing J_v (She et al., 2012a), although this effect was less important in the current study due to the overwhelming influence of the diffusion coefficient.

The TFC-N had an interesting behavior in the AL-FS orientation (Figure 6-3(c)). A slightly higher J_v was obtained for the Na_2SO_4 DS compared to trisodium citrate, which can be explained by the larger diffusion coefficient of Na_2SO_4 and thus its lower level of dilutive ICP. Nevertheless, NaCl, with the highest diffusion coefficient among the three draw solutes, performed poorly as a DS for the TFC-N. Once again, the low rejection of TFC-N against NaCl resulted in severe reverse diffusion of NaCl from the DS, which led to a low J_v controlled by $M_{ICP\text{-}Js}$ (Section 6.3.3.1).

6.3.4 Membrane fouling resistance

Fouling is a critical issue in membrane separations (Lay et al., 2010; Lee et al.,

2010; Mi and Elimelech, 2010b; Tang et al., 2010; Wang and Tang, 2011a; b; Qi et al., 2012b). This section compares the fouling propensity of the poly(piperazine-amide) based NF-like and fully-aromatic polyamide RO-like TFC membranes using alginate as a model foulant. The fouling tests were run in the AL-FS orientation. This orientation is often adapted when the feed has a high fouling tendency, in order to avoid foulant entering the porous support and causing internal pore clogging (Mi and Elimelech, 2010b; Tang et al., 2010; Zou et al., 2011). During the fouling tests, no significant flux decline was observed for both membranes over the 14 h tests (Figure 6-7(a)). SEM was used to examine the fouled membranes; foulant extraction was performed to determine the amount of foulant mass deposited on the membrane surface. For the TFC-N, there was no obvious change in the membrane surface morphology after a fouling test (Figure 6-7(b), compared to the virgin TFC-N in Figure 6-2(b)). Furthermore, foulant deposition was not detectable based on our extraction results. In contrast, a moderate amount of foulant mass (8.8 ± 2.1 $\mu g/cm^2$) was measured for the fouled TFC-R; its ridge-and-valley surface roughness structure was completely covered by the foulant layer (see fouled TFC-R in Figure 6-7(c) and virgin TFC-R in Figure 6-2(c)). The more foulant deposition for TFC-R can be attributed to its relatively more hydrophobic and rougher surface (Table 6-2) (Vrijenhoek et al., 2001; Tang et al., 2007a; Wang and Tang, 2011c). Prior studies on RO and NF membrane fouling have indicated that surface roughness could be one of the most influential membrane properties contributing to fouling, since the foulant would preferentially accumulate within the valleys of the rough polyamide layer and causes clogging (Vrijenhoek et al., 2001; Tang et al., 2007a; Wang and Tang, 2011c). It is also worthwhile to note that the commercial CTA FO membranes also have relatively smooth membrane surfaces (roughness ~36 nm and lack of the ridge-and-valley structure, see (Tang et al., 2010)), which is consistent with the low fouling tendency of these membranes reported in the literature (Lay et al., 2010; Mi and Elimelech, 2010b).

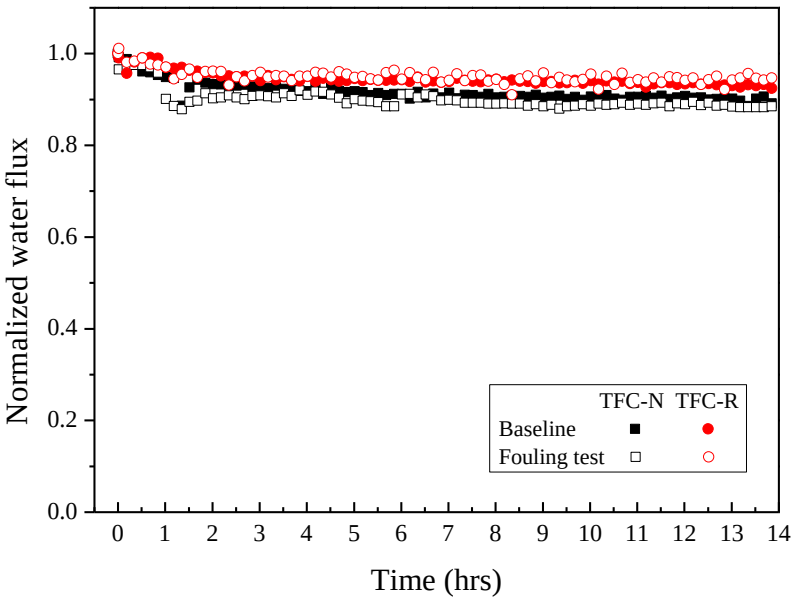

(a)

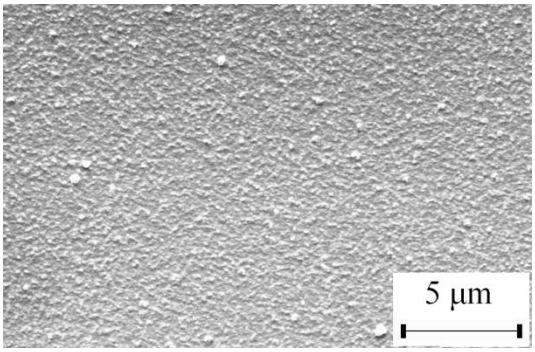

(b) Foulant mass: not detected

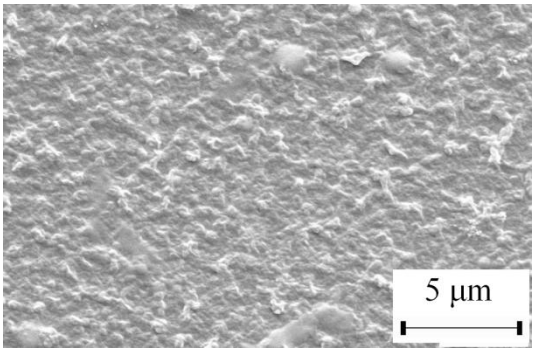

(c) Foulant mass: 8.8 ±2.1 µg/cm^2

Figure 6-7 Membrane fouling results: (a) normalized water flux (actual flux/initial flux) in FO fouling tests for the TFC-N and TFC-R, (b) SEM image of the fouled TFC-N membrane, and (c) SEM image of the fouled TFC-R membrane. FO fouling tests conditions: feed contained 7 mM NaCl, 1 mM $CaCl_2$ and 100 mg/L alginate; pH was 6.0 ± 0.1; draw solution was 1.5 M Na_2SO_4; initial water flux was 9.8 ± 0.9 L/(m^2 h) for the TFC-N and 8.1 ± 0.8 L/(m^2 h) for the TFC-R; the fouling test duration was 14 h (23 ℃). Baseline tests were similarly conducted without alginate addition. The normalized water flux was determined as the ratio of real-time FO water flux versus the initial water flux.

The foulant deposition on the TFC-R did not appear to significantly affect its FO water flux performance, which may be explained by the inherent flux stability in the AL-FS orientation possibly due to the ICP self-compensation effect (Tang et al.,

2010). While the increased membrane resistance tends to reduce the FO water flux, this is compensated by a reduced level of ICP (thus increasing the effective driving force) that moderates the flux reduction. Nevertheless, the greater foulant deposition propensity of the fully aromatic polyamide based TFC-R may still be a potential concern; its long term flux stability needs to be further investigated in future studies.

6.3.5 Implications for FO membrane processes

Table 6-3 summarizes the various competing mechanisms governing flux performance of the FO process. $M_{ICP\text{-}feed}$ is only applicable to the AL-DS orientation, whereas $M_{ICP\text{-}draw}$ is only applicable to the AL-FS orientation. In addition, M_R and $M_{ICP\text{-}Js}$ are applicable to both membrane orientations. These mechanisms are affected by various membrane-related, DS-related, and FS-related parameters, as listed in Table 6-3. In general, FS parameters (such as its osmotic pressure π_{feed} and the diffusion coefficient of the feed solutes D_{feed}) are fixed for a given FO application. On the other hand, one can choose the membrane type/properties (and sometimes DS type/properties) to optimize FO performance. It is generally known that membranes with a lower structural parameter, higher water permeability, and lower solute permeability are preferred (McCutcheon and Elimelech, 2006; Hancock and Cath, 2009; Wei et al., 2011b). However, the difficulty in FO optimization often lies in the complicated trade-off relationships between the different parameters and their competing effects on various mechanisms. For instance, a higher permeability membrane (large A) reduces M_R at the possible expense of more severe $M_{ICP\text{-}Js}$ due to the trade-off in its rejection to draw solutes (larger B_{draw}). Similarly, large draw solutes reduce B_{draw} (less severe $M_{ICP\text{-}Js}$) but their lower D_{draw} reduces the mass transfer of the draw solutes in the support layer (more severe $M_{ICP\text{-}draw}$ in the AL-FS orientation).

From a process optimization point of view, a set of systematic criteria for the selection of FO membranes and draw solutes will be highly valuable. First of all, a critical criterion is having a high rejection to the draw solute ($B_{draw}/A << \pi_{feed}$ (Xiao et al., 2011)) to minimize the detrimental $M_{ICP\text{-}Js}$ effect. This can be done by

carefully selecting the draw solute and membrane combination (e.g., NaCl/TFC-R couple or trisodium citrate /TFC-N couple). For the draw solute selection, the D_{draw} value should be as high as possible so long as $M_{ICP\text{-}Js}$ is not the dominant mechanism. Other draw solute properties, such as its solubility and available osmotic pressure, the ease of regeneration, toxicity, cost (Achilli et al., 2010), and their potential to promote membrane fouling on the FS side (Zou et al., 2011; She et al., 2012a) should be considered as well. Similarly, a high A value is favored to minimize M_R as long as $M_{ICP\text{-}Js}$ is not important by ensuring $B_{draw}/A << \pi_{feed}$. Additional criteria for the membrane and orientation selection include their effect on fouling and on the required feed solute rejection (e.g., internal concentration polarization of feed solutes in AL-DS may reduce contaminant rejection (Jin et al., 2011)).

Table 6-4 presents some potential osmotically driven applications, including FO desalination, PRO osmotic power generation, and OMBR (Cath et al., 2006; Zhao et al., 2012b) to illustrate the principles for FO membrane selection. In FO based desalination, dissolved solutes (e.g., NaCl and boron) in the seawater feed need to be adequately rejected. In this case, the rejection of the feed solutes requires the use of RO-like FO membranes. The AL-FS orientation is preferred to minimize membrane fouling and also to maintain high rejection of feed contaminants such as boron (Jin et al., 2011). For PRO applications, seawater or seawater RO brines may be used as the DS (Yip et al., 2011; She et al., 2012b). To avoid severe $M_{ICP\text{-}Js}$, RO-like FO membranes with a high NaCl rejection are needed. Since feed solute rejection is generally not a concern in PRO, the AL-DS orientation is preferred for its higher water flux (thus higher power density). However, fouling in this orientation can be a significant concern. When a FS with a high fouling potential (such as treated effluent) is used, one may be forced to operate PRO in the AL-FS orientation for improved flux stability.

Table 6-4 Parameters for membrane selection and process optimization in osmotically driven membrane processes

Application	Feed solution	Draw solution	Fouling potential of feed solution	Membrane orientation	Type of FO membrane
FO desalination	Seawater (contaminant to be removed, NaCl and other major ions, boron)	Synthetic draw solutions ($B_{draw}/A << \pi_{feed}$)	Mild to moderate	AL-FS to minimize fouling and maintain high rejection	RO-like, good NaCl and boron rejection
PRO power generation	River water	Seawater, RO brine	Mild to moderate	AL-DS	RO-like, good NaCl rejection
	Treated effluent or wastewater	Seawater, RO brine	High	Maybe AL-FS to reduce fouling	RO-like
OMBR	Activated sludge (TDS, biomass, waste organics)	Seawater, RO brine	High	AL-FS	RO-like, good NaCl rejection
		Synthetic draw solutions ($B_{draw}/A << \pi_{feed}$)	High	AL-FS	NF-like or RO-like

For OMBR applications, the feed solution has a very high fouling propensity, which dictates that the AL-FS orientation shall be applied. When synthetic draw solutes are used, one may either use RO-like or NF-like membranes as long as adequate rejection can be achieved against the draw solutes. Indeed, the adoption of NF-like FO membranes can be advantageous for several reasons: (1) their higher water permeability reduces membrane frictional loss, (2) their better surface chemistry reduces fouling potential, and (3) their lower retention to TDS reduces accumulation of feed salts in the bioreactor that can hinder the FO performance and biological activities (Xiao et al., 2011; Alturki et al., 2012). Similarly, in other applications where the primary intention is to concentrate organic/biological components rather than to reclaim water (e.g., concentrating liquid foods (Petrotos and Lazarides, 2001) and microalgal biomass (Zou et al., 2011), the use of high permeability NF-like FO membranes can be promising.

6.4 Conclusions

NF-like and RO-like TFC FO membranes were fabricated and systematically compared in terms of FO performance and fouling behavior in this chapter. The results revealed that the water flux in the FO process is governed by several important mechanisms, i.e., M_R, $M_{ICP\text{-}Js}$ and $M_{ICP\text{-}feed}$ in the AL-DS orientation and M_R, $M_{ICP\text{-}Js}$ and $M_{ICP\text{-}draw}$ in the AL-FS orientation. In particular, the $M_{ICP\text{-}Js}$ is of uppermost importance in influencing the membrane flux behavior. Thus, much higher water flux was achieved by the TFC-R in NaCl based processes, while the TFC-N with low NaCl rejection (33.3 ± 0.2% at 5 bar) performed poorly, with a low water flux and a J_s/J_v ratio about two orders of magnitude higher than that of the TFC-R. When Na_2SO_4 and trisodium citrate were used as draw solutes, the TFC-N exhibited a high FO water flux due to the minimized effect of the $M_{ICP\text{-}Js}$ and the high water permeability of the NF-like rejection layer. In the AL-FS orientation, however, the TFC-N and TFC-R had similar water fluxes when using Na_2SO_4 or trisodium citrate as the draw solute, as a result of the dominant effect of the $M_{ICP\text{-}draw}$. When the solute flux was low, J_v increased with higher draw solute diffusion coefficient (NaCl > Na_2SO_4 > trisodium citrate). According to the above, the aforementioned governing mechanisms are affected by various membrane-

related, DS-related and FS-related parameters, e.g., A, B_{draw}, D_{draw}, S, π_{feed}, etc. Criteria for membranes and operating conditions were proposed. Application of these criteria in potential FO applications such as FO desalination, PRO power generation and OMBR had important implications for the selection of NF-like or RO-like membranes in FO processes as well as process optimization.

Chapter 7
Conclusions and recommendations

7.1 Conclusions

High-performance flat-sheet TFC FO membranes were synthesized in this study. The membranes consisted of a porous substrate prepared by phase inversion and an ultrathin polyamide rejection layer formed by interfacial polymerization. Both layers were specially tailored for FO operating conditions. Using the TFC FO membranes, mechanisms that govern the membrane performance in FO processes were systematically studied. Conclusions from this research are summarized in the following.

(1) High performance FO membranes should have a small structural parameter (*S* value), high water permeability (*A* value) and low solute permeability (*B* value). In other words, both the membrane support and rejection layer properties are of critical importance to FO performance. Fabrication of TFC membranes allows individual optimization of the membrane substrate and rejection layer. Hence, it provides TFC FO membranes an important advantage over integral asymmetric membranes. This is proved by the experimental results, since the TFC FO membranes synthesized in this study generally achieved higher water fluxes while maintaining a relatively low salt flux/water flux ratio, compared to the evaluated commercial integral asymmetric FO membranes.

(2) The synthesized TFC FO membranes were characterized and compared with asymmetric FO membranes and TFC RO membranes to understand the effects of the support structure on the structural parameter and on the FO performance. The TFC FO membranes appeared to have highly porous substrate structures with long finger-like pores formed under a thin sponge-like skin layer. The FO results showed that this finger-like pore structure can minimize the tortuosity, and thus is preferred for reducing the structural parameter and for minimizing the ICP. In addition, increasing the porosity and reducing the membrane

thickness are also beneficial to reduce the structural parameter. On the other hand, the poor performance of commercial TFC RO membranes under FO conditions can be attributed to their thick and highly tortuous spongy-like support structure where severe ICP could take place during the FO process.

(3) FO membranes with different separation properties were obtained by systematically changing the monomer concentrations during interfacial polymerization. A strong trade-off between membrane water permeability and salt rejection was demonstrated during membrane fabrication. Membranes prepared with higher MPD concentrations or lower TMC concentrations had a lower water permeability but improved salt rejection.

(4) The FO water flux is affected by both the membrane water permeability and the salt rejection. While the higher water permeability of membrane tends to enhance the FO water flux due to reduced membrane frictional resistance loss, the coupled lower salt rejection may simultaneously cause more severe internal concentration polarization due to the solute reverse diffusion, which has an opposing effect that cuts down the FO water flux. A balance between the water permeability and salt rejection should be achieved during the optimization of FO membranes.

(5) As a result of the highly non-linear dependence of the FO performance on the operating conditions and membrane properties, an optimized membrane for one specific application does not necessarily guarantee good performance for other applications. In view of the trade-off between membrane-related and operating parameters as well as their competing effects, FO membranes should be optimized according to the dominating mechanism for specific operating conditions.

(6) The FO water flux is governed by several important mechanisms: the frictional resistance loss mechanism (M_R), the solute-reverse-diffusion-induced ICP mechanism ($M_{ICP\text{-}Js}$), the concentrative ICP of feed solutes in the AL-DS

orientation ($M_{ICP\text{-}feed}$) or the dilutive ICP of draw solutes in the AL-FS orientation ($M_{ICP\text{-}draw}$). These mechanisms are affected by various membrane-related, draw-solution-related and feed-solution-related parameters. A set of systematic criteria for the selection of FO membranes and draw solutes is proposed. The most important criterion is a high rejection to draw solutes, which can be achieved by optimal combination of membrane rejection and draw solute. The water permeability of the membrane and diffusion coefficient of the draw solute should be as high as possible when $M_{ICP\text{-}Js}$ is not a dominant mechanism. Additional criteria also include the fouling resistance and feed solute rejection.

(7) RO-like and NF-like TFC FO membranes were compared in FO processes to shed light on the selection of membranes for FO applications. RO-like FO membranes exhibited better performance than the NF-like counterpart in the NaCl based tests, due to the superior NaCl rejection of the former. By using draw solutes with a lower permeability coefficient (e.g., Na_2SO_4 and trisodium citrate), however, the highly permeable NF-like FO membrane exhibited comparable, or even better performance than RO-like membranes when M_R dominates over the other mechanisms (e.g., $M_{ICP\text{-}Js}$, $M_{ICP\text{-}feed}$, and $M_{ICP\text{-}draw}$). In addition, the more hydrophilic and smoother surface of the NF-like rejection layer tended to have better fouling resistance and thus is advantageous in applications with high fouling potential.

7.2 Recommendations

According to the findings from this research, several future studies are recommended to further improve the TFC FO membranes as well as the potential engineering applications of osmotically driven membrane technology.

(1) The skin layer of substrate has critical influence on the formation of rejection layer as mentioned in Section 4.3.1. A relatively dense skin layer with appropriate surface pore size is necessary to reduce the defects in the polyamide rejection layer. On the other hand, this dense layer would become a main

contribution to large structural parameter for FO membranes because of its high tortuosity and low porosity. Therefore, studies on the effects of the substrate skin layer from the aspects of surface pore size, pore structure and thickness are suggested.

(2) Systematic studies on the formation of finger-like pore structure in the membrane support layer can be conducted in the future. The cross-sections of S-1 and S-2 in Chapter 4 showed different morphologies due to the different compositions of casting solutions used. Straight finger-like pores were observed in the S-2 substrate, whereas distorted macrovoids were observed on the bottom of the S-1 substrate. The mechanisms how the macrovoids formed and decreased are not clear yet. The relevant parameters may include polymer concentration in the casting solution, compatibility between the additives and the polymer-solvent-non-solvent system, viscosity of the casting solution, composition of the coagulant bath, etc.

(3) The fully aromatic polyamide based TFC FO membranes appeared to have rough surface morphology due to the very fast reaction between MPD and TMC during the rejection layer formation, which makes the membranes very susceptible to foulant deposition. Approaches to reduce the surface roughness should be explored. For example, a molecular layer-by-layer deposition process was proposed recently to form a polyamide film with small roughness (Johnson et al., 2012). The effects of reactive monomers, additives and organic solvents on the surface roughness are suggested to investigate as well.

(4) In view of the increasing interest in FO technologies, large scale applications like OMBR and osmotic power generation are expected in the near future. Fabrication of high mechanical strength FO membranes would be a crucial topic to facilitate module design and assembly. More polymers with excellent mechanical strength should be tested. In addition, it is an efficient way to incorporate a reinforcing fabric in the substrate, for which the influence on the pore structure of the polymer layer and the structural parameter has yet to be

studied.

(5) Selection of draw solute is another technical challenge in the FO applications as discussed in Chapter 6. More attentions should be paid to the development of draw solutes, which could be the conventional salts as used in this study as well as advanced synthetic solutes with high osmotic pressure, high diffusion coefficient and low permeability. Efficient regeneration technology of the draw solution should be developed as well.

(6) The commercially available FO membrane modules from HTI are with the spiral-wound configuration, which is widely used in the NF and RO modules. In the FO process, a high concentration draw solution rather than pure water needs to be circulated in the permeate side. The ICP phenomenon could occur on each side of the membrane. These unique problems impose special requirements on the FO modules design (Xiao et al., 2012), which could be varied depending on the applications. Thus, the FO modules with either flat-sheet or hollow fibre membranes have yet to be optimized in terms of module dimension, spacer and even module configuration.

(7) Major mechanisms and parameters that govern the FO performance have been investigated in this study. Modeling work to simulate the effect of these mechanisms could be carried on in the future study. Most of the current FO modeling studies are using the analytical ICP model developed by Loeb. Other methods such as computational fluid dynamics (Gruber et al., 2011; Gruber et al., 2012) could also be used for more comprehensive modeling in the FO process as well as FO module study.

Appendix

Modeling the effects of membrane optimization on FO performance

Section A Introduction

FO water flux is determined by the membrane properties in a highly non-linear manner due to the presence of ICP (Loeb et al., 1997; McCutcheon et al., 2005b; Tang et al., 2010). Meanwhile, the severity of ICP depends on several membrane-related, DS-related and FS-related parameters (see section 6.3.5). Net effect of these parameters on FO water flux can be predicted by an ICP model, which was developed by Loeb et al. (Loeb et al., 1997) and has been verified in many studies (Gray et al., 2006; McCutcheon and Elimelech, 2006; Tang et al., 2010; Wang et al., 2010b):

AL-DS:
$$J_v = \frac{D}{S}\ln\frac{A\pi_{draw} - J_v + B}{A\pi_{feed} + B} \quad \text{(A1)}$$

AL-FS:
$$J_v = \frac{D}{S}\ln\frac{A\pi_{draw} + B}{A\pi_{feed} + J_v + B} \quad \text{(A2)}$$

where J_v is the FO water flux, D is the diffusion coefficient of solute, S is the structural parameter of membrane, π_{draw} and π_{feed} are the osmotic pressures of draw solution and feed solution, respectively, A and B are the membrane water and salt permeability coefficients, respectively.

According to the ICP model, three membrane-related parameters, i.e., structural parameter (S value), water permeability (A value) and salt permeability (B value), are determinant to FO water flux. Experimental investigation on the influence of these parameters and related governing mechanisms has been presented in Chapters 4-6. In this appendix, simulation based on the ICP model was conducted from the

membrane property point of view, to provide theoretical knowledge of the influence of membrane optimization. Reference values of the modeling parameters (Table A1) were determined according to the membrane properties and experimental conditions in this study.

Table A1 Reference values of modeling parameters

Parameter	Reference value
Solute diffusion coefficient, D	1.3×10^{-9} m^2/s
Osmotic pressure of draw solution, π_{draw}	99.9 bar for 2.0 M NaCl
Osmotic pressure of feed solution, π_{feed}	0.5 bar for 10 mM NaCl
Membrane water permeability, A	5.0×10^{-12} m/(s Pa)
Membrane salt permeability, B	1.0×10^{-7} m/s
Structural parameter, S	0.7 mm

Section B Effect of structural parameter

The influence of membrane structural parameter on the FO water flux is shown in Figure A1. A lower J_v is achieved when a membrane with larger S value is used. Increasing the membrane S value leads to higher resistance of support layer to mass diffusion and thus enhances ICP. It is also the main reason for the poor FO performance of typical RO membranes, despite their superior water permeability and salt rejection (see Chapter 4). In the current simulation, a water flux of 179 L/(m^2 h) (equal to the water flux under an equivalent hydraulic pressure) can be achieved in both the AL-DS and AL-FS orientations if the membrane is support-free (S = 0). The influence of S value is especially important in the AL-FS orientation due to the presence of serious dilutive ICP. Since it may not be practical to use a support-free FO membrane, developing substrates with minimum S value and sufficient mechanical strength is important for FO membrane fabrication.

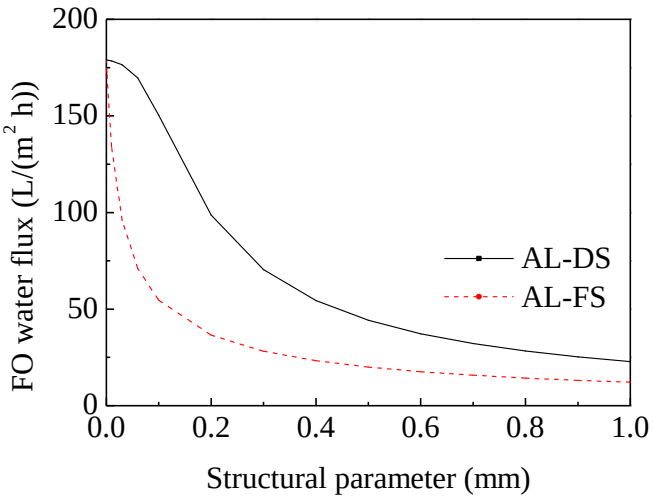

Figure A1 The predicted FO water flux as a function of membrane structural parameter. Simulation parameters: A = 5.0 × 10^{-12} m/(s Pa), B = 1.0 × 10^{-7} m/s, D = 1.3 × 10^{-9} m^2/s, π_{draw} = 99.9 bar, π_{feed} = 0.45 bar.

Section C Effect of membrane water permeability

The influence of membrane water permeability on the FO water flux is shown in Figure A2. Initially, J_v increases almost proportionally to A value when other parameters are constant. However, less enhancement of water flux can be achieved by further increasing A value after a certain region. The results suggest that for FO membranes with low water permeability, the frictional resistance loss mechanism (M_R) plays a dominant role. For example, the commercial asymmetric FO membranes studied in Chapter 4 had relatively low water permeability (Table 4-3). The A values of CTA-W and CTA-NW were only 0.9 × 10^{-12} m/(s Pa) and 1.3 × 10^{-12} m/(s Pa), respectively. Thus, much higher water flux was obtained by using the more permeable CTA-HW membrane (A = 3.3 × 10^{-12} m/(s Pa)). On the other hand, in view of the trade-off between the membrane water permeability and rejection (Section 5.3.2), FO membranes with A values in the plateau region are not suggested to further improve the permeability, in order to avoid the negative effect of the corresponding lower salt rejection.

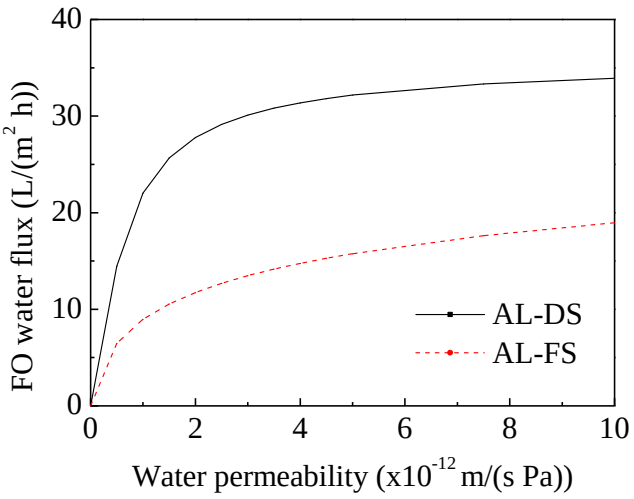

Figure A2 The predicted FO water flux with increasing membrane water permeability. Simulation parameters: B = 1.0 × 10^{-7} m/s, S = 0.7 mm, D = 1.3 × 10^{-9} m^2/s, π_{draw} = 99.9 bar, π_{feed} = 0.45 bar.

Section D Effect of membrane salt permeability

The effect of adjusting salt permeability on the FO water flux is shown in Figure A3. A lower J_v is achieved with a higher membrane salt permeability. With constant membrane water permeability, the increasing salt permeability leads to a higher B/A ratio (i.e., lower membrane selectivity). It was suggested by previous study that the salt flux/water flux ratio (J_s/J_v) is directly determined by the membrane selectivity (Tang et al., 2010). A larger B/A value may lead to severe reverse diffusion of draw solute and correspondingly lower water flux (i.e. the $M_{ICP\text{-}Js}$ mechanism).

J_v is less sensitive to the change in B value in the AL-FS orientation because of the overwhelming effect of DS dilution ($M_{ICP\text{-}draw}$) over the draw solute leakage ($M_{ICP\text{-}Js}$), as well as the self-compensation mechanism in this orientation. In the AL-DS orientation, ICP on the feed side is contributed by the accumulation of feed solute ($M_{ICP\text{-}feed}$) as well as the reverse diffusion of draw solute ($M_{ICP\text{-}Js}$). Optimizing B value is more effective when $M_{ICP\text{-}Js}$ dominates over $M_{ICP\text{-}feed}$, i.e., $B/A >> \pi_{feed}$. For example, the water flux of a "loose" membrane with B value of 1 × 10^{-6} m/s (B/A = 2 bar, much higher than π_{feed} 0.5 bar) can be improved from 23.9 L/(m^2 h) to 29.8 L/(m^2 h) via reduction of B value by 75% (B/A reduced to 0.5 bar). For a high-rejection membranes, e.g., the membrane with B value of 1 × 10^{-7} m/s (B/A = 0.2

bar, lower than π_{feed} 0.5 bar) as TFC-2, reducing the *B* value by 90% (*B*/*A* reduced to 0.02 bar) can only enhance the water flux from 32.2 L/(m^2 h) to 34.2 L/(m^2 h). In addition, modification of the membrane rejection layer may result in a lower *B* value but also a lower *A* value, of which the net effect would depend on the testing conditions (Section 5.3.2). Thus, an optimal combination of *A* and *B* values should be decided according to the membrane properties and operating conditions.

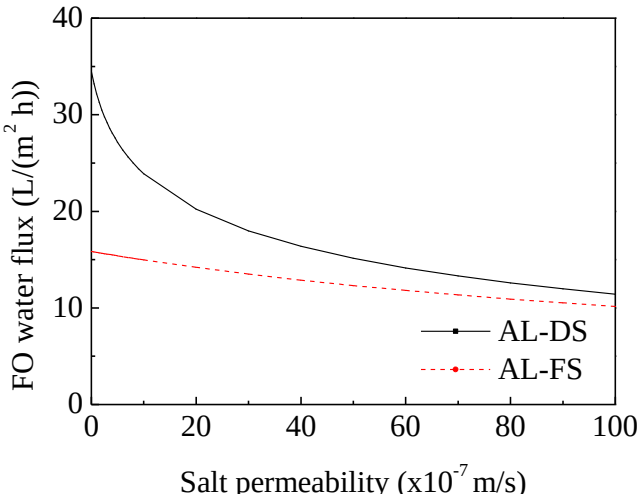

Figure A3 The predicted FO water flux with increasing membrane salt permeability. Simulation parameters: A = 5.0 × 10^{-12} m/(s Pa), S = 0.7 mm, D = 1.3 × 10^{-9} m^2/s, π_{draw} = 99.9 bar, π_{feed} = 0.45 bar.

Section E Conclusions

In this appendix, the effects of membrane optimization in terms of structural parameter *S*, water permeability *A* and salt permeability *B* on the FO water flux was predicted using the ICP model. According to the results, ideal FO membranes should have small structural parameter, higher water permeability and lower salt permeability. The *S* value is a critical parameter for FO membranes, which can be individually tailored during substrate fabrication. On the other hand, the optimization of membrane rejection layer would be constrained by the trade-off between the membrane permeability and salt rejection. For the low permeability membranes of which the J_v is mainly constrained by the membrane frictional resistance loss, membranes should be improved to have water permeability as high as possible. While for the membranes with high permeability, J_v tends to be less

affected by the water permeability change but severe J_s-induced-ICP may occur and lead to a low water flux. In this case, membranes should be optimized to have higher salt rejection.

References

(2009a), "Contract signals commercial deployment of forward osmosis system", Membrane Technology, Vol. 2009, No. 4, pp. 2-2.

(2009b), "High BOD and COD carpetdyeing wastewater recycled using forward osmosis", Membrane Technology, Vol. 2009, No. 4, pp. 8-8.

(2009c), "New Product Developments", Filtration Industry Analyst, Vol. 2009, No. 2, pp. 14-14.

(2010), "Thinner is better", Water Desalination Report, Vol. 46, No. 18, pp. 1.

Aaberg, R.J. (2003), "Osmotic Power: A new and powerful renewable energy source?", Refocus, Vol. 4, No. 6, pp. 48-50.

Achilli, A., Cath, T.Y. and Childress, A.E. (2009a), "Power generation with pressure retarded osmosis: An experimental and theoretical investigation", Journal of Membrane Science, Vol. 343, No. 1-2, pp. 42-52.

Achilli, A., Cath, T.Y. and Childress, A.E. (2010), "Selection of inorganic-based draw solutions for forward osmosis applications", Journal of Membrane Science, Vol. 364, No. 1-2, pp. 233-241.

Achilli, A., Cath, T.Y., Marchand, E.A. and Childress, A.E. (2009b), "The forward osmosis membrane bioreactor: A low fouling alternative to MBR processes", Desalination, Vol. 239, No. 1-3, pp. 10-21.

Achilli, A. and Childress, A.E. (2010), "Pressure retarded osmosis: From the vision of Sidney Loeb to the first prototype installation - Review", Desalination, Vol. 261, No. 3, pp. 205-211.

Ajay Babu, C., Prasada Rao, M. and Vijaya Ratna, J. (2010), "Controlled-porosity osmotic pump tablets-an overview", Journal of Pharmaceutical Research and Health Care, Vol. 2, No. 1, pp. 114-126.

Alturki, A., McDonald, J., Khan, S.J., Hai, F.I., Price, W.E. and Nghiem, L.D. (2012), "Performance of a novel osmotic membrane bioreactor (OMBR) system: Flux stability and removal of trace organics", Bioresource Technology, Vol. 113, No., pp. 201-206.

Arena, J.T., McCloskey, B., Freeman, B.D. and McCutcheon, J.R. (2011), "Surface modification of thin film composite membrane support layers with polydopamine: Enabling

use of reverse osmosis membranes in pressure retarded osmosis", Journal of Membrane Science, Vol. 375, No. 1-2, pp. 55-62.

Bai, H., Liu, Z. and Sun, D.D. (2011), "Highly water soluble and recovered dextran coated Fe_3O_4 magnetic nanoparticles for brackish water desalination", Separation and Purification Technology, Vol. 81, No. 3, pp. 392-399.

Bamaga, O.A., Yokochi, A. and Beaudry, E.G. (2009), "Application of forward osmosis in pretreatment of seawater for small reverse osmosis desalination units", Desalination and Water Treatment, Vol. 5, No. 1-3, pp. 183-191.

Bamaga, O.A., Yokochi, A., Zabara, B. and Babaqi, A.S. (2011), "Hybrid FO/RO desalination system: Preliminary assessment of osmotic energy recovery and designs of new FO membrane module configurations", Desalination, Vol. 268, No. 1-3, pp. 163-169.

Bolto, B., Tran, T. and Hoang, M. (2007), "Membrane magic - Desalting by forward osmosis", Water, Vol. 34, No. 2, pp. 46-48.

Boo, C., Lee, S., Elimelech, M., Meng, Z. and Hong, S. (2012), "Colloidal fouling in forward osmosis: Role of reverse salt diffusion", Journal of Membrane Science, Vol. 390-391, No., pp. 277-284.

Bui, N.N., Lind, M.L., Hoek, E.M.V. and McCutcheon, J.R. (2011), "Electrospun nanofiber supported thin film composite membranes for engineered osmosis", Journal of Membrane Science, Vol. 385-386, No. 1, pp. 10-19.

Cartinella, J.L., Cath, T.Y., Flynn, M.T., Miller, G.C., Hunter, K.W. and Childress, A.E. (2006), "Removal of natural steroid hormones from wastewater using membrane contactor processes", Environmental Science and Technology, Vol. 40, No. 23, pp. 7381-7386.

Cath, T.Y., Adams, D. and Childress, A.E. (2005a), "Membrane contactor processes for wastewater reclamation in space: II. Combined direct osmosis, osmotic distillation, and membrane distillation for treatment of metabolic wastewater", Journal of Membrane Science, Vol. 257, No. 1-2, pp. 111-119.

Cath, T.Y., Childress, A.E. and Elimelech, M. (2006), "Forward osmosis: Principles, applications, and recent developments", Journal of Membrane Science, Vol. 281, No. 1-2, pp. 70-87.

Cath, T.Y., Gormly, S., Beaudry, E.G., Flynn, M.T., Adams, V.D. and Childress, A.E. (2005b), "Membrane contactor processes for wastewater reclamation in space: Part I. Direct osmotic concentration as pretreatment for reverse osmosis", Journal of Membrane Science, Vol. 257, No. 1-2, pp. 85-98.

Cath, T.Y., Hancock, N.T., Lundin, C.D., Hoppe-Jones, C. and Drewes, J.E. (2010), "A multi-barrier osmotic dilution process for simultaneous desalination and purification of impaired water", Journal of Membrane Science, Vol. 362, No. 1-2, pp. 417-426.

Chai, G.-Y. and Krantz, W.B. (1994), "Formation and characterization of polyamide membranes via interfacial polymerization", Journal of Membrane Science, Vol. 93, No. 2, pp. 175-192.

Chanukya, B.S., Patil, S. and Rastogi, N.K. (2012), "Influence of concentration polarization on flux behavior in forward osmosis during desalination using ammonium bicarbonate", Desalination, Vol. 312, No., pp. 39-44.

Chekli, L., Phuntsho, S., Shon, H.K., Vigneswaran, S., Kandasamy, J. and Chanan, A. (2012), "A review of draw solutes in forward osmosis process and their use in modern applications", Desalination and Water Treatment, Vol. 43, No. 1-3, pp. 167-184.

Choi, Y.J., Choi, J.S., Oh, H.J., Lee, S., Yang, D.R. and Kim, J.H. (2009), "Toward a combined system of forward osmosis and reverse osmosis for seawater desalination", Desalination, Vol. 247, No. 1-3, pp. 239-246.

Chou, S., Shi, L., Wang, R., Tang, C.Y., Qiu, C. and Fane, A.G. (2010), "Characteristics and potential applications of a novel forward osmosis hollow fiber membrane", Desalination, Vol. 261, No. 3, pp. 365-372.

Chou, S., Wang, R., Shi, L., She, Q., Tang, C. and Fane, A.G. (2012), "Thin-film composite hollow fiber membranes for pressure retarded osmosis (PRO) process with high power density", Journal of Membrane Science, Vol. 389, No., pp. 25-33.

Cohen, D. (2004), "Mixing moves osmosis technology forward", Chemical Processing, Vol. 67, No. 10, pp. 29-32.

Cornelissen, E.R., Harmsen, D., Beerendonk, E.F., Qin, J.J., Oo, H., De Korte, K.F. and Kappelhof, J.W.M.N. (2011), "The innovative Osmotic Membrane Bioreactor (OMBR) for reuse of wastewater", Water Science and Technology, Vol. 63, No. 8, pp. 1557-1565.

Cornelissen, E.R., Harmsen, D., de Korte, K.F., Ruiken, C.J., Qin, J.J., Oo, H. and Wessels, L.P. (2008), "Membrane fouling and process performance of forward osmosis membranes on activated sludge", Journal of Membrane Science, Vol. 319, No. 1-2, pp. 158-168.

Decher, G. (1997), "Fuzzy nanoassemblies: Toward layered polymeric multicomposites", Science, Vol. 277, No. 5330, pp. 1232-1237.

Dova, M.I., Petrotos, K.B. and Lazarides, H.N. (2007), "On the direct osmotic concentration of liquid foods. Part I: Impact of process parameters on process performance",

Journal of Food Engineering, Vol. 78, No. 2, pp. 422-430.

Eckenhoff, B. and Yum, S.I. (1981), "The osmotic pump: novel research tool for optimizing drug regimens", Biomaterials, Vol. 2, No. 2, pp. 89-97.

Elimelech, M. (2007), "Yale constructs forward osmosis desalination pilot plant", Membrane Technology, Vol. 2007, No. 1, pp. 7-8.

Elimelech, M. and Bhattacharjee, S. (1998), "A novel approach for modeling concentration polarization in crossflow membrane filtration based on the equivalence of osmotic pressure model and filtration theory", Journal of Membrane Science, Vol. 145, No. 2, pp. 223-241.

Fang, W., Wang, R., Chou, S., Setiawan, L. and Fane, A.G. (2012), "Composite forward osmosis hollow fiber membranes: Integration of RO- and NF-like selective layers to enhance membrane properties of anti-scaling and anti-internal concentration polarization", Journal of Membrane Science, Vol. 394-395, No., pp. 140-150.

Gao, Y., Li, W., Lay, W.C.L., Coster, H.G.L., Fane, A.G. and Tang, C.Y. (2012), "Characterization of forward osmosis membranes by electrochemical impedance spectroscopy", Desalination, Vol., No., pp. In press.

Garcia-Castello, E.M., McCutcheon, J.R. and Elimelech, M. (2009), "Performance evaluation of sucrose concentration using forward osmosis", Journal of Membrane Science, Vol. 338, No. 1-2, pp. 61-66.

Ge, Q., Su, J., Amy, G.L. and Chung, T.S. (2012a), "Exploration of polyelectrolytes as draw solutes in forward osmosis processes", Water Research, Vol. 46, No. 4, pp. 1318-1326.

Ge, Q., Su, J., Chung, T.S. and Amy, G. (2011), "Hydrophilic superparamagnetic nanoparticles: Synthesis, characterization, and performance in forward osmosis processes", Industrial and Engineering Chemistry Research, Vol. 50, No. 1, pp. 382-388.

Ge, Q., Wang, P., Wan, C. and Chung, T.S. (2012b), "Polyelectrolyte-promoted Forward Osmosis-Membrane Distillation (FO-MD) hybrid process for dye wastewater treatment", Environmental Science and Technology, Vol. 46, No. 11, pp. 6236-6243.

Ge, Z. and He, Z. (2012), "Effects of draw solutions and membrane conditions on electricity generation and water flux in osmotic microbial fuel cells", Bioresource Technology, Vol. 109, No., pp. 70-76.

Geise, G.M., Park, H.B., Sagle, A.C., Freeman, B.D. and McGrath, J.E. (2011), "Water permeability and water/salt selectivity tradeoff in polymers for desalination", Journal of Membrane Science, Vol. 369, No. 1-2, pp. 130-138.

Gerstandt, K., Peinemann, K.V., Skilhagen, S.E., Thorsen, T. and Holt, T. (2008), "Membrane processes in energy supply for an osmotic power plant", Desalination, Vol. 224, No. 1-3, pp. 64-70.

Gormly, S., Richardson, T.M.J., Flynn, M. and Kliss, M. (2009), "Lightweight contingency water recovery system concept development", SAE International Journal of Aerospace, Vol. 1, No. 1, pp. 444-453.

Gourley, S. (2006), "US military fields new water filtration system", Jane's Defence Weekly, Vol., No. AUG., pp.

Gray, G.T., McCutcheon, J.R. and Elimelech, M. (2006), "Internal concentration polarization in forward osmosis: role of membrane orientation", Desalination, Vol. 197, No. 1-3, pp. 1-8.

Gregor, H.P. (1974), "Osmotic power plant", Science, Vol. 185, No. 4146, pp. 101-102.

Gruber, M.F., Johnson, C.J., Tang, C., Jensen, M.H., Yde, L. and Helix-Nielsen, C. (2012), "Validation and analysis of forward osmosis CFD model in complex 3D geometries", Membranes, Vol. 2, No. 4, pp. 764-782.

Gruber, M.F., Johnson, C.J., Tang, C.Y., Jensen, M.H., Yde, L. and Helix-Nielsen, C. (2011), "Computational fluid dynamics simulations of flow and concentration polarization in forward osmosis membrane systems", Journal of Membrane Science, Vol. 379, No. 1-2, pp. 488-495.

Guan, J., Zhou, L., Nie, S., Yan, T., Tang, X. and Pan, W. (2009), "A novel gastric-resident osmotic pump tablet: In vitro and in vivo evaluation", International Journal of Pharmaceutics, Vol. 383, No. 1-2, pp. 30-36.

Hammond, P.T. (2011), "Engineering materials layer-by-layer: Challenges and opportunities in multilayer assembly", AIChE Journal, Vol. 57, No. 11, pp. 2928-2940.

Hancock, N.T. and Cath, T.Y. (2009), "Solute coupled diffusion in osmotically driven membrane processes", Environmental Science and Technology, Vol. 43, No. 17, pp. 6769-6775.

Hancock, N.T., Phillip, W.A., Elimelech, M. and Cath, T.Y. (2011), "Bidirectional permeation of electrolytes in osmotically driven membrane processes", Environmental Science and Technology, Vol. 45, No. 24, pp. 10642-10651.

Herron, J. (2005), "Asymmetric forward osmosis membranes", United States Patent 7,445,712.

Holloway, R.W., Childress, A.E., Dennett, K.E. and Cath, T.Y. (2007), "Forward osmosis for concentration of anaerobic digester centrate", Water Research, Vol. 41, No. 17, pp. 4005-4014.

Hoover, L.A., Phillip, W.A., Tiraferri, A., Yip, N.Y. and Elimelech, M. (2011), "Forward with osmosis: Emerging applications for greater sustainability", Environmental Science and Technology, Vol. 45, No. 23, pp. 9824-9830.

Hutchings, N.R., Appleton, E.W. and McGinnis, R.A. (2010), Making high quality frac water out of oilfield waste, pp. 4991-5000, Florence.

Jia, Y.X., Li, H.L., Wang, M., Wu, L.Y. and Hu, Y.D. (2010), "Carbon nanotube: Possible candidate for forward osmosis", Separation and Purification Technology, Vol. 75, No. 1, pp. 55-60.

Jiao, B., Cassano, A. and Drioli, E. (2004), "Recent advances on membrane processes for the concentration of fruit juices: a review", Journal of Food Engineering, Vol. 63, No. 3, pp. 303-324.

Jin, X., Shan, J., Wang, C., Wei, J. and Tang, C.Y. (2012a), "Rejection of pharmaceuticals by forward osmosis membranes", Journal of Hazardous Materials, Vol. 227-228, No., pp. 55-61.

Jin, X., She, Q., Ang, X. and Tang, C.Y. (2012b), "Removal of boron and arsenic by forward osmosis membrane: Influence of membrane orientation and organic fouling", Journal of Membrane Science, Vol. 389, No., pp. 182-187.

Jin, X., Tang, C.Y., Gu, Y., She, Q. and Qi, S. (2011), "Boric acid permeation in forward osmosis membrane processes: Modeling, experiments, and implications", Environmental Science and Technology, Vol. 45, No. 6, pp. 2323-2330.

Jin, Y. and Su, Z. (2009), "Effects of polymerization conditions on hydrophilic groups in aromatic polyamide thin films", Journal of Membrane Science, Vol. 330, No. 1-2, pp. 175-179.

Johnson, P.M., Yoon, J., Kelly, J.Y., Howarter, J.A. and Stafford, C.M. (2012), "Molecular layer-by-layer deposition of highly crosslinked polyamide films", Journal of Polymer Science, Part B: Polymer Physics, Vol. 50, No. 3, pp. 168-173.

Judd, S. (2008), "The status of membrane bioreactor technology", Trends in Biotechnology, Vol. 26, No. 2, pp. 109-116.

Kessler, J.O. and Moody, C.D. (1976), "Drinking water from sea water by forward

osmosis", Desalination, Vol. 18, No. 3, pp. 297-306.

Khare, V.P., Greenberg, A.R. and Krantz, W.B. (2003), "Development of pendant drop mechanical analysis as a technique for determining the stress-relaxation and water-permeation properties of interfacially polymerized barrier layers", Journal of Applied Polymer Science, Vol. 90, No. 10, pp. 2618-2628.

Khare, V.P., Greenberg, A.R. and Krantz, W.B. (2004), "Investigation of the viscoelastic and transport properties of interfacially polymerized barrier layers using pendant drop mechanical analysis", Journal of Applied Polymer Science, Vol. 94, No. 2, pp. 558-568.

Kim, T.W., Kim, Y., Yun, C., Jang, H., Kim, W. and Park, S. (2012), "Systematic approach for draw solute selection and optimal system design for forward osmosis desalination", Desalination, Vol. 284, No., pp. 253-260.

Kim, Y.C. and Elimelech, M. (2012), "Adverse impact of feed channel spacers on the performance of pressure retarded osmosis", Environmental Science and Technology, Vol. 46, No. 8, pp. 4673-4681.

Kim, Y.C., Han, S. and Hong, S. (2011), "A feasibility study of magnetic separation of magnetic nanoparticle for forward osmosis", Water Science and Technology, Vol. 64, No. 2, pp. 469-476.

Kosaraju, P.B. and Sirkar, K.K. (2008), "Interfacially polymerized thin film composite membranes on microporous polypropylene supports for solvent-resistant nanofiltration", Journal of Membrane Science, Vol. 321, No. 2, pp. 155-161.

Kwon, Y.-N., Tang, C.Y. and Leckie, J.O. (2008), "Change of chemical composition and hydrogen bonding behavior due to chlorination of crosslinked polyamide membranes", Journal of Applied Polymer Science, Vol. 108, No. 4, pp. 2061-2066.

Lay, W.C.L., Chong, T.H., Tang, C.Y., Fane, A.G., Zhang, J. and Liu, Y. (2010), "Fouling propensity of forward osmosis: Investigation of the slower flux decline phenomenon", Water Science and Technology, Vol. 61, No. 4, pp. 927-936.

Lay, W.C.L., Zhang, J., Tang, C., Wang, R., Liu, Y. and Fane, A.G. (2012a), "Factors affecting flux performance of forward osmosis systems", Journal of Membrane Science, Vol. 394-395, No., pp. 151-168.

Lay, W.C.L., Zhang, Q., Zhang, J., McDougald, D., Tang, C., Wang, R., Liu, Y. and Fane, A.G. (2011), "Study of integration of forward osmosis and biological process: Membrane performance under elevated salt environment", Desalination, Vol. 283, No., pp. 123-130.

Lay, W.C.L., Zhang, Q., Zhang, J., McDougald, D., Tang, C., Wang, R., Liu, Y. and Fane,

A.G. (2012b), "Effect of pharmaceuticals on the performance of a novel osmotic membrane bioreactor (OMBR)", Separation Science and Technology, Vol. 47, No. 4, pp. 543-554.

Lee, K.L., Baker, R.W. and Lonsdale, H.K. (1981), "Membranes for power generation by pressure-retarded osmosis", Journal of Membrane Science, Vol. 8, No. 2, pp. 141-171.

Lee, K.P., Arnot, T.C. and Mattia, D. (2011), "A review of reverse osmosis membrane materials for desalination-Development to date and future potential", Journal of Membrane Science, Vol. 370, No. 1-2, pp. 1-22.

Lee, S., Boo, C., Elimelech, M. and Hong, S. (2010), "Comparison of fouling behavior in forward osmosis (FO) and reverse osmosis (RO)", Journal of Membrane Science, Vol. 365, No. 1-2, pp. 34-39.

Levenspiel, O. and De Nevers, N. (1974), "Osmotic power plant", Science, Vol. 185, No. 4146, pp. 102.

Li, D., Zhang, X., Yao, J., Simon, G.P. and Wang, H. (2011a), "Stimuli-responsive polymer hydrogels as a new class of draw agent for forward osmosis desalination", Chemical Communications, Vol. 47, No. 6, pp. 1710-1712.

Li, D., Zhang, X., Yao, J., Zeng, Y., Simon, G.P. and Wang, H. (2011b), "Composite polymer hydrogels as draw agents in forward osmosis and solar dewatering", Soft Matter, Vol. 7, No. 21, pp. 10048-10056.

Li, Q., Xu, Z. and Pinnau, I. (2007), "Fouling of reverse osmosis membranes by biopolymers in wastewater secondary effluent: Role of membrane surface properties and initial permeate flux", Journal of Membrane Science, Vol. 290, No. 1-2, pp. 173-181.

Li, W., Gao, Y. and Tang, C.Y. (2011c), "Network modeling for studying the effect of support structure on internal concentration polarization during forward osmosis: Model development and theoretical analysis with FEM", Journal of Membrane Science, Vol. 379, No. 1-2, pp. 307-321.

Li, X.M., Xu, G., Liu, Y. and He, T. (2011d), "Magnetic Fe_3O_4 nanoparticles: Synthesis and application in water treatment", Nanoscience and Nanotechnology - Asia, Vol. 1, No. 1, pp. 14-24.

Li, Z.Y., Yangali-Quintanilla, V., Valladares-Linares, R., Li, Q., Zhan, T. and Amy, G. (2012), "Flux patterns and membrane fouling propensity during desalination of seawater by forward osmosis", Water Research, Vol. 46, No. 1, pp. 195-204.

Ling, M.M. and Chung, T.S. (2011a), "Desalination process using super hydrophilic nanoparticles via forward osmosis integrated with ultrafiltration regeneration", Desalination,

Vol. 278, No. 1-3, pp. 194-202.

Ling, M.M. and Chung, T.S. (2011b), "Novel dual-stage FO system for sustainable protein enrichment using nanoparticles as intermediate draw solutes", Journal of Membrane Science, Vol. 372, No. 1-2, pp. 201-209.

Ling, M.M., Wang, K.Y. and Chung, T.S. (2010), "Highly water-soluble magnetic nanoparticles as novel draw solutes in forward osmosis for water reuse", Industrial and Engineering Chemistry Research, Vol. 49, No. 12, pp. 5869-5876.

Liu, Z., Bai, H., Lee, J. and Sun, D.D. (2011), "A low-energy forward osmosis process to produce drinking water", Energy and Environmental Science, Vol. 4, No. 7, pp. 2582-2585.

Loeb, S. (1975), "Osmotic power plants", Science, Vol. 189, No. 4203, pp. 654-655.

Loeb, S. (1976), "Production of energy from concentrated brines by pressure retarded osmosis. I. Preliminary technical and economic correlations", Journal of Membrane Science, Vol. 1, No. 1, pp. 49-63.

Loeb, S. (2002), "Large-scale power production by pressure-retarded osmosis, using river water and sea water passing through spiral modules", Desalination, Vol. 143, No. 2, pp. 115-122.

Loeb, S., Titelman, L., Korngold, E. and Freiman, J. (1997), "Effect of porous support fabric on osmosis through a Loeb-Sourirajan type asymmetric membrane", Journal of Membrane Science, Vol. 129, No. 2, pp. 243-249.

Loeb, S., Van Hessen, F. and Shahaf, D. (1976), "Production of energy from concentrated brines by pressure retarded osmosis. II. Experimental results and projected energy costs", Journal of Membrane Science, Vol. 1, No. 3, pp. 249-269.

Lonsdale, H.K. (1982), "The growth of membrane technology", Journal of Membrane Science, Vol. 10, No. 2-3, pp. 81-181.

Lonsdale, H.K. (1987), "The evolution of ultrathin synthetic membranes", Journal of Membrane Science, Vol. 33, No. 2, pp. 121-136.

Low, S.C. (2009), "Preliminary studies of seawater desalination using forward osmosis", Desalination and Water Treatment, Vol. 7, No. 1-3, pp. 41-46.

Lutchmiah, K., Cornelissen, E.R., Harmsen, D.J.H., Post, J.W., Lampi, K., Ramaekers, H., Rietveld, L.C. and Roest, K. (2011), "Water recovery from sewage using forward osmosis", Water Science and Technology, Vol. 64, No. 7, pp. 1443-1449.

Ma, N., Wei, J., Liao, R. and Tang, C.Y. (2012), "Zeolite-polyamide thin film nanocomposite membranes: Towards enhanced performance for forward osmosis", Journal of Membrane Science, Vol. 405-406, No., pp. 149-157.

Martinetti, C.R., Childress, A.E. and Cath, T.Y. (2009), "High recovery of concentrated RO brines using forward osmosis and membrane distillation", Journal of Membrane Science, Vol. 331, No. 1-2, pp. 31-39.

McCutcheon, J.R. and Elimelech, M. (2006), "Influence of concentrative and dilutive internal concentration polarization on flux behavior in forward osmosis", Journal of Membrane Science, Vol. 284, No. 1-2, pp. 237-247.

McCutcheon, J.R. and Elimelech, M. (2007), "Modeling water flux in forward osmosis: Implications for improved membrane design", AIChE Journal, Vol. 53, No. 7, pp. 1736-1744.

McCutcheon, J.R. and Elimelech, M. (2008), "Influence of membrane support layer hydrophobicity on water flux in osmotically driven membrane processes", Journal of Membrane Science, Vol. 318, No. 1-2, pp. 458-466.

McCutcheon, J.R., McGinnis, R. and Elimelech, M. (2005a), Desalination using a novel ammonia-carbon dioxide forward osmosis process: Evaluation of process performance, p. 2094, Cincinnati, OH.

McCutcheon, J.R., McGinnis, R.L. and Elimelech, M. (2005b), "A novel ammonia-carbon dioxide forward (direct) osmosis desalination process", Desalination, Vol. 174, No. 1, pp. 1-11.

McCutcheon, J.R., McGinnis, R.L. and Elimelech, M. (2006), "Desalination by ammonia-carbon dioxide forward osmosis: Influence of draw and feed solution concentrations on process performance", Journal of Membrane Science, Vol. 278, No. 1-2, pp. 114-123.

McGinnis, R.L. and Elimelech, M. (2007), "Energy requirements of ammonia-carbon dioxide forward osmosis desalination", Desalination, Vol. 207, No. 1-3, pp. 370-382.

McGinnis, R.L., McCutcheon, J.R. and Elimelech, M. (2007), "A novel ammonia-carbon dioxide osmotic heat engine for power generation", Journal of Membrane Science, Vol. 305, No. 1-2, pp. 13-19.

Mehta, G.D. and Loeb, S. (1978), "Internal polarization in the porous substructure of a semipermeable membrane under pressure-retarded osmosis", Journal of Membrane Science, Vol. 4, No., pp. 261-265.

Mehta, G.D. and Loeb, S. (1979), "Performance of permasep B-9 and B-10 membranes in various osmotic regions and at high osmotic pressures", Journal of Membrane Science, Vol. 4, No. 3, pp. 335-349.

Mi, B. and Elimelech, M. (2008), "Chemical and physical aspects of organic fouling of forward osmosis membranes", Journal of Membrane Science, Vol. 320, No. 1-2, pp. 292-302.

Mi, B. and Elimelech, M. (2010a), "Gypsum scaling and cleaning in forward osmosis: Measurements and mechanisms", Environmental Science and Technology, Vol. 44, No. 6, pp. 2022-2028.

Mi, B. and Elimelech, M. (2010b), "Organic fouling of forward osmosis membranes: Fouling reversibility and cleaning without chemical reagents", Journal of Membrane Science, Vol. 348, No. 1-2, pp. 337-345.

Moody, C.D. and Kessler, J.O. (1976), "Forward osmosis extractors", Desalination, Vol. 18, No. 3, pp. 283-295.

Mulder, M. (1996), Basic principles of membrane technology, 2nd, Kluwer Academic Publishers.

Ng, H.Y., Tang, W. and Wong, W.S. (2006), "Performance of forward (direct) osmosis process: Membrane structure and transport phenomenon", Environmental Science and Technology, Vol. 40, No. 7, pp. 2408-2413.

Norman, R.S. (1975), "Osmotic power plants", Science, Vol. 189, No. 4203, pp. 655.

Ong, R.C. and Chung, T.S. (2012), "Fabrication and positron annihilation spectroscopy (PAS) characterization of cellulose triacetate membranes for forward osmosis", Journal of Membrane Science, Vol. 394-395, No., pp. 230-240.

Patel-Predd, P. (2006), "Technology solutions: Water desalination takes a step forward", Environmental Science and Technology, Vol. 40, No. 11, pp. 3454-3455.

Patel, S. (2010), "Norway inaugurates osmotic power plant", Power, Vol. 154, No. 2, pp.

Pattle, R.E. (1954), "Production of electric power by mixing fresh and salt water in the hydroelectric pile [19]", Nature, Vol. 174, No. 4431, pp. 660.

Pearce, G. (2010-2011), "Desalination shake up: Forward thinking membrane developments", Water and Wastewater International, Vol. 25, No. 6, pp. 36-37.

Petersen, R.J. (1993), "Composite reverse osmosis and nanofiltration membranes", Journal of Membrane Science, Vol. 83, No. 1, pp. 81-150.

Petrotos, K.B. and Lazarides, H.N. (2001), "Osmotic concentration of liquid foods", Journal of Food Engineering, Vol. 49, No. 2-3, pp. 201-206.

Petrotos, K.B., Quantick, P. and Petropakis, H. (1998), "A study of the direct osmotic concentration of tomato juice in tubular membrane - module configuration. I. The effect of certain basic process parameters on the process performance", Journal of Membrane Science, Vol. 150, No. 1, pp. 99-110.

Phillip, W.A., Yong, J.S. and Elimelech, M. (2010), "Reverse draw solute permeation in forward osmosis: Modeling and experiments", Environmental Science and Technology, Vol. 44, No. 13, pp. 5170-5176.

Phuntsho, S., Shon, H.K., Hong, S., Lee, S. and Vigneswaran, S. (2011), "A novel low energy fertilizer driven forward osmosis desalination for direct fertigation: Evaluating the performance of fertilizer draw solutions", Journal of Membrane Science, Vol. 375, No. 1-2, pp. 172-181.

Phuntsho, S., Shon, H.K., Hong, S., Lee, S., Vigneswaran, S. and Kandasamy, J. (2012a), "Fertiliser drawn forward osmosis desalination: The concept, performance and limitations for fertigation", Reviews in Environmental Science and Biotechnology, Vol. 11, No. 2, pp. 147-168.

Phuntsho, S., Shon, H.K., Majeed, T., El Saliby, I., Vigneswaran, S., Kandasamy, J., Hong, S. and Lee, S. (2012b), "Blended fertilizers as draw solutions for fertilizer-drawn forward osmosis desalination", Environmental Science and Technology, Vol. 46, No. 8, pp. 4567-4575.

Post, J.W., Veerman, J., Hamelers, H.V.M., Euverink, G.J.W., Metz, S.J., Nymeijer, K. and Buisman, C.J.N. (2007), "Salinity-gradient power: Evaluation of pressure-retarded osmosis and reverse electrodialysis", Journal of Membrane Science, Vol. 288, No. 1-2, pp. 218-230.

Prakash Rao, A., Desai, N.V. and Rangarajan, R. (1997), "Interfacially synthesized thin film composite RO membranes for seawater desalination", Journal of Membrane Science, Vol. 124, No. 2, pp. 263-272.

Qi, S., Li, W., Zhao, Y., Ma, N., Wei, J., Chin, T.W. and Tang, C.Y. (2012a), "Influence of the properties of layer-by-layer active layers on forward osmosis performance", Journal of Membrane Science, Vol. 423-424, No., pp. 536-542.

Qi, S., Qiu, C.Q., Zhao, Y. and Tang, C.Y. (2012b), "Double-skinned forward osmosis membranes based on layer-by-layer assembly-FO performance and fouling behavior",

Journal of Membrane Science, Vol. 405-406, No., pp. 20-29.

Qin, J.J., Kekre, K.A., Oo, M.H., Tao, G., Lay, C.L., Lew, C.H., Cornelissen, E.R. and Ruiken, C.J. (2010), "Preliminary study of osmotic membrane bioreactor: Effects of draw solution on water flux and air scouring on fouling", Water Science and Technology, Vol. 62, No. 6, pp. 1353-1360.

Qin, J.J., Oo, M.H., Tao, G., Cornelissen, E.R., Ruiken, C.J., de Korte, K.F., Wessels, L.P. and Kekre, K.A. (2009), "Optimization of operating conditions in forward osmosis for osmotic membrane bioreactor", Open Chemical Engineering Journal, Vol. 3, No., pp. 27-32.

Qiu, C., Qi, S. and Tang, C.Y. (2011a), "Synthesis of high flux forward osmosis membranes by chemically crosslinked layer-by-layer polyelectrolytes", Journal of Membrane Science, Vol. 381, No. 1-2, pp. 74-80.

Qiu, C., Setiawan, L., Wang, R., Tang, C.Y. and Fane, A.G. (2011b), "High performance flat sheet forward osmosis membrane with an NF-like selective layer on a woven fabric embedded substrate", Desalination, Vol. 287, No., pp. 266-270.

Reali, M. (1980), "Closed cycle osmotic power plants for electric power production", Energy, Vol. 5, No. 4, pp. 325-329.

Reali, M. (1981), "Submarine hydro-electro-osmotic power plants for an efficient exploitation of salinity gradients", Energy, Vol. 6, No. 3, pp. 227-231.

Roh, I.J., Greenberg, A.R. and Khare, V.P. (2006), "Synthesis and characterization of interfacially polymerized polyamide thin films", Desalination, Vol. 191, No. 1-3, pp. 279-290.

Roh, I.J., Park, S.Y., Kim, J.J. and Kim, C.K. (1998), "Effects of the polyamide molecular structure on the performance of reverse osmosis membranes", Journal of Polymer Science, Part B: Polymer Physics, Vol. 36, No. 11, pp. 1821-1830.

Sablani, S., Goosen, M., Al-Belushi, R. and Wilf, M. (2001), "Concentration polarization in ultrafiltration and reverse osmosis: A critical review", Desalination, Vol. 141, No. 3, pp. 269-289.

Sairam, M., Sereewatthanawut, E., Li, K., Bismarck, A. and Livingston, A.G. (2011), "Method for the preparation of cellulose acetate flat sheet composite membranes for forward osmosis-Desalination using $MgSO_4$ draw solution", Desalination, Vol. 273, No. 2-3, pp. 299-307.

Sant'Anna, V., Marczak, L.D.F. and Tessaro, I.C. (2012), "Membrane concentration of liquid foods by forward osmosis: Process and quality view", Journal of Food Engineering,

Vol. 111, No. 3, pp. 483-489.

Saren, Q., Qiu, C.Q. and Tang, C.Y. (2011), "Synthesis and characterization of novel forward osmosis membranes based on layer-by-layer assembly", Environmental Science and Technology, Vol. 45, No. 12, pp. 5201-5208.

Sarp, S., Lee, S., Park, K., Park, M., Kim, J.H. and Cho, J. (2012), "Using macromolecules as osmotically active compounds in osmosis followed by filtration (OF) system", Desalination and Water Treatment, Vol. 43, No. 1-3, pp. 131-137.

Schultz, W.L. (2010), "Going forward", Pollution Engineering, Vol. 42, No. 6, pp. 37-38.

Setiawan, L., Shi, L., Krantz, W.B. and Wang, R. (2012a), "Explorations of delamination and irregular structure in poly(amide-imide)-polyethersulfone dual layer hollow fiber membranes", Journal of Membrane Science, Vol. 423-424, No., pp. 73-84.

Setiawan, L., Wang, R., Li, K. and Fane, A.G. (2011), "Fabrication of novel poly(amide-imide) forward osmosis hollow fiber membranes with a positively charged nanofiltration-like selective layer", Journal of Membrane Science, Vol. 369, No. 1-2, pp. 196-205.

Setiawan, L., Wang, R., Li, K. and Fane, A.G. (2012b), "Fabrication and characterization of forward osmosis hollow fiber membranes with antifouling NF-like selective layer", Journal of Membrane Science, Vol. 394-395, No., pp. 80-88.

Setiawan, L., Wang, R., Shi, L., Li, K. and Fane, A.G. (2012c), "Novel dual-layer hollow fiber membranes applied for forward osmosis process", Journal of Membrane Science, Vol. 421-422, No., pp. 238-246.

She, Q., Jin, X., Li, Q. and Tang, C.Y. (2012a), "Relating reverse and forward solute diffusion to membrane fouling in osmotically driven membrane processes", Water Research, Vol. 46, No. 7, pp. 2478-2486.

She, Q., Jin, X. and Tang, C.Y. (2012b), "Osmotic power production from salinity gradient resource by pressure retarded osmosis: Effects of operating conditions and reverse solute diffusion", Journal of Membrane Science, Vol. 401-402, No., pp. 262-273.

Shi, L., Chou, S.R., Wang, R., Fang, W.X., Tang, C.Y. and Fane, A.G. (2011), "Effect of substrate structure on the performance of thin-film composite forward osmosis hollow fiber membranes", Journal of Membrane Science, Vol. 382, No. 1-2, pp. 116-123.

Shi, L., Wang, R., Cao, Y., Liang, D.T. and Tay, J.H. (2008), "Effect of additives on the fabrication of poly(vinylidene fluoride-co-hexafluropropylene) (PVDF-HFP) asymmetric microporous hollow fiber membranes", Journal of Membrane Science, Vol. 315, No. 1-2, pp. 195-204.

Skilhagen, S.E., Dugstad, J.E. and Aaberg, R.J. (2008), "Osmotic power - power production based on the osmotic pressure difference between waters with varying salt gradients", Desalination, Vol. 220, No. 1-3, pp. 476-482.

Song, X., Liu, Z. and Sun, D.D. (2011), "Nano gives the answer: Breaking the bottleneck of internal concentration polarization with a nanofiber composite forward osmosis membrane for a high water production rate", Advanced Materials, Vol. 23, No. 29, pp. 3256-3260.

Song, Y., Sun, P., Henry, L.L. and Sun, B. (2005), "Mechanisms of structure and performance controlled thin film composite membrane formation via interfacial polymerization process", Journal of Membrane Science, Vol. 251, No. 1-2, pp. 67-79.

Strathmann, H. (1981), "Membrane separation processes", Journal of Membrane Science, Vol. 9, No. 1-2, pp. 121-189.

Strathmann, H. and Kock, K. (1977), "The formation mechanism of phase inversion membranes", Desalination, Vol. 21, No. 3, pp. 241-255.

Su, J. and Chung, T.S. (2011), "Sublayer structure and reflection coefficient and their effects on concentration polarization and membrane performance in FO processes", Journal of Membrane Science, Vol. 376, No. 1-2, pp. 214-224.

Su, J., Chung, T.S., Helmer, B.J. and de Wit, J.S. (2012), "Enhanced double-skinned FO membranes with inner dense layer for wastewater treatment and macromolecule recycle using Sucrose as draw solute", Journal of Membrane Science, Vol. 396, No., pp. 92-100.

Su, J., Yang, Q., Teo, J.F. and Chung, T.S. (2010a), "Cellulose acetate nanofiltration hollow fiber membranes for forward osmosis processes", Journal of Membrane Science, Vol. 355, No. 1-2, pp. 36-44.

Su, J., Zhang, S., Chen, H., Jean, Y.C. and Chung, T.S. (2010b), "Effects of annealing on the microstructure and performance of cellulose acetate membranes for pressure-retarded osmosis processes", Journal of Membrane Science, Vol. 364, No. 1-2, pp. 344-353.

Subramani, A., Badruzzaman, M., Oppenheimer, J. and Jacangelo, J.G. (2011), "Energy minimization strategies and renewable energy utilization for desalination: A review", Water Research, Vol. 45, No. 5, pp. 1907-1920.

Sukitpaneenit, P. and Chung, T.S. (2009), "Molecular elucidation of morphology and mechanical properties of PVDF hollow fiber membranes from aspects of phase inversion, crystallization and rheology", Journal of Membrane Science, Vol. 340, No. 1-2, pp. 192-205.

Tan, C.H. and Ng, H.Y. (2008), "Modified models to predict flux behavior in forward osmosis in consideration of external and internal concentration polarizations", Journal of Membrane Science, Vol. 324, No. 1-2, pp. 209-219.

Tan, C.H. and Ng, H.Y. (2010), "A novel hybrid forward osmosis - nanofiltration (FO-NF) process for seawater desalination: Draw solution selection and system configuration", Desalination and Water Treatment, Vol. 13, No. 1-3, pp. 356-361.

Tang, C.Y., Fu, Q.S., Criddle, C.S. and Leckie, J.O. (2007a), "Effect of flux (transmembrane pressure) and membrane properties on fouling and rejection of reverse osmosis and nanofiltration membranes treating perfluorooctane sulfonate containing wastewater", Environmental Science and Technology, Vol. 41, No. 6, pp. 2008-2014.

Tang, C.Y., Kwon, Y.-N. and Leckie, J.O. (2007b), "Characterization of humic acid fouled reverse osmosis and nanofiltration membranes by transmission electron microscopy and streaming potential Measurements", Environmental Science & Technology, Vol. 41, No. 3, pp. 942-949.

Tang, C.Y., Kwon, Y.-N. and Leckie, J.O. (2007c), "Probing the nano- and micro-scales of reverse osmosis membranes--A comprehensive characterization of physiochemical properties of uncoated and coated membranes by XPS, TEM, ATR-FTIR, and streaming potential measurements", Journal of Membrane Science, Vol. 287, No. 1, pp. 146-156.

Tang, C.Y., Kwon, Y.-N. and Leckie, J.O. (2009a), "Effect of membrane chemistry and coating layer on physiochemical properties of thin film composite polyamide RO and NF membranes: I. FTIR and XPS characterization of polyamide and coating layer chemistry", Desalination, Vol. 242, No. 1-3, pp. 149-167.

Tang, C.Y., Kwon, Y.N. and Leckie, J.O. (2009b), "Effect of membrane chemistry and coating layer on physiochemical properties of thin film composite polyamide RO and NF membranes. II. Membrane physiochemical properties and their dependence on polyamide and coating layers", Desalination, Vol. 242, No. 1-3, pp. 168-182.

Tang, C.Y., She, Q., Lay, W.C.L., Wang, R. and Fane, A.G. (2010), "Coupled effects of internal concentration polarization and fouling on flux behavior of forward osmosis membranes during humic acid filtration", Journal of Membrane Science, Vol. 354, No. 1-2, pp. 123-133.

Tang, C.Y., She, Q., Lay, W.C.L., Wang, R., Field, R. and Fane, A.G. (2011), "Modeling double-skinned FO membranes", Desalination, Vol. 283, No., pp. 178-186.

Tang, W. and Ng, H.Y. (2008), "Concentration of brine by forward osmosis: Performance and influence of membrane structure", Desalination, Vol. 224, No. 1-3, pp. 143-153.

Theeuwes, F. and Yum, S.I. (1976), "Principles of the design and operation of generic

osmotic pumps for the delivery of semisolid or liquid drug formulations", Annals of Biomedical Engineering, Vol. 4, No. 4, pp. 343-353.

Thorsen, T. and Holt, T. (2009), "The potential for power production from salinity gradients by pressure retarded osmosis", Journal of Membrane Science, Vol. 335, No. 1-2, pp. 103-110.

Tiraferri, A., Yip, N.Y., Phillip, W.A., Schiffman, J.D. and Elimelech, M. (2011), "Relating performance of thin-film composite forward osmosis membranes to support layer formation and structure", Journal of Membrane Science, Vol. 367, No. 1-2, pp. 340-352.

Ulbricht, M. (2006), "Advanced functional polymer membranes", Polymer, Vol. 47, No. 7, pp. 2217-2262.

Van De Witte, P., Dijkstra, P.J., Van Den Berg, J.W.A. and Feijen, J. (1996), "Phase separation processes in polymer solutions in relation to membrane formation", Journal of Membrane Science, Vol. 117, No. 1-2, pp. 1-31.

Ver śsimo, S., Peinemann, K.V. and Bordado, J. (2006), "Influence of the diamine structure on the nanofiltration performance, surface morphology and surface charge of the composite polyamide membranes", Journal of Membrane Science, Vol. 279, No. 1-2, pp. 266-275.

Vigo, F. and Uliana, C. (1986), "Suitability of reverse osmosis membranes for energy recovery by submarine osmotic power plants", Desalination, Vol. 60, No. 1, pp. 45-57.

Vrijenhoek, E.M., Hong, S. and Elimelech, M. (2001), "Influence of membrane surface properties on initial rate of colloidal fouling of reverse osmosis and nanofiltration membranes", Journal of Membrane Science, Vol. 188, No. 1, pp. 115-128.

Wallace, M., Cui, Z. and Hankins, N.P. (2008), "A thermodynamic benchmark for assessing an emergency drinking water device based on forward osmosis", Desalination, Vol. 227, No. 1-3, pp. 34-45.

Wang, H., Chung, T.S., Tong, Y.W., Jeyaseelan, K., Armugam, A., Chen, Z., Hong, M. and Meier, W. (2012a), "Highly permeable and selective pore-spanning biomimetic membrane embedded with aquaporin Z", Small, Vol. 8, No. 8, pp. 1185-1190.

Wang, K.Y., Chung, T.-S. and Qin, J.-J. (2007), "Polybenzimidazole (PBI) nanofiltration hollow fiber membranes applied in forward osmosis process", Journal of Membrane Science, Vol. 300, No. 1-2, pp. 6-12.

Wang, K.Y., Chung, T.S. and Amy, G. (2012b), "Developing thin-film-composite forward osmosis membranes on the PES/SPSf substrate through interfacial polymerization", AIChE Journal, Vol. 58, No. 3, pp. 770-781.

Wang, K.Y., Ong, R.C. and Chung, T.S. (2010a), "Double-skinned forward osmosis membranes for reducing internal concentration polarization within the porous sublayer", Industrial and Engineering Chemistry Research, Vol. 49, No. 10, pp. 4824-4831.

Wang, K.Y., Teoh, M.M., Nugroho, A. and Chung, T.S. (2011), "Integrated forward osmosis-membrane distillation (FO-MD) hybrid system for the concentration of protein solutions", Chemical Engineering Science, Vol. 66, No. 11, pp. 2421-2430.

Wang, K.Y., Yang, Q., Chung, T.S. and Rajagopalan, R. (2009), "Enhanced forward osmosis from chemically modified polybenzimidazole (PBI) nanofiltration hollow fiber membranes with a thin wall", Chemical Engineering Science, Vol. 64, No. 7, pp. 1577-1584.

Wang, R., Shi, L., Tang, C.Y., Chou, S., Qiu, C. and Fane, A.G. (2010b), "Characterization of novel forward osmosis hollow fiber membranes", Journal of Membrane Science, Vol. 355, No. 1-2, pp. 158-167.

Wang, Y., Wicaksana, F., Tang, C.Y. and Fane, A.G. (2010c), "Direct microscopic observation of forward osmosis membrane fouling", Environmental Science and Technology, Vol. 44, No. 18, pp. 7102-7109.

Wang, Y.N. and Tang, C.Y. (2011a), "Fouling of nanofiltration, reverse osmosis, and ultrafiltration membranes by protein mixtures: The role of inter-foulant-species interaction", Environmental Science and Technology, Vol. 45, No. 15, pp. 6373-6379.

Wang, Y.N. and Tang, C.Y. (2011b), "Nanofiltration membrane fouling by oppositely charged macromolecules: Investigation on flux behavior, foulant mass deposition, and solute rejection", Environmental Science and Technology, Vol. 45, No. 20, pp. 8941-8947.

Wang, Y.N. and Tang, C.Y. (2011c), "Protein fouling of nanofiltration, reverse osmosis, and ultrafiltration membranes-The role of hydrodynamic conditions, solution chemistry, and membrane properties", Journal of Membrane Science, Vol. 376, No. 1-2, pp. 275-282.

Wang, Y.N., Wei, J., She, Q., Pacheco, F. and Tang, C.Y. (2012c), "Microscopic characterization of FO/PRO membranes - A comparative study of CLSM, TEM and SEM", Environmental Science and Technology, Vol. 46, No. 18, pp. 9995-10003.

Waterman, K.C., MacDonald, B.C. and Roy, M.C. (2009), "Extrudable core system: Development of a single-layer osmotic controlled-release tablet", Journal of Controlled Release, Vol. 134, No. 3, pp. 201-206.

Wei, J., Liu, X., Qiu, C., Wang, R. and Tang, C.Y. (2011a), "Influence of monomer concentrations on the performance of polyamide-based thin film composite forward osmosis membranes", Journal of Membrane Science, Vol. 381, No. 1-2, pp. 110-117.

Wei, J., Qiu, C., Tang, C.Y., Wang, R. and Fane, A.G. (2011b), "Synthesis and characterization of flat-sheet thin film composite forward osmosis membranes", Journal of Membrane Science, Vol. 372, No. 1-2, pp. 292-302.

Wei, J., Qiu, C., Wang, Y.-N., Wang, R. and Tang, C.Y. (2013), "Comparison of NF-like and RO-like thin film composite osmotically-driven membranes—Implications for membrane selection and process optimization", Journal of Membrane Science, Vol. 427, No., pp. 460-471.

Widjojo, N., Chung, T.S., Weber, M., Maletzko, C. and Warzelhan, V. (2011), "The role of sulphonated polymer and macrovoid-free structure in the support layer for thin-film composite (TFC) forward osmosis (FO) membranes", Journal of Membrane Science, Vol. 383, No. 1-2, pp. 214-223.

Xiao, D., Li, W., Chou, S., Wang, R. and Tang, C.Y. (2012), "A modeling investigation on optimizing the design of forward osmosis hollow fiber modules", Journal of Membrane Science, Vol. 392-393, No., pp. 76-87.

Xiao, D., Tang, C.Y., Zhang, J., Lay, W.C.L., Wang, R. and Fane, A.G. (2011), "Modeling salt accumulation in osmotic membrane bioreactors: Implications for FO membrane selection and system operation", Journal of Membrane Science, Vol. 366, No. 1-2, pp. 314-324.

Xie, M., Nghiem, L.D., Price, W.E. and Elimelech, M. (2012a), "Comparison of the removal of hydrophobic trace organic contaminants by forward osmosis and reverse osmosis", Water Research, Vol. 46, No. 8, pp. 2683-2692.

Xie, M., Price, W.E. and Nghiem, L.D. (2012b), "Rejection of pharmaceutically active compounds by forward osmosis: Role of solution pH and membrane orientation", Separation and Purification Technology, Vol. 93, No., pp. 107-114.

Xu, Y., Peng, X., Tang, C.Y., Fu, Q.S. and Nie, S. (2010), "Effect of draw solution concentration and operating conditions on forward osmosis and pressure retarded osmosis performance in a spiral wound module", Journal of Membrane Science, Vol. 348, No. 1-2, pp. 298-309.

Yang, Q., Wang, K.Y. and Chung, T.S. (2009a), "Dual-layer hollow fibers with enhanced flux as novel forward osmosis membranes for water production", Environmental Science and Technology, Vol. 43, No. 8, pp. 2800-2805.

Yang, Q., Wang, K.Y. and Chung, T.S. (2009b), "A novel dual-layer forward osmosis membrane for protein enrichment and concentration", Separation and Purification Technology, Vol. 69, No. 3, pp. 269-274.

Yangali-Quintanilla, V., Li, Z., Valladares, R., Li, Q. and Amy, G. (2011), "Indirect desalination of Red Sea water with forward osmosis and low pressure reverse osmosis for water reuse", Desalination, Vol. 280, No. 1-3, pp. 160-166.

Yap, W.J., Zhang, J., Lay, W.C.L., Cao, B., Fane, A.G. and Liu, Y. (2012), "State of the art of osmotic membrane bioreactors for water reclamation", Bioresource Technology, Vol. 122, No., pp. 217-222.

Yen, S.K., Mehnas Haja N, F., Su, M., Wang, K.Y. and Chung, T.S. (2010), "Study of draw solutes using 2-methylimidazole-based compounds in forward osmosis", Journal of Membrane Science, Vol. 364, No. 1-2, pp. 242-252.

Yip, N.Y. and Elimelech, M. (2011), "Performance limiting effects in power generation from salinity gradients by pressure retarded osmosis", Environmental Science and Technology, Vol. 45, No. 23, pp. 10273-10282.

Yip, N.Y., Tiraferri, A., Phillip, W.A., Schiffman, J.D. and Elimelech, M. (2010), "High performance thin-film composite forward osmosis membrane", Environmental Science and Technology, Vol. 44, No. 10, pp. 3812-3818.

Yip, N.Y., Tiraferri, A., Phillip, W.A., Schiffman, J.D., Hoover, L.A., Kim, Y.C. and Elimelech, M. (2011), "Thin-film composite pressure retarded osmosis membranes for sustainable power generation from salinity gradients", Environmental Science and Technology, Vol. 45, No. 10, pp. 4360-4369.

Yu, Y., Seo, S., Kim, I.C. and Lee, S. (2011), "Nanoporous polyethersulfone (PES) membrane with enhanced flux applied in forward osmosis process", Journal of Membrane Science, Vol. 375, No. 1-2, pp. 63-68.

Zhang, F., Brastad, K.S. and He, Z. (2011a), "Integrating forward osmosis into microbial fuel cells for wastewater treatment, water extraction and bioelectricity generation", Environmental Science and Technology, Vol. 45, No. 15, pp. 6690-6696.

Zhang, H., Ma, Y., Jiang, T., Zhang, G. and Yang, F. (2012a), "Influence of activated sludge properties on flux behavior in osmosis membrane bioreactor (OMBR)", Journal of Membrane Science, Vol. 390-391, No., pp. 270-276.

Zhang, J., Loong, W.L.C., Chou, S., Tang, C., Wang, R. and Fane, A.G. (2012b), "Membrane biofouling and scaling in forward osmosis membrane bioreactor", Journal of Membrane Science, Vol. 403-404, No., pp. 8-14.

Zhang, S., Wang, K.Y., Chung, T.S., Chen, H., Jean, Y.C. and Amy, G. (2010), "Well-constructed cellulose acetate membranes for forward osmosis: Minimized internal concentration polarization with an ultra-thin selective layer", Journal of Membrane Science, Vol. 360, No. 1-2, pp. 522-535.

Zhang, S., Wang, K.Y., Chung, T.S., Jean, Y.C. and Chen, H. (2011b), "Molecular design of the cellulose ester-based forward osmosis membranes for desalination", Chemical Engineering Science, Vol. 66, No. 9, pp. 2008-2018.

Zhang, S., Zhang, R., Jean, Y.C., Paul, D.R. and Chung, T.S. (2012c), "Cellulose esters for forward osmosis: Characterization of water and salt transport properties and free volume", Polymer (United Kingdom), Vol. 53, No. 13, pp. 2664-2672.

Zhao, S. and Zou, L. (2011a), "Effects of working temperature on separation performance, membrane scaling and cleaning in forward osmosis desalination", Desalination, Vol. 278, No. 1-3, pp. 157-164.

Zhao, S. and Zou, L. (2011b), "Relating solution physicochemical properties to internal concentration polarization in forward osmosis", Journal of Membrane Science, Vol. 379, No. 1-2, pp. 459-467.

Zhao, S., Zou, L. and Mulcahy, D. (2012a), "Brackish water desalination by a hybrid forward osmosis-nanofiltration system using divalent draw solute", Desalination, Vol. 284, No., pp. 175-181.

Zhao, S., Zou, L., Tang, C.Y. and Mulcahy, D. (2012b), "Recent developments in forward osmosis: Opportunities and challenges", Journal of Membrane Science, Vol. 396, No., pp. 1-21.

Zou, S., Gu, Y., Xiao, D. and Tang, C.Y. (2011), "The role of physical and chemical parameters on forward osmosis membrane fouling during algae separation", Journal of Membrane Science, Vol. 366, No. 1-2, pp. 356-362.

ELSEVIER LICENSE
TERMS AND CONDITIONS

Jul 03, 2013

This is a License Agreement between Jing Wei ("You") and Elsevier ("Elsevier") provided by Copyright Clearance Center ("CCC"). The license consists of your order details, the terms and conditions provided by Elsevier, and the payment terms and conditions.

All payments must be made in full to CCC. For payment instructions, please see information listed at the bottom of this form.

Supplier	Elsevier Limited The Boulevard,Langford Lane Kidlington,Oxford,OX5 1GB,UK
Registered Company Number	1982084
Customer name	Jing Wei
Customer address	1 Cleantech Loop, CleanTech One, #06-08 Singapore, 637141
License number	3181260660941
License date	Jul 03, 2013
Licensed content publisher	Elsevier
Licensed content publication	Journal of Membrane Science
Licensed content title	Synthesis and characterization of flat-sheet thin film composite forward osmosis membranes
Licensed content author	Jing Wei,Changquan Qiu,Chuyang Y. Tang,Rong Wang,Anthony G. Fane
Licensed content date	15 April 2011
Licensed content volume number	372
Licensed content issue number	1–2
Number of pages	11
Start Page	292
End Page	302
Type of Use	reuse in a thesis/dissertation
Intended publisher of new work	other
Portion	full article
Format	both print and electronic
Are you the author of this Elsevier article?	Yes

Will you be translating?	No
Order reference number	
Title of your thesis/dissertation	Synthesis of Flat-sheet Thin Film Composite Forward Osmosis Membranes
Expected completion date	Jul 2013
Estimated size (number of pages)	200
Elsevier VAT number	GB 494 6272 12
Permissions price	0.00 USD
VAT/Local Sales Tax	0.00 USD / 0.00 GBP
Total	0.00 USD
Terms and Conditions	

INTRODUCTION

1. The publisher for this copyrighted material is Elsevier. By clicking "accept" in connection with completing this licensing transaction, you agree that the following terms and conditions apply to this transaction (along with the Billing and Payment terms and conditions established by Copyright Clearance Center, Inc. ("CCC"), at the time that you opened your Rightslink account and that are available at any time at http://myaccount.copyright.com).

GENERAL TERMS

2. Elsevier hereby grants you permission to reproduce the aforementioned material subject to the terms and conditions indicated.

3. Acknowledgement: If any part of the material to be used (for example, figures) has appeared in our publication with credit or acknowledgement to another source, permission must also be sought from that source. If such permission is not obtained then that material may not be included in your publication/copies. Suitable acknowledgement to the source must be made, either as a footnote or in a reference list at the end of your publication, as follows:

"Reprinted from Publication title, Vol /edition number, Author(s), Title of article / title of chapter, Pages No., Copyright (Year), with permission from Elsevier [OR APPLICABLE SOCIETY COPYRIGHT OWNER]." Also Lancet special credit - "Reprinted from The Lancet, Vol. number, Author(s), Title of article, Pages No., Copyright (Year), with permission from Elsevier."

4. Reproduction of this material is confined to the purpose and/or media for which permission is hereby given.

5. Altering/Modifying Material: Not Permitted. However figures and illustrations may be altered/adapted minimally to serve your work. Any other abbreviations, additions, deletions and/or any other alterations shall be made only with prior written authorization of Elsevier Ltd. (Please contact Elsevier at permissions@elsevier.com)

6. If the permission fee for the requested use of our material is waived in this instance, please be advised that your future requests for Elsevier materials may attract a fee.

7. Reservation of Rights: Publisher reserves all rights not specifically granted in the combination of (i) the license details provided by you and accepted in the course of this licensing transaction, (ii) these terms and conditions and (iii) CCC's Billing and Payment terms and conditions.

8. License Contingent Upon Payment: While you may exercise the rights licensed immediately upon issuance of the license at the end of the licensing process for the transaction, provided that you have disclosed complete and accurate details of your proposed use, no license is finally effective unless and until full payment is received from you (either by publisher or by CCC) as provided in CCC's Billing and Payment terms and conditions. If full payment is not received on a timely basis, then any license preliminarily granted shall be deemed automatically revoked and shall be void as if never granted. Further, in the event that you breach any of these terms and conditions or any of CCC's Billing and Payment terms and conditions, the license is automatically revoked and shall be void as if never granted. Use of materials as described in a revoked license, as well as any use of the materials beyond the scope of an unrevoked license, may constitute copyright infringement and publisher reserves the right to take any and all action to protect its copyright in the materials.

9. Warranties: Publisher makes no representations or warranties with respect to the licensed material.

10. Indemnity: You hereby indemnify and agree to hold harmless publisher and CCC, and their respective officers, directors, employees and agents, from and against any and all claims arising out of your use of the licensed material other than as specifically authorized pursuant to this license.

11. No Transfer of License: This license is personal to you and may not be sublicensed, assigned, or transferred by you to any other person without publisher's written permission.

12. No Amendment Except in Writing: This license may not be amended except in a writing signed by both parties (or, in the case of publisher, by CCC on publisher's behalf).

13. Objection to Contrary Terms: Publisher hereby objects to any terms contained in any purchase order, acknowledgment, check endorsement or other writing prepared by you, which terms are inconsistent with these terms and conditions or CCC's Billing and Payment terms and conditions. These terms and conditions, together with CCC's Billing and Payment terms and conditions (which are incorporated herein), comprise the entire agreement between you and publisher (and CCC) concerning this licensing transaction. In the event of any conflict between your obligations established by these terms and conditions and those established by CCC's Billing and Payment terms and conditions, these terms and conditions shall control.

14. Revocation: Elsevier or Copyright Clearance Center may deny the permissions described in this License at their sole discretion, for any reason or no reason, with a full refund payable to you. Notice of such denial will be made using the contact information provided by you.

Failure to receive such notice will not alter or invalidate the denial. In no event will Elsevier or Copyright Clearance Center be responsible or liable for any costs, expenses or damage incurred by you as a result of a denial of your permission request, other than a refund of the amount(s) paid by you to Elsevier and/or Copyright Clearance Center for denied permissions.

LIMITED LICENSE

The following terms and conditions apply only to specific license types:

15. **Translation**: This permission is granted for non-exclusive world **English** rights only unless your license was granted for translation rights. If you licensed translation rights you may only translate this content into the languages you requested. A professional translator must perform all translations and reproduce the content word for word preserving the integrity of the article. If this license is to re-use 1 or 2 figures then permission is granted for non-exclusive world rights in all languages.

16. **Website**: The following terms and conditions apply to electronic reserve and author websites:
Electronic reserve: If licensed material is to be posted to website, the web site is to be password-protected and made available only to bona fide students registered on a relevant course if:
This license was made in connection with a course,
This permission is granted for 1 year only. You may obtain a license for future website posting,
All content posted to the web site must maintain the copyright information line on the bottom of each image,
A hyper-text must be included to the Homepage of the journal from which you are licensing at http://www.sciencedirect.com/science/journal/xxxxx or the Elsevier homepage for books at http://www.elsevier.com , and
Central Storage: This license does not include permission for a scanned version of the material to be stored in a central repository such as that provided by Heron/XanEdu.

17. **Author website** for journals with the following additional clauses:

All content posted to the web site must maintain the copyright information line on the bottom of each image, and the permission granted is limited to the personal version of your paper. You are not allowed to download and post the published electronic version of your article (whether PDF or HTML, proof or final version), nor may you scan the printed edition to create an electronic version. A hyper-text must be included to the Homepage of the journal from which you are licensing at http://www.sciencedirect.com/science/journal/xxxxx . As part of our normal production process, you will receive an e-mail notice when your article appears on Elsevier's online service ScienceDirect (www.sciencedirect.com). That e-mail will include the article's Digital Object Identifier (DOI). This number provides the electronic link to the published article and should be included in the posting of your personal version. We ask that you wait until you receive this e-mail and have the DOI to do any posting.

Central Storage: This license does not include permission for a scanned version of the

material to be stored in a central repository such as that provided by Heron/XanEdu.

18. **Author website** for books with the following additional clauses:
Authors are permitted to place a brief summary of their work online only.
A hyper-text must be included to the Elsevier homepage at http://www.elsevier.com . All content posted to the web site must maintain the copyright information line on the bottom of each image. You are not allowed to download and post the published electronic version of your chapter, nor may you scan the printed edition to create an electronic version.

Central Storage: This license does not include permission for a scanned version of the material to be stored in a central repository such as that provided by Heron/XanEdu.

19. **Website** (regular and for author): A hyper-text must be included to the Homepage of the journal from which you are licensing at http://www.sciencedirect.com/science/journal/xxxxx. or for books to the Elsevier homepage at http://www.elsevier.com

20. **Thesis/Dissertation**: If your license is for use in a thesis/dissertation your thesis may be submitted to your institution in either print or electronic form. Should your thesis be published commercially, please reapply for permission. These requirements include permission for the Library and Archives of Canada to supply single copies, on demand, of the complete thesis and include permission for UMI to supply single copies, on demand, of the complete thesis. Should your thesis be published commercially, please reapply for permission.

21. **Other Conditions**:

v1.6

If you would like to pay for this license now, please remit this license along with your payment made payable to "COPYRIGHT CLEARANCE CENTER" otherwise you will be invoiced within 48 hours of the license date. Payment should be in the form of a check or money order referencing your account number and this invoice number RLNK501057345.
Once you receive your invoice for this order, you may pay your invoice by credit card. Please follow instructions provided at that time.

Make Payment To:
Copyright Clearance Center
Dept 001
P.O. Box 843006
Boston, MA 02284-3006

For suggestions or comments regarding this order, contact RightsLink Customer Support: customercare@copyright.com or +1-877-622-5543 (toll free in the US) or +1-978-646-2777.

Gratis licenses (referencing $0 in the Total field) are free. Please retain this printable license for your reference. No payment is required.

ELSEVIER LICENSE
TERMS AND CONDITIONS

Jul 03, 2013

This is a License Agreement between Jing Wei ("You") and Elsevier ("Elsevier") provided by Copyright Clearance Center ("CCC"). The license consists of your order details, the terms and conditions provided by Elsevier, and the payment terms and conditions.

All payments must be made in full to CCC. For payment instructions, please see information listed at the bottom of this form.

Supplier	Elsevier Limited The Boulevard,Langford Lane Kidlington,Oxford,OX5 1GB,UK
Registered Company Number	1982084
Customer name	Jing Wei
Customer address	1 Cleantech Loop, CleanTech One, #06-08 Singapore, 637141
License number	3181251113535
License date	Jul 03, 2013
Licensed content publisher	Elsevier
Licensed content publication	Journal of Membrane Science
Licensed content title	Influence of monomer concentrations on the performance of polyamide-based thin film composite forward osmosis membranes
Licensed content author	Jing Wei,Xin Liu,Changquan Qiu,Rong Wang,Chuyang Y. Tang
Licensed content date	30 September 2011
Licensed content volume number	381
Licensed content issue number	1–2
Number of pages	8
Start Page	110
End Page	117
Type of Use	reuse in a thesis/dissertation
Intended publisher of new work	other
Portion	full article
Format	both print and electronic
Are you the author of this Elsevier article?	Yes
Will you be translating?	No

Order reference number	
Title of your thesis/dissertation	Synthesis of Flat-sheet Thin Film Composite Forward Osmosis Membranes
Expected completion date	Jul 2013
Estimated size (number of pages)	200
Elsevier VAT number	GB 494 6272 12
Permissions price	0.00 USD
VAT/Local Sales Tax	0.00 USD / 0.00 GBP
Total	0.00 USD
Terms and Conditions	

INTRODUCTION

1. The publisher for this copyrighted material is Elsevier. By clicking "accept" in connection with completing this licensing transaction, you agree that the following terms and conditions apply to this transaction (along with the Billing and Payment terms and conditions established by Copyright Clearance Center, Inc. ("CCC"), at the time that you opened your Rightslink account and that are available at any time at http://myaccount.copyright.com).

GENERAL TERMS

2. Elsevier hereby grants you permission to reproduce the aforementioned material subject to the terms and conditions indicated.

3. Acknowledgement: If any part of the material to be used (for example, figures) has appeared in our publication with credit or acknowledgement to another source, permission must also be sought from that source. If such permission is not obtained then that material may not be included in your publication/copies. Suitable acknowledgement to the source must be made, either as a footnote or in a reference list at the end of your publication, as follows:

"Reprinted from Publication title, Vol /edition number, Author(s), Title of article / title of chapter, Pages No., Copyright (Year), with permission from Elsevier [OR APPLICABLE SOCIETY COPYRIGHT OWNER]." Also Lancet special credit - "Reprinted from The Lancet, Vol. number, Author(s), Title of article, Pages No., Copyright (Year), with permission from Elsevier."

4. Reproduction of this material is confined to the purpose and/or media for which permission is hereby given.

5. Altering/Modifying Material: Not Permitted. However figures and illustrations may be altered/adapted minimally to serve your work. Any other abbreviations, additions, deletions and/or any other alterations shall be made only with prior written authorization of Elsevier Ltd. (Please contact Elsevier at permissions@elsevier.com)

6. If the permission fee for the requested use of our material is waived in this instance, please be advised that your future requests for Elsevier materials may attract a fee.

7. Reservation of Rights: Publisher reserves all rights not specifically granted in the combination of (i) the license details provided by you and accepted in the course of this licensing transaction, (ii) these terms and conditions and (iii) CCC's Billing and Payment terms and conditions.

8. License Contingent Upon Payment: While you may exercise the rights licensed immediately upon issuance of the license at the end of the licensing process for the transaction, provided that you have disclosed complete and accurate details of your proposed use, no license is finally effective unless and until full payment is received from you (either by publisher or by CCC) as provided in CCC's Billing and Payment terms and conditions. If full payment is not received on a timely basis, then any license preliminarily granted shall be deemed automatically revoked and shall be void as if never granted. Further, in the event that you breach any of these terms and conditions or any of CCC's Billing and Payment terms and conditions, the license is automatically revoked and shall be void as if never granted. Use of materials as described in a revoked license, as well as any use of the materials beyond the scope of an unrevoked license, may constitute copyright infringement and publisher reserves the right to take any and all action to protect its copyright in the materials.

9. Warranties: Publisher makes no representations or warranties with respect to the licensed material.

10. Indemnity: You hereby indemnify and agree to hold harmless publisher and CCC, and their respective officers, directors, employees and agents, from and against any and all claims arising out of your use of the licensed material other than as specifically authorized pursuant to this license.

11. No Transfer of License: This license is personal to you and may not be sublicensed, assigned, or transferred by you to any other person without publisher's written permission.

12. No Amendment Except in Writing: This license may not be amended except in a writing signed by both parties (or, in the case of publisher, by CCC on publisher's behalf).

13. Objection to Contrary Terms: Publisher hereby objects to any terms contained in any purchase order, acknowledgment, check endorsement or other writing prepared by you, which terms are inconsistent with these terms and conditions or CCC's Billing and Payment terms and conditions. These terms and conditions, together with CCC's Billing and Payment terms and conditions (which are incorporated herein), comprise the entire agreement between you and publisher (and CCC) concerning this licensing transaction. In the event of any conflict between your obligations established by these terms and conditions and those established by CCC's Billing and Payment terms and conditions, these terms and conditions shall control.

14. Revocation: Elsevier or Copyright Clearance Center may deny the permissions described in this License at their sole discretion, for any reason or no reason, with a full refund payable to you. Notice of such denial will be made using the contact information provided by you.

Failure to receive such notice will not alter or invalidate the denial. In no event will Elsevier or Copyright Clearance Center be responsible or liable for any costs, expenses or damage incurred by you as a result of a denial of your permission request, other than a refund of the amount(s) paid by you to Elsevier and/or Copyright Clearance Center for denied permissions.

LIMITED LICENSE

The following terms and conditions apply only to specific license types:

15. **Translation**: This permission is granted for non-exclusive world **English** rights only unless your license was granted for translation rights. If you licensed translation rights you may only translate this content into the languages you requested. A professional translator must perform all translations and reproduce the content word for word preserving the integrity of the article. If this license is to re-use 1 or 2 figures then permission is granted for non-exclusive world rights in all languages.

16. **Website**: The following terms and conditions apply to electronic reserve and author websites:
Electronic reserve: If licensed material is to be posted to website, the web site is to be password-protected and made available only to bona fide students registered on a relevant course if:
This license was made in connection with a course,
This permission is granted for 1 year only. You may obtain a license for future website posting,
All content posted to the web site must maintain the copyright information line on the bottom of each image,
A hyper-text must be included to the Homepage of the journal from which you are licensing at http://www.sciencedirect.com/science/journal/xxxxx or the Elsevier homepage for books at http://www.elsevier.com , and
Central Storage: This license does not include permission for a scanned version of the material to be stored in a central repository such as that provided by Heron/XanEdu.

17. **Author website** for journals with the following additional clauses:

All content posted to the web site must maintain the copyright information line on the bottom of each image, and the permission granted is limited to the personal version of your paper. You are not allowed to download and post the published electronic version of your article (whether PDF or HTML, proof or final version), nor may you scan the printed edition to create an electronic version. A hyper-text must be included to the Homepage of the journal from which you are licensing at http://www.sciencedirect.com/science/journal/xxxxx . As part of our normal production process, you will receive an e-mail notice when your article appears on Elsevier's online service ScienceDirect (www.sciencedirect.com). That e-mail will include the article's Digital Object Identifier (DOI). This number provides the electronic link to the published article and should be included in the posting of your personal version. We ask that you wait until you receive this e-mail and have the DOI to do any posting.

Central Storage: This license does not include permission for a scanned version of the

material to be stored in a central repository such as that provided by Heron/XanEdu.

18. **Author website** for books with the following additional clauses:
Authors are permitted to place a brief summary of their work online only.
A hyper-text must be included to the Elsevier homepage at http://www.elsevier.com . All content posted to the web site must maintain the copyright information line on the bottom of each image. You are not allowed to download and post the published electronic version of your chapter, nor may you scan the printed edition to create an electronic version.

Central Storage: This license does not include permission for a scanned version of the material to be stored in a central repository such as that provided by Heron/XanEdu.

19. **Website** (regular and for author): A hyper-text must be included to the Homepage of the journal from which you are licensing at http://www.sciencedirect.com/science/journal/xxxxx. or for books to the Elsevier homepage at http://www.elsevier.com

20. **Thesis/Dissertation**: If your license is for use in a thesis/dissertation your thesis may be submitted to your institution in either print or electronic form. Should your thesis be published commercially, please reapply for permission. These requirements include permission for the Library and Archives of Canada to supply single copies, on demand, of the complete thesis and include permission for UMI to supply single copies, on demand, of the complete thesis. Should your thesis be published commercially, please reapply for permission.

21. **Other Conditions**:

v1.6

If you would like to pay for this license now, please remit this license along with your payment made payable to "COPYRIGHT CLEARANCE CENTER" otherwise you will be invoiced within 48 hours of the license date. Payment should be in the form of a check or money order referencing your account number and this invoice number RLNK501057322.
Once you receive your invoice for this order, you may pay your invoice by credit card. Please follow instructions provided at that time.

Make Payment To:
Copyright Clearance Center
Dept 001
P.O. Box 843006
Boston, MA 02284-3006

For suggestions or comments regarding this order, contact RightsLink Customer Support: customercare@copyright.com or +1-877-622-5543 (toll free in the US) or +1-978-646-2777.

Gratis licenses (referencing $0 in the Total field) are free. Please retain this printable license for your reference. No payment is required.

ELSEVIER LICENSE
TERMS AND CONDITIONS

Jul 03, 2013

This is a License Agreement between Jing Wei ("You") and Elsevier ("Elsevier") provided by Copyright Clearance Center ("CCC"). The license consists of your order details, the terms and conditions provided by Elsevier, and the payment terms and conditions.

All payments must be made in full to CCC. For payment instructions, please see information listed at the bottom of this form.

Supplier	Elsevier Limited The Boulevard,Langford Lane Kidlington,Oxford,OX5 1GB,UK
Registered Company Number	1982084
Customer name	Jing Wei
Customer address	1 Cleantech Loop, CleanTech One, #06-08 Singapore, 637141
License number	3181260499763
License date	Jul 03, 2013
Licensed content publisher	Elsevier
Licensed content publication	Journal of Membrane Science
Licensed content title	Comparison of NF-like and RO-like thin film composite osmotically-driven membranes—Implications for membrane selection and process optimization
Licensed content author	Jing Wei,Changquan Qiu,Yi-Ning Wang,Rong Wang,Chuyang Y. Tang
Licensed content date	15 January 2013
Licensed content volume number	427
Licensed content issue number	
Number of pages	12
Start Page	460
End Page	471
Type of Use	reuse in a thesis/dissertation
Intended publisher of new work	other
Portion	full article
Format	both print and electronic
Are you the author of this Elsevier article?	Yes

Will you be translating?	No
Order reference number	
Title of your thesis/dissertation	Synthesis of Flat-sheet Thin Film Composite Forward Osmosis Membranes
Expected completion date	Jul 2013
Estimated size (number of pages)	200
Elsevier VAT number	GB 494 6272 12
Permissions price	0.00 USD
VAT/Local Sales Tax	0.00 USD / 0.00 GBP
Total	0.00 USD
Terms and Conditions	

INTRODUCTION

1. The publisher for this copyrighted material is Elsevier. By clicking "accept" in connection with completing this licensing transaction, you agree that the following terms and conditions apply to this transaction (along with the Billing and Payment terms and conditions established by Copyright Clearance Center, Inc. ("CCC"), at the time that you opened your Rightslink account and that are available at any time at http://myaccount.copyright.com).

GENERAL TERMS

2. Elsevier hereby grants you permission to reproduce the aforementioned material subject to the terms and conditions indicated.

3. Acknowledgement: If any part of the material to be used (for example, figures) has appeared in our publication with credit or acknowledgement to another source, permission must also be sought from that source. If such permission is not obtained then that material may not be included in your publication/copies. Suitable acknowledgement to the source must be made, either as a footnote or in a reference list at the end of your publication, as follows:

"Reprinted from Publication title, Vol /edition number, Author(s), Title of article / title of chapter, Pages No., Copyright (Year), with permission from Elsevier [OR APPLICABLE SOCIETY COPYRIGHT OWNER]." Also Lancet special credit - "Reprinted from The Lancet, Vol. number, Author(s), Title of article, Pages No., Copyright (Year), with permission from Elsevier."

4. Reproduction of this material is confined to the purpose and/or media for which permission is hereby given.

5. Altering/Modifying Material: Not Permitted. However figures and illustrations may be altered/adapted minimally to serve your work. Any other abbreviations, additions, deletions and/or any other alterations shall be made only with prior written authorization of Elsevier Ltd. (Please contact Elsevier at permissions@elsevier.com)

6. If the permission fee for the requested use of our material is waived in this instance, please be advised that your future requests for Elsevier materials may attract a fee.

7. Reservation of Rights: Publisher reserves all rights not specifically granted in the combination of (i) the license details provided by you and accepted in the course of this licensing transaction, (ii) these terms and conditions and (iii) CCC's Billing and Payment terms and conditions.

8. License Contingent Upon Payment: While you may exercise the rights licensed immediately upon issuance of the license at the end of the licensing process for the transaction, provided that you have disclosed complete and accurate details of your proposed use, no license is finally effective unless and until full payment is received from you (either by publisher or by CCC) as provided in CCC's Billing and Payment terms and conditions. If full payment is not received on a timely basis, then any license preliminarily granted shall be deemed automatically revoked and shall be void as if never granted. Further, in the event that you breach any of these terms and conditions or any of CCC's Billing and Payment terms and conditions, the license is automatically revoked and shall be void as if never granted. Use of materials as described in a revoked license, as well as any use of the materials beyond the scope of an unrevoked license, may constitute copyright infringement and publisher reserves the right to take any and all action to protect its copyright in the materials.

9. Warranties: Publisher makes no representations or warranties with respect to the licensed material.

10. Indemnity: You hereby indemnify and agree to hold harmless publisher and CCC, and their respective officers, directors, employees and agents, from and against any and all claims arising out of your use of the licensed material other than as specifically authorized pursuant to this license.

11. No Transfer of License: This license is personal to you and may not be sublicensed, assigned, or transferred by you to any other person without publisher's written permission.

12. No Amendment Except in Writing: This license may not be amended except in a writing signed by both parties (or, in the case of publisher, by CCC on publisher's behalf).

13. Objection to Contrary Terms: Publisher hereby objects to any terms contained in any purchase order, acknowledgment, check endorsement or other writing prepared by you, which terms are inconsistent with these terms and conditions or CCC's Billing and Payment terms and conditions. These terms and conditions, together with CCC's Billing and Payment terms and conditions (which are incorporated herein), comprise the entire agreement between you and publisher (and CCC) concerning this licensing transaction. In the event of any conflict between your obligations established by these terms and conditions and those established by CCC's Billing and Payment terms and conditions, these terms and conditions shall control.

14. Revocation: Elsevier or Copyright Clearance Center may deny the permissions described in this License at their sole discretion, for any reason or no reason, with a full refund payable to you. Notice of such denial will be made using the contact information provided by you.

Failure to receive such notice will not alter or invalidate the denial. In no event will Elsevier or Copyright Clearance Center be responsible or liable for any costs, expenses or damage incurred by you as a result of a denial of your permission request, other than a refund of the amount(s) paid by you to Elsevier and/or Copyright Clearance Center for denied permissions.

LIMITED LICENSE

The following terms and conditions apply only to specific license types:

15. **Translation**: This permission is granted for non-exclusive world **English** rights only unless your license was granted for translation rights. If you licensed translation rights you may only translate this content into the languages you requested. A professional translator must perform all translations and reproduce the content word for word preserving the integrity of the article. If this license is to re-use 1 or 2 figures then permission is granted for non-exclusive world rights in all languages.

16. **Website**: The following terms and conditions apply to electronic reserve and author websites:
Electronic reserve: If licensed material is to be posted to website, the web site is to be password-protected and made available only to bona fide students registered on a relevant course if:
This license was made in connection with a course,
This permission is granted for 1 year only. You may obtain a license for future website posting,
All content posted to the web site must maintain the copyright information line on the bottom of each image,
A hyper-text must be included to the Homepage of the journal from which you are licensing at http://www.sciencedirect.com/science/journal/xxxxx or the Elsevier homepage for books at http://www.elsevier.com , and
Central Storage: This license does not include permission for a scanned version of the material to be stored in a central repository such as that provided by Heron/XanEdu.

17. **Author website** for journals with the following additional clauses:

All content posted to the web site must maintain the copyright information line on the bottom of each image, and the permission granted is limited to the personal version of your paper. You are not allowed to download and post the published electronic version of your article (whether PDF or HTML, proof or final version), nor may you scan the printed edition to create an electronic version. A hyper-text must be included to the Homepage of the journal from which you are licensing at http://www.sciencedirect.com/science/journal/xxxxx . As part of our normal production process, you will receive an e-mail notice when your article appears on Elsevier's online service ScienceDirect (www.sciencedirect.com). That e-mail will include the article's Digital Object Identifier (DOI). This number provides the electronic link to the published article and should be included in the posting of your personal version. We ask that you wait until you receive this e-mail and have the DOI to do any posting.

Central Storage: This license does not include permission for a scanned version of the

material to be stored in a central repository such as that provided by Heron/XanEdu.

18. **Author website** for books with the following additional clauses:
Authors are permitted to place a brief summary of their work online only.
A hyper-text must be included to the Elsevier homepage at http://www.elsevier.com . All content posted to the web site must maintain the copyright information line on the bottom of each image. You are not allowed to download and post the published electronic version of your chapter, nor may you scan the printed edition to create an electronic version.

Central Storage: This license does not include permission for a scanned version of the material to be stored in a central repository such as that provided by Heron/XanEdu.

19. **Website** (regular and for author): A hyper-text must be included to the Homepage of the journal from which you are licensing at http://www.sciencedirect.com/science/journal/xxxxx. or for books to the Elsevier homepage at http://www.elsevier.com

20. **Thesis/Dissertation**: If your license is for use in a thesis/dissertation your thesis may be submitted to your institution in either print or electronic form. Should your thesis be published commercially, please reapply for permission. These requirements include permission for the Library and Archives of Canada to supply single copies, on demand, of the complete thesis and include permission for UMI to supply single copies, on demand, of the complete thesis. Should your thesis be published commercially, please reapply for permission.

21. **Other Conditions**:

v1.6

If you would like to pay for this license now, please remit this license along with your payment made payable to "COPYRIGHT CLEARANCE CENTER" otherwise you will be invoiced within 48 hours of the license date. Payment should be in the form of a check or money order referencing your account number and this invoice number RLNK501057338.
Once you receive your invoice for this order, you may pay your invoice by credit card. Please follow instructions provided at that time.

Make Payment To:
Copyright Clearance Center
Dept 001
P.O. Box 843006
Boston, MA 02284-3006

For suggestions or comments regarding this order, contact RightsLink Customer Support: customercare@copyright.com or +1-877-622-5543 (toll free in the US) or +1-978-646-2777.

Gratis licenses (referencing $0 in the Total field) are free. Please retain this printable license for your reference. No payment is required.